ISYA 2024 – THE INTERSTELLAR MEDIUM (ISM): LECTURE 3.
Heating & Cooling – The Phases of the ISM

Frédéric GALLIANO

CEA Paris-Saclay, France

October 1st, 2024

Outline of the Lecture

1. **COOLING & HEATING OF THE GAS**
   - The gas heating processes
   - The gas cooling function
   - The five thermal phases of the ISM

Outline of the Lecture

1. **COOLING & HEATING OF THE GAS**
   - The gas heating processes
   - The gas cooling function
   - The five thermal phases of the ISM

2. **THE PRINCIPLES OF RADIATIVE TRANSFER**
   - The radiative transfer equation
   - Solutions in simple cases
   - Dust radiative transfer with more complex geometries

Outline of the Lecture

1. **COOLING & HEATING OF THE GAS**
   - The gas heating processes
   - The gas cooling function
   - The five thermal phases of the ISM
2. **THE PRINCIPLES OF RADIATIVE TRANSFER**
   - The radiative transfer equation
   - Solutions in simple cases
   - Dust radiative transfer with more complex geometries
3. **STAR-FORMING REGIONS**
   - The Structure of Star-Forming Regions
   - H II regions
   - PhotoDissociation Regions (PDRs)

Outline of the Lecture

Outline of the Lecture

1. **COOLING & HEATING OF THE GAS**
   - The gas heating processes
   - The gas cooling function
   - The five thermal phases of the ISM
2. **THE PRINCIPLES OF RADIATIVE TRANSFER**
   - The radiative transfer equation
   - Solutions in simple cases
   - Dust radiative transfer with more complex geometries
3. **STAR-FORMING REGIONS**
   - The Structure of Star-Forming Regions
   - H II regions
   - PhotoDissociation Regions (PDRs)
4. **CONCLUSION**
   - Take-away points
   - References

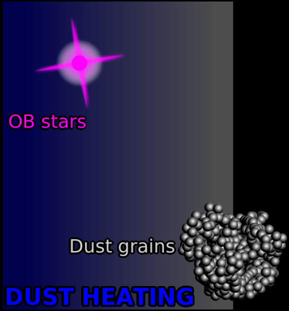
OB stars
Dust grains
DUST HEATING

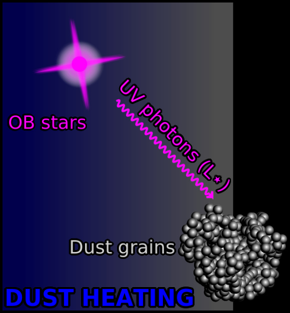
UV photons ($L_\star$)
OB stars
Dust grains
DUST HEATING

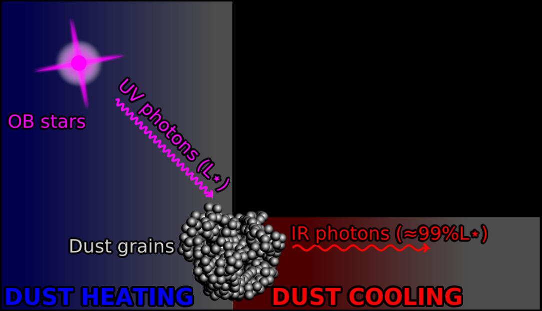
OB stars
UV photons ($L_\star$)
Dust grains
IR photons ($\approx$99%$L_\star$)
DUST HEATING
DUST COOLING

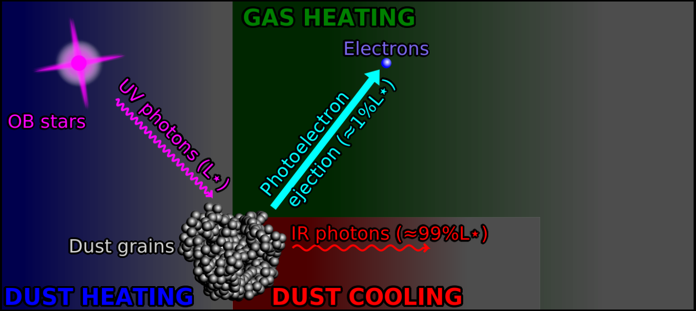
GAS HEATING
Electrons
OB stars
UV photons (L⋆)
Photoelectron ejection (≈1%L⋆)
IR photons (≈99%L⋆)
Dust grains
DUST HEATING
DUST COOLING

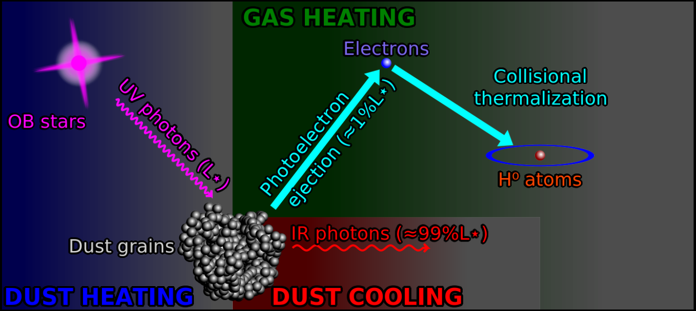
GAS HEATING
Electrons
Collisional thermalization
OB stars
UV photons ($L_\star$)
Photoelectron ejection ($\approx 1\% L_\star$)
H⁰ atoms
Dust grains
IR photons ($\approx 99\% L_\star$)
DUST HEATING
DUST COOLING

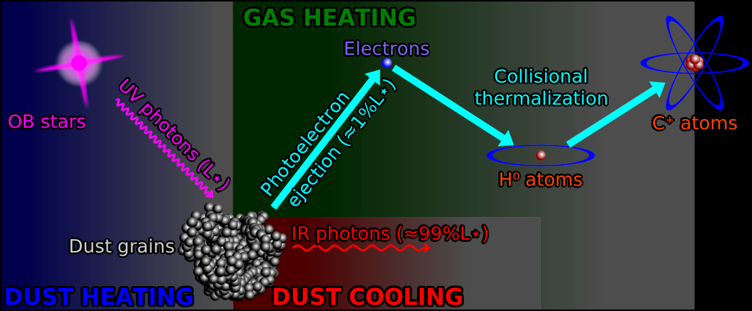
GAS HEATING
Electrons
Collisional thermalization
OB stars
UV photons ($L_\star$)
Photoelectron ejection ($\approx 1\% L_\star$)
C⁺ atoms
H⁰ atoms
Dust grains
IR photons ($\approx 99\% L_\star$)
DUST HEATING
DUST COOLING

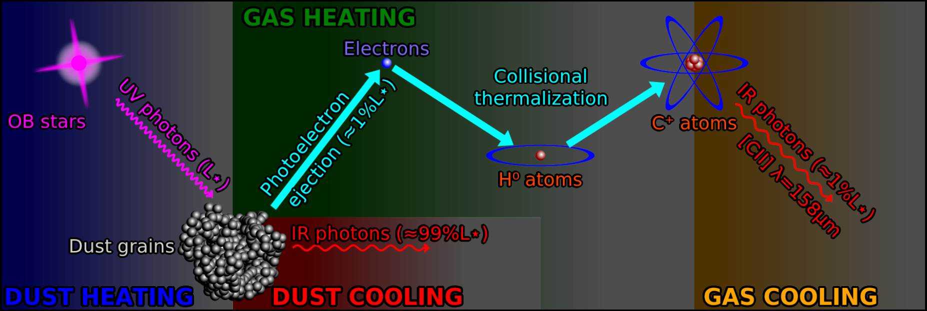
GAS HEATING
Electrons
OB stars
UV photons (L⋆)
Photoelectron ejection (≈1%L⋆)
Collisional thermalization
H⁰ atoms
C⁺ atoms
IR photons (≈1%L⋆)
[CII] λ=158µm
Dust grains
IR photons (≈99%L⋆)
DUST HEATING
DUST COOLING
GAS COOLING

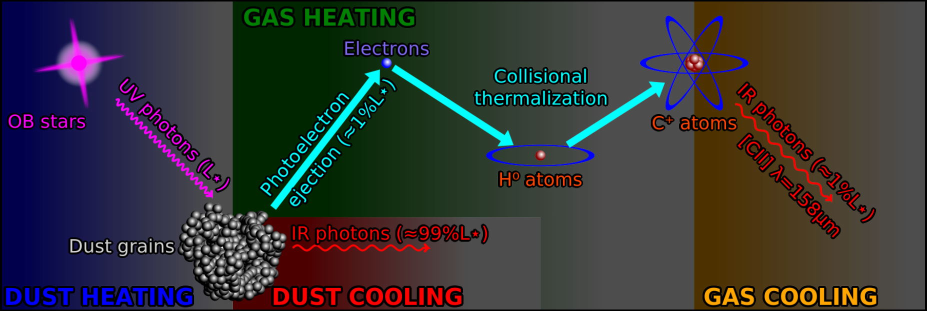

The main neutral gas heating mechanism

[C II]$_{158\mu m}$, [O I]$_{63\mu m}$ → usually the brightest ISM lines in galaxies (*e.g.*; Cormier et al. 2019).

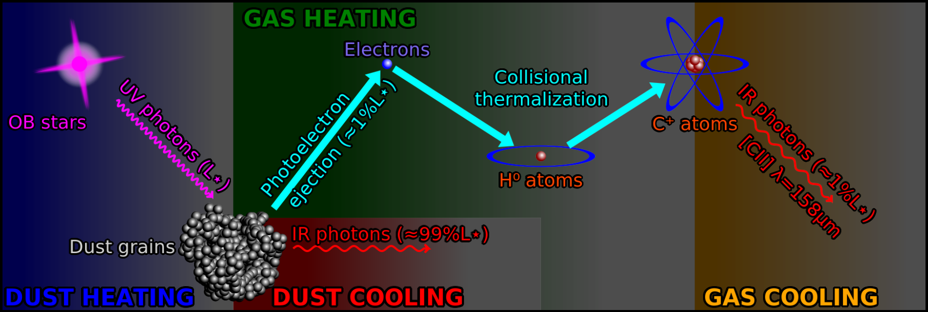

The main neutral gas heating mechanism

$[\mathrm{C\,II}]_{158\mu m}$, $[\mathrm{O\,I}]_{63\mu m}$ $\rightarrow$ usually the brightest ISM lines in galaxies (*e.g.*; Cormier et al. 2019).

A process dominated by small grains

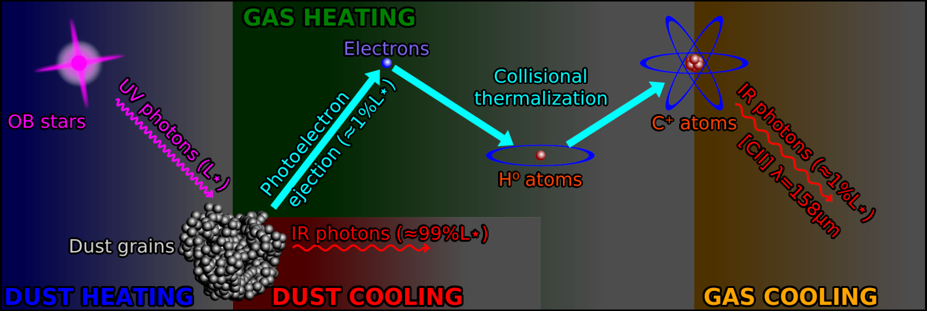

The main neutral gas heating mechanism

[C II]$_{158\mu m}$, [O I]$_{63\mu m}$ $\rightarrow$ usually the brightest ISM lines in galaxies (*e.g.*; Cormier et al. 2019).

A process dominated by small grains

For PAHs & nanograins: absorption of a $h\nu \gtrsim 11$ eV photon $\Rightarrow$ electron ejection probability high.

Thermal Phases | The PhotoElectric (PE) Heating

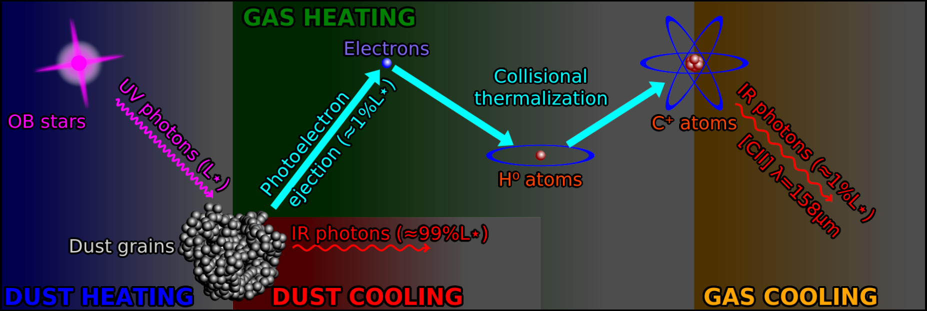

The main neutral gas heating mechanism

[C II]$_{158\mu m}$, [O I]$_{63\mu m}$ $\rightarrow$ usually the brightest ISM lines in galaxies (*e.g.*; Cormier et al. 2019).

A process dominated by small grains

For PAHs & nanograins: absorption of a $h\nu \gtrsim 11$ eV photon $\Rightarrow$ electron ejection probability high.

For medium / large grains: photon absorption within the grain $\Rightarrow$ low diffusion probability of the electron to the surface.

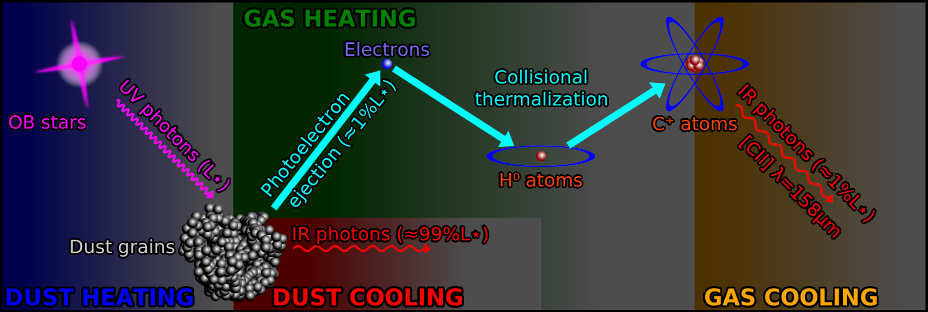

The main neutral gas heating mechanism

$[\mathrm{C\,II}]_{158\mu m}$, $[\mathrm{O\,I}]_{63\mu m}$ $\rightarrow$ usually the brightest ISM lines in galaxies (*e.g.*; Cormier et al. 2019).

A process dominated by small grains

For PAHs & nanograins: absorption of a $h\nu \gtrsim 11$ eV photon $\Rightarrow$ electron ejection probability high.

For medium / large grains: photon absorption within the grain $\Rightarrow$ low diffusion probability of the electron to the surface.

Most of the grain cumulated area is in small sizes $\Rightarrow$ PE dominated by PAHs & nanograins.

The UV *Interstellar Radiation Field* (ISRF)

The UV *Interstellar Radiation Field* (ISRF)

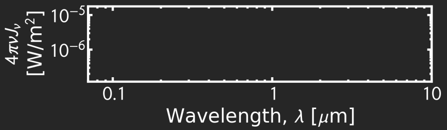

The UV *Interstellar Radiation Field* (ISRF)

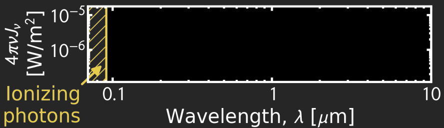

The UV *Interstellar Radiation Field* (ISRF)

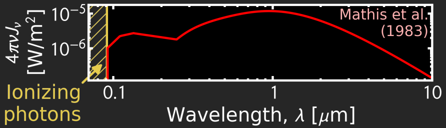

The UV *Interstellar Radiation Field* (ISRF)

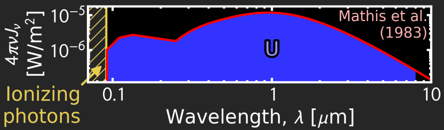

The UV *Interstellar Radiation Field* (ISRF)

The UV field: $G_0 \equiv \dfrac{\int_{0.0912\,\mu m}^{0.24\,\mu m} 4\pi J_\lambda(\lambda)\,\mathrm{d}\lambda}{1.6 \times 10^{-6}\ \mathrm{W/m^2}}$

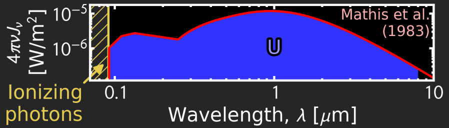

The UV *Interstellar Radiation Field* (ISRF)

The UV field: $G_0 \equiv \dfrac{\int_{0.0912\,\mu m}^{0.24\,\mu m} 4\pi J_\lambda(\lambda)\,\mathrm{d}\lambda}{1.6\times 10^{-6}\ \mathrm{W/m^2}}$

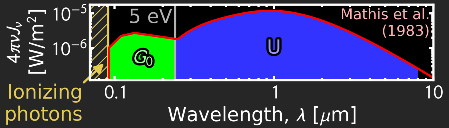

The UV *Interstellar Radiation Field* (ISRF)

The UV field: $G_0 \equiv \dfrac{\int_{0.0912\,\mu m}^{0.24\,\mu m} 4\pi J_\lambda(\lambda)\,\mathrm{d}\lambda}{1.6\times 10^{-6}\ \mathrm{W/m^2}}$

The charge parameter: $\gamma \equiv G_0\sqrt{T}/n_e$

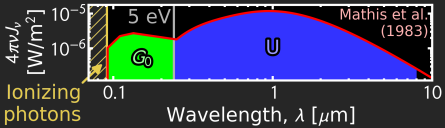

The UV *Interstellar Radiation Field* (ISRF)

The UV field: $G_0 \equiv \dfrac{\int_{0.0912\,\mu m}^{0.24\,\mu m} 4\pi J_\lambda(\lambda)\,\mathrm{d}\lambda}{1.6\times10^{-6}\ \mathrm{W/m^2}}$

The charge parameter: $\gamma \equiv G_0\sqrt{T}/n_e$

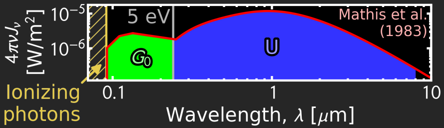

The photoelectric effect on PAHs

The UV *Interstellar Radiation Field* (ISRF)

The UV field: $G_0 \equiv \dfrac{\int_{0.0912\,\mu m}^{0.24\,\mu m} 4\pi J_\lambda(\lambda)\,\mathrm{d}\lambda}{1.6\times10^{-6}\ \mathrm{W/m^2}}$

The charge parameter: $\gamma \equiv G_0\sqrt{T}/n_e$

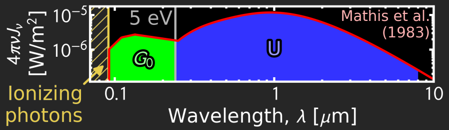

The photoelectric effect on PAHs

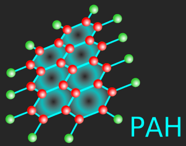

The UV *Interstellar Radiation Field* (ISRF)

The UV field: $G_0 \equiv \dfrac{\int_{0.0912\,\mu m}^{0.24\,\mu m} 4\pi J_\lambda(\lambda)\,\mathrm{d}\lambda}{1.6\times10^{-6}\ \mathrm{W/m^2}}$

The charge parameter: $\gamma \equiv G_0\sqrt{T}/n_e$

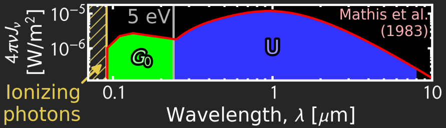

The photoelectric effect on PAHs

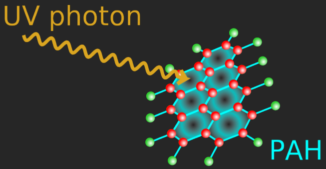

The UV *Interstellar Radiation Field* (ISRF)

The UV field: $G_0 \equiv \dfrac{\int_{0.0912\,\mu m}^{0.24\,\mu m} 4\pi J_\lambda(\lambda)\,\mathrm{d}\lambda}{1.6\times10^{-6}\ \mathrm{W/m^2}}$

The charge parameter: $\gamma \equiv G_0\sqrt{T}/n_e$

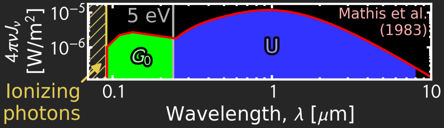

The photoelectric effect on PAHs

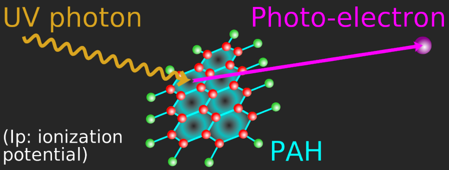

(Ip: ionization potential)

The UV *Interstellar Radiation Field* (ISRF)

The UV field: $G_0 \equiv \dfrac{\int_{0.0912\,\mu m}^{0.24\,\mu m} 4\pi J_\lambda(\lambda)\,\mathrm{d}\lambda}{1.6\times10^{-6}\ \mathrm{W/m^2}}$

The charge parameter: $\gamma \equiv G_0\sqrt{T}/n_e$

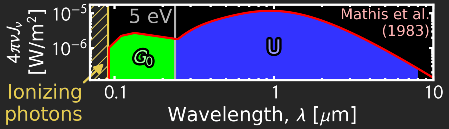

The photoelectric effect on PAHs

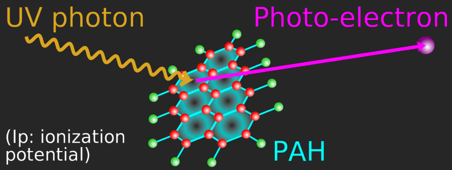

(Ip: ionization potential)

$$\epsilon_{PE}^{PAH}(\nu) \simeq Y\left(\frac{h\nu - I_P}{h\nu}\right)$$

The UV *Interstellar Radiation Field* (ISRF)

The UV field: $G_0 \equiv \frac{\int_{0.0912\,\mu m}^{0.24\,\mu m} 4\pi J_\lambda(\lambda)\,d\lambda}{1.6\times10^{-6}\ \mathrm{W/m^2}}$

The charge parameter: $\gamma \equiv G_0\sqrt{T}/n_e$

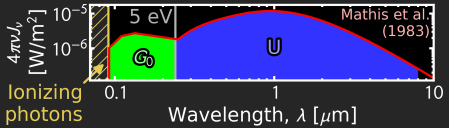

The photoelectric effect on PAHs

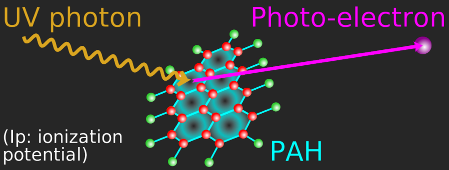

(Ip: ionization potential)

$$\epsilon_{PE}^{PAH}(\nu) \simeq Y\left(\frac{h\nu - I_P}{h\nu}\right)$$

The photoelectric effect on grains

The UV *Interstellar Radiation Field* (ISRF)

The UV field: $G_0 \equiv \dfrac{\int_{0.0912\,\mu m}^{0.24\,\mu m} 4\pi J_\lambda(\lambda)\,\mathrm{d}\lambda}{1.6\times10^{-6}\ \mathrm{W/m^2}}$

The charge parameter: $\gamma \equiv G_0\sqrt{T}/n_e$

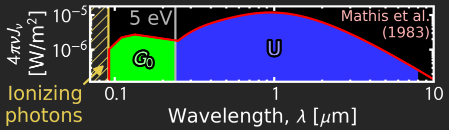

The photoelectric effect on PAHs

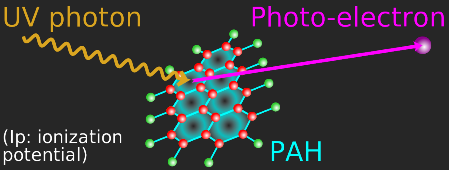

(Ip: ionization potential)

$$\epsilon_{PE}^{PAH}(\nu) \simeq Y\left(\frac{h\nu - I_P}{h\nu}\right)$$

The photoelectric effect on grains

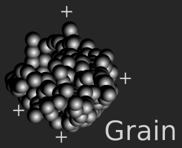

The UV *Interstellar Radiation Field* (ISRF)

The UV field: $G_0 \equiv \dfrac{\int_{0.0912\,\mu m}^{0.24\,\mu m} 4\pi J_\lambda(\lambda)\,\mathrm{d}\lambda}{1.6 \times 10^{-6}\ \mathrm{W/m^2}}$

The charge parameter: $\gamma \equiv G_0\sqrt{T}/n_e$

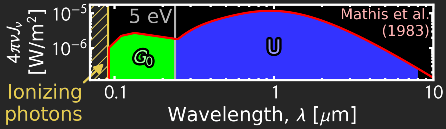

The photoelectric effect on PAHs

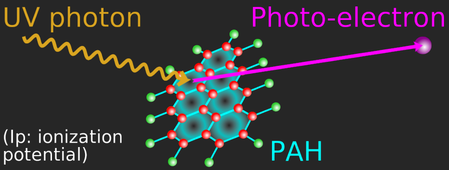

(Ip: ionization potential)

$$\epsilon_{PE}^{PAH}(\nu) \simeq Y\left(\frac{h\nu - I_P}{h\nu}\right)$$

The photoelectric effect on grains

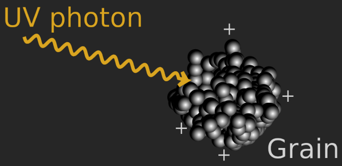

The UV *Interstellar Radiation Field* (ISRF)

The UV field: $G_0 \equiv \frac{\int_{0.0912\,\mu m}^{0.24\,\mu m} 4\pi J_\lambda(\lambda)\,\mathrm{d}\lambda}{1.6\times10^{-6}\ \mathrm{W/m^2}}$

The charge parameter: $\gamma \equiv G_0\sqrt{T}/n_e$

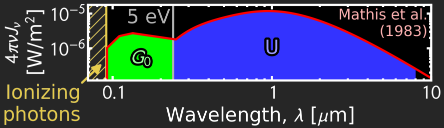

The photoelectric effect on PAHs

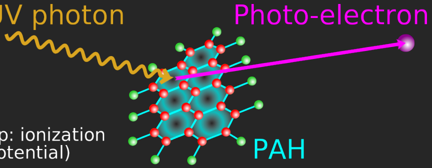

(Ip: ionization potential)

$$\epsilon_{PE}^{PAH}(\nu) \simeq Y\left(\frac{h\nu - I_P}{h\nu}\right)$$

The photoelectric effect on grains

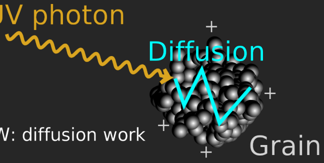

(W: diffusion work

The UV *Interstellar Radiation Field* (ISRF)

The UV field: $G_0 \equiv \frac{\int_{0.0912\,\mu m}^{0.24\,\mu m} 4\pi J_\lambda(\lambda)\,d\lambda}{1.6 \times 10^{-6}\ \mathrm{W/m^2}}$

The charge parameter: $\gamma \equiv G_0\sqrt{T}/n_e$

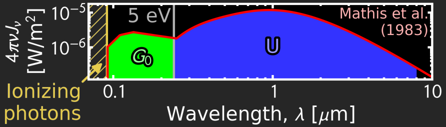

The photoelectric effect on PAHs

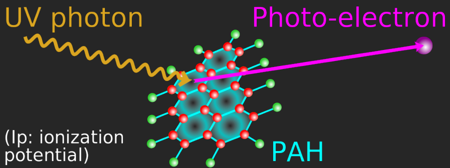

$$\epsilon_{PE}^{PAH}(\nu) \simeq Y\left(\frac{h\nu - I_P}{h\nu}\right)$$

The photoelectric effect on grains

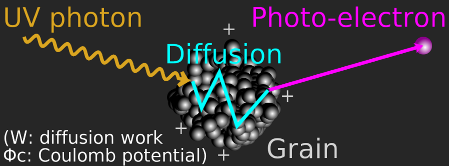

The UV *Interstellar Radiation Field* (ISRF)

The UV field: $G_0 \equiv \dfrac{\int_{0.0912\,\mu m}^{0.24\,\mu m} 4\pi J_\lambda(\lambda)\,\mathrm{d}\lambda}{1.6\times10^{-6}\ \mathrm{W/m^2}}$

The charge parameter: $\gamma \equiv G_0\sqrt{T}/n_e$

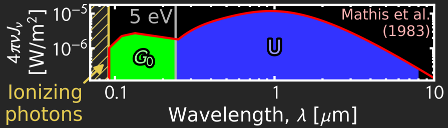

The photoelectric effect on PAHs

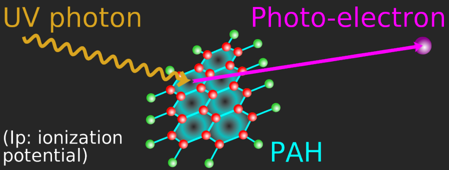

$$\epsilon_{PE}^{PAH}(\nu) \simeq Y\left(\frac{h\nu - I_P}{h\nu}\right)$$

The photoelectric effect on grains

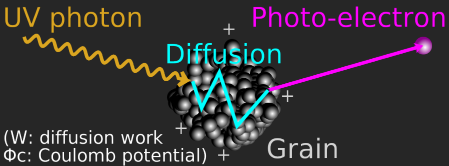

$$\epsilon_{PE}^{grain}(\nu) \simeq Y\left(\frac{h\nu - W - \phi_c}{h\nu}\right)$$

The UV *Interstellar Radiation Field* (ISRF)

The UV field: $$G_0 \equiv \frac{\int_{0.0912\,\mu m}^{0.24\,\mu m} 4\pi J_\lambda(\lambda)\,\mathrm{d}\lambda}{1.6\times10^{-6}\ \mathrm{W/m^2}}$$

The charge parameter: $\gamma \equiv G_0\sqrt{T}/n_e$

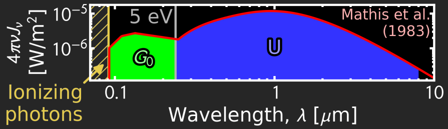

The photoelectric effect on PAHs

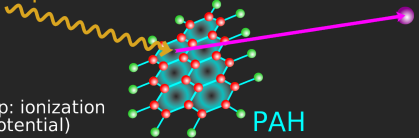

(Ip: ionization potential)

$$\epsilon_{\mathrm{PE}}^{\mathrm{PAH}}(\nu) \simeq Y\left(\frac{h\nu - I_\mathrm{P}}{h\nu}\right)$$

The photoelectric effect on grains

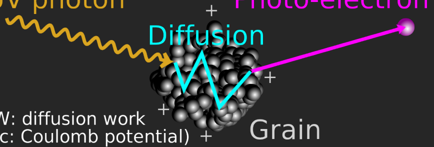

(W: diffusion work
Φc: Coulomb potential)

$$\epsilon_{\mathrm{PE}}^{\mathrm{grain}}(\nu) \simeq Y\left(\frac{h\nu - W - \phi_c}{h\nu}\right)$$

Empirical heating rate (Bakes & Tielens, 1994; Wolfire et al., 2022)

The UV *Interstellar Radiation Field* (ISRF)

The UV field: $G_0 \equiv \dfrac{\int_{0.0912\,\mu m}^{0.24\,\mu m} 4\pi J_\lambda(\lambda)\,\mathrm{d}\lambda}{1.6\times10^{-6}\ \mathrm{W/m^2}}$

The charge parameter: $\gamma \equiv G_0\sqrt{T}/n_e$

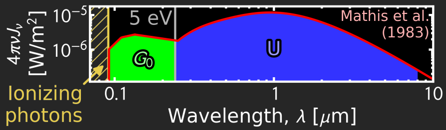

The photoelectric effect on PAHs

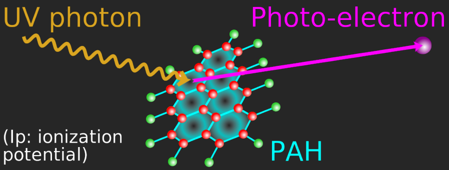

(Ip: ionization potential)

$$\epsilon_{\rm PE}^{\rm PAH}(\nu) \simeq Y\left(\frac{h\nu - I_P}{h\nu}\right)$$

The photoelectric effect on grains

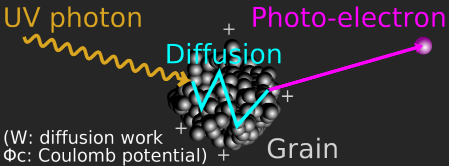

(W: diffusion work
Φc: Coulomb potential)

$$\epsilon_{\rm PE}^{\rm grain}(\nu) \simeq Y\left(\frac{h\nu - W - \phi_c}{h\nu}\right)$$

Empirical heating rate (Bakes & Tielens, 1994; Wolfire et al., 2022)

$$\epsilon_{\rm PE} \simeq \frac{4.87\times10^{-2}}{1+4\times10^{-3}\gamma^{0.73}} + \frac{3.65\times10^{-2}(T/10^4\ \mathrm{K})^{0.7}}{1+2\times10^{-2}\gamma}$$

The UV *Interstellar Radiation Field* (ISRF)

The UV field: $G_0 \equiv \dfrac{\int_{0.0912\,\mu m}^{0.24\,\mu m} 4\pi J_\lambda(\lambda)\,\mathrm{d}\lambda}{1.6\times10^{-6}\ \mathrm{W/m^2}}$

The charge parameter: $\gamma \equiv G_0\sqrt{T}/n_e$

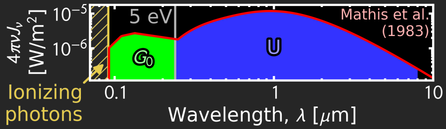

The photoelectric effect on PAHs

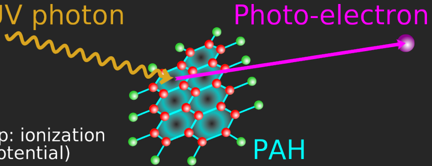

(Ip: ionization potential)

$$\epsilon_{\rm PE}^{\rm PAH}(\nu) \simeq Y\left(\frac{h\nu - I_{\rm P}}{h\nu}\right)$$

The photoelectric effect on grains

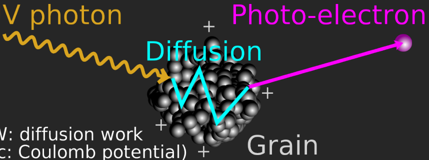

(W: diffusion work
Φc: Coulomb potential)

$$\epsilon_{\rm PE}^{\rm grain}(\nu) \simeq Y\left(\frac{h\nu - W - \phi_c}{h\nu}\right)$$

Empirical heating rate (Bakes & Tielens, 1994; Wolfire et al., 2022)

$$\epsilon_{\rm PE} \simeq \frac{4.87\times10^{-2}}{1+4\times10^{-3}\gamma^{0.73}} + \frac{3.65\times10^{-2}(T/10^4\ \mathrm{K})^{0.7}}{1+2\times10^{-2}\gamma} \rightarrow \Gamma_{\rm PE} = 10^{-31}\epsilon_{\rm PE}G_0\ [\mathrm{W}].$$

The heating rate due to the photoionization of specie i

The heating rate due to the photoionization of specie *i*

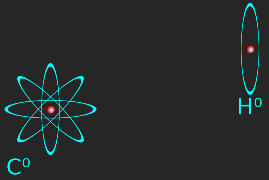

(*e.g.* Tielens, 2005)

The heating rate due to the photoionization of specie i

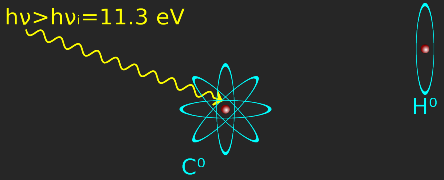

$h\nu_i$: photoionization potential.

(*e.g.* Tielens, 2005)

The heating rate due to the photoionization of specie *i*

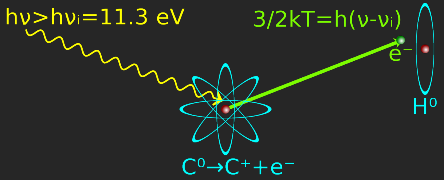

$h\nu_i$: photoionization potential.

(*e.g.* Tielens, 2005)

The heating rate due to the photoionization of specie *i*

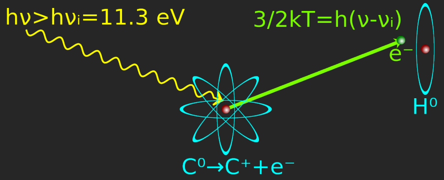

$\Gamma_{\rm PI}^i =$

$h\nu_i$: photoionization potential.

(*e.g.* Tielens, 2005)

The heating rate due to the photoionization of specie i

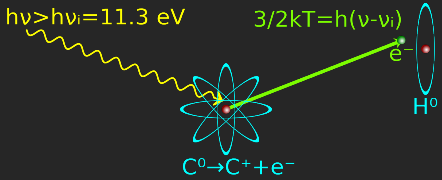

$$\Gamma^i_{\rm PI} = \int_{\nu_i}^{\infty} \underbrace{\frac{4\pi J_\nu(\nu)}{h\nu}}_{\text{photon rate}} \times$$

$h\nu_i$: photoionization potential.

(*e.g.* Tielens, 2005)

The heating rate due to the photoionization of specie *i*

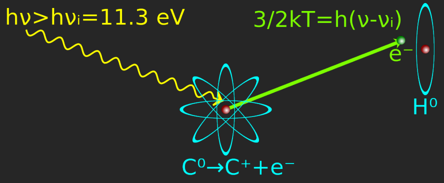

$$\Gamma^i_{\text{PI}} = \int_{\nu_i}^{\infty} \underbrace{\frac{4\pi J_\nu(\nu)}{h\nu}}_{\text{photon rate}} \times \underbrace{\alpha_i(\nu)}_{\text{cross-section}} \times$$

$h\nu_i$: photoionization potential.

(*e.g.* Tielens, 2005)

The heating rate due to the photoionization of specie *i*

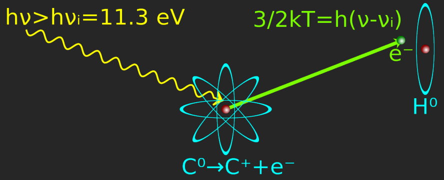

$$\Gamma^i_{\rm PI} = \int_{\nu_i}^{\infty} \underbrace{\frac{4\pi J_\nu(\nu)}{h\nu}}_{\text{photon rate}} \times \underbrace{\alpha_i(\nu)}_{\text{cross-section}} \times \underbrace{h(\nu-\nu_i)}_{\text{excess energy}} \,{\rm d}\nu,$$

$h\nu_i$: photoionization potential.

(*e.g.* Tielens, 2005)

The heating rate due to the photoionization of specie *i*

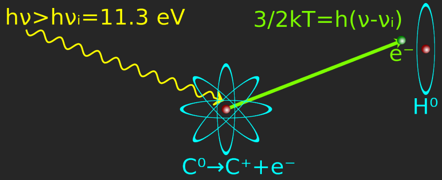

$$\Gamma^i_{\mathrm{PI}} = \int_{\nu_i}^{\infty} \underbrace{\frac{4\pi J_\nu(\nu)}{h\nu}}_{\text{photon rate}} \times \underbrace{\alpha_i(\nu)}_{\text{cross-section}} \times \underbrace{h(\nu-\nu_i)}_{\text{excess energy}} \, \mathrm{d}\nu,$$

$h\nu_i$: photoionization potential.

(*e.g.* Tielens, 2005)

In the ionized gas

The heating rate due to the photoionization of specie *i*

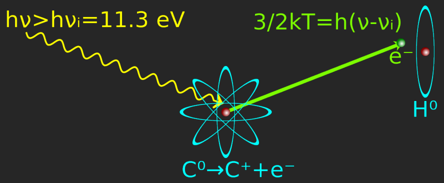

$$\Gamma_{\rm PI}^i = \int_{\nu_i}^{\infty} \underbrace{\frac{4\pi J_\nu(\nu)}{h\nu}}_{\text{photon rate}} \times \underbrace{\alpha_i(\nu)}_{\text{cross-section}} \times \underbrace{h(\nu-\nu_i)}_{\text{excess energy}} \,{\rm d}\nu,$$

$h\nu_i$: photoionization potential.

(*e.g.* Tielens, 2005)

In the ionized gas

- Most electrons coming from the photoionization $H^0 + \gamma \rightarrow H^+ + e^-$.

The heating rate due to the photoionization of specie i

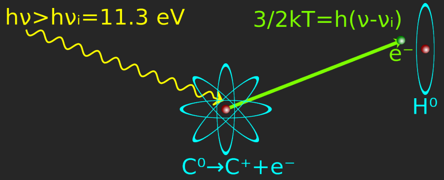

$$\Gamma_{\rm PI}^i = \int_{\nu_i}^{\infty} \underbrace{\frac{4\pi J_\nu(\nu)}{h\nu}}_{\text{photon rate}} \times \underbrace{\alpha_i(\nu)}_{\text{cross-section}} \times \underbrace{h(\nu-\nu_i)}_{\text{excess energy}} \, d\nu,$$

$h\nu_i$: photoionization potential.

(*e.g.* Tielens, 2005)

In the ionized gas

- Most electrons coming from the photoionization $H^0 + \gamma \rightarrow H^+ + e^-$.

$\Rightarrow$ dominant heating process in H II.

The heating rate due to the photoionization of specie *i*

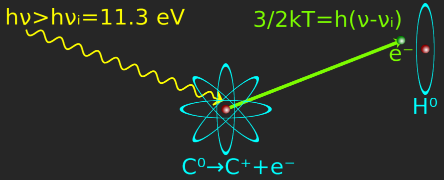

$$\Gamma^i_{\rm PI} = \int_{\nu_i}^{\infty} \underbrace{\frac{4\pi J_\nu(\nu)}{h\nu}}_{\text{photon rate}} \times \underbrace{\alpha_i(\nu)}_{\text{cross-section}} \times \underbrace{h(\nu-\nu_i)}_{\text{excess energy}} \, {\rm d}\nu,$$

$h\nu_i$: photoionization potential.

(*e.g.* Tielens, 2005)

In the ionized gas

- Most electrons coming from the photoionization $H^0 + \gamma \rightarrow H^+ + e^-$.

⇒ dominant heating process in H II.

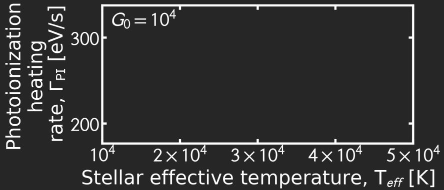

The heating rate due to the photoionization of specie *i*

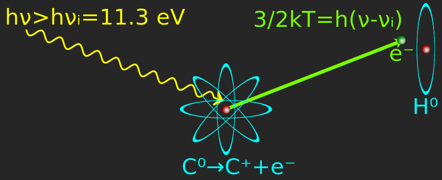

$$\Gamma^i_{\rm PI} = \int_{\nu_i}^{\infty} \underbrace{\frac{4\pi J_\nu(\nu)}{h\nu}}_{\text{photon rate}} \times \underbrace{\alpha_i(\nu)}_{\text{cross-section}} \times \underbrace{h(\nu-\nu_i)}_{\text{excess energy}} \,{\rm d}\nu,$$

$h\nu_i$: photoionization potential.

(*e.g.* Tielens, 2005)

In the ionized gas

- Most electrons coming from the photoionization $H^0 + \gamma \rightarrow H^+ + e^-$.

$\Rightarrow$ dominant heating process in H II.

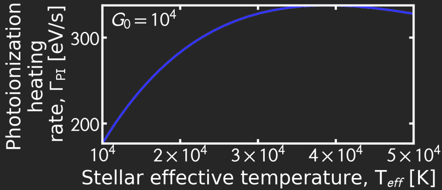

The heating rate due to the photoionization of specie *i*

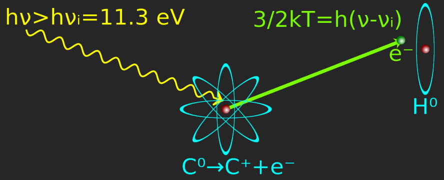

$$\Gamma_{\rm PI}^i = \int_{\nu_i}^{\infty} \underbrace{\frac{4\pi J_\nu(\nu)}{h\nu}}_{\text{photon rate}} \times \underbrace{\alpha_i(\nu)}_{\text{cross-section}} \times \underbrace{h(\nu-\nu_i)}_{\text{excess energy}}\, {\rm d}\nu,$$

$h\nu_i$: photoionization potential.

(*e.g.* Tielens, 2005)

In the ionized gas

- Most electrons coming from the photoionization $H^0 + \gamma \rightarrow H^+ + e^-$.

⇒ dominant heating process in H II.

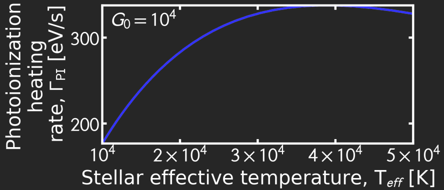

In the neutral gas

The heating rate due to the photoionization of specie *i*

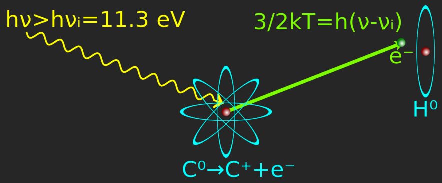

$$\Gamma^i_{\rm PI} = \int_{\nu_i}^{\infty} \underbrace{\frac{4\pi J_\nu(\nu)}{h\nu}}_{\text{photon rate}} \times \underbrace{\alpha_i(\nu)}_{\text{cross-section}} \times \underbrace{h(\nu-\nu_i)}_{\text{excess energy}} \,{\rm d}\nu,$$

$h\nu_i$: photoionization potential.

(*e.g.* Tielens, 2005)

In the ionized gas

- Most electrons coming from the photoionization $H^0 + \gamma \rightarrow H^+ + e^-$.

$\Rightarrow$ dominant heating process in H II.

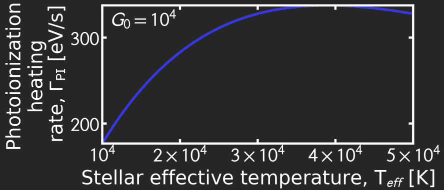

In the neutral gas

- Most electrons coming from photoionization $C^0 + \gamma \rightarrow C^+ + e^-$.

The heating rate due to the photoionization of specie *i*

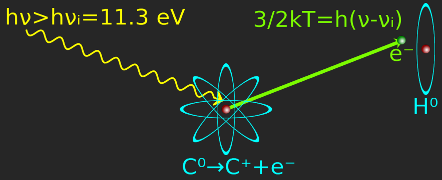

$$\Gamma_{\rm PI}^i = \int_{\nu_i}^{\infty} \underbrace{\frac{4\pi J_\nu(\nu)}{h\nu}}_{\text{photon rate}} \times \underbrace{\alpha_i(\nu)}_{\text{cross-section}} \times \underbrace{h(\nu-\nu_i)}_{\text{excess energy}} \, \mathrm{d}\nu,$$

$h\nu_i$: photoionization potential.

(*e.g.* Tielens, 2005)

In the ionized gas

- Most electrons coming from the photoionization $\mathrm{H}^0 + \gamma \rightarrow \mathrm{H}^+ + e^-$.

$\Rightarrow$ dominant heating process in H II.

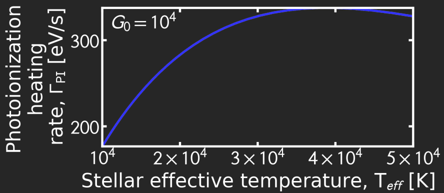

In the neutral gas

- Most electrons coming from photoionization $\mathrm{C}^0 + \gamma \rightarrow \mathrm{C}^+ + e^-$.
- At $Z \simeq Z_\odot$, $N(\mathrm{C})/N(\mathrm{H}) \simeq 1.6 \times 10^{-4}$.

The heating rate due to the photoionization of specie i

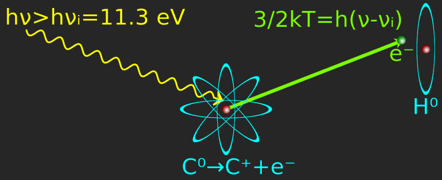

$$\Gamma_{\rm PI}^i = \int_{\nu_i}^{\infty} \underbrace{\frac{4\pi J_\nu(\nu)}{h\nu}}_{\text{photon rate}} \times \underbrace{\alpha_i(\nu)}_{\text{cross-section}} \times \underbrace{h(\nu-\nu_i)}_{\text{excess energy}} \,\mathrm{d}\nu,$$

$h\nu_i$: photoionization potential.

(*e.g.* Tielens, 2005)

In the ionized gas

- Most electrons coming from the photoionization $\mathrm{H}^0 + \gamma \rightarrow \mathrm{H}^+ + e^-$.

⇒ dominant heating process in H II.

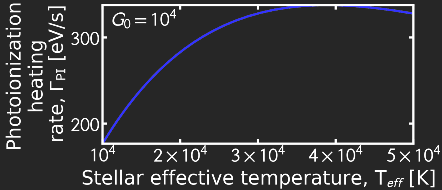

In the neutral gas

- Most electrons coming from photoionization $\mathrm{C}^0 + \gamma \rightarrow \mathrm{C}^+ + e^-$.
- At $Z \simeq Z_\odot$, $N(\mathrm{C})/N(\mathrm{H}) \simeq 1.6 \times 10^{-4}$.

⇒ secondary heating source in H I.

Cosmic-Ray (CR) heating

Cosmic-Ray (CR) heating

- Low-energy CRs (1–10 MeV) are the most numerous.

Cosmic-Ray (CR) heating

- Low-energy CRs (1–10 MeV) are the most numerous.
- They penetrate dense clouds where there are no UV photons.

Cosmic-Ray (CR) heating

- Low-energy CRs (1–10 MeV) are the most numerous.
- They penetrate dense clouds where there are no UV photons.
- CR rate: $\boxed{\zeta_{\rm CR} \simeq (0.5-3)\times 10^{-16}\ \rm s^{-1}}$.

Cosmic-Ray (CR) heating

- Low-energy CRs (1–10 MeV) are the most numerous.
- They penetrate dense clouds where there are no UV photons.
- CR rate: $\boxed{\zeta_{\rm CR} \simeq (0.5 - 3) \times 10^{-16}\ {\rm s}^{-1}}$.

$\rightarrow$ $\Gamma_{\rm CR} \simeq \zeta_{\rm CR} \times 10$ [eV/s].

Cosmic-Ray (CR) heating

- Low-energy CRs (1–10 MeV) are the most numerous.
- They penetrate dense clouds where there are no UV photons.
- CR rate: $\boxed{\zeta_{\text{CR}} \simeq (0.5 - 3) \times 10^{-16}\ \text{s}^{-1}}$.

$\longrightarrow$ $\Gamma_{\text{CR}} \simeq \zeta_{\text{CR}} \times 10$ [eV/s].

$\Rightarrow$ CRs are the most efficient heating source in dense molecular clouds.

Cosmic-Ray (CR) heating

- Low-energy CRs (1–10 MeV) are the most numerous.
- They penetrate dense clouds where there are no UV photons.
- CR rate: $\boxed{\zeta_{\rm CR} \simeq (0.5-3)\times 10^{-16}\ {\rm s}^{-1}}$.

→ $\Gamma_{\rm CR} \simeq \zeta_{\rm CR} \times 10$ [eV/s].

⇒ CRs are the most efficient heating source in dense molecular clouds.

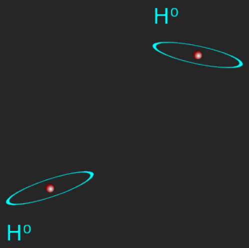

Cosmic-Ray (CR) heating

- Low-energy CRs (1–10 MeV) are the most numerous.
- They penetrate dense clouds where there are no UV photons.
- CR rate: $\boxed{\zeta_{\rm CR} \simeq (0.5 - 3) \times 10^{-16}\ {\rm s}^{-1}}$.

→ $\Gamma_{\rm CR} \simeq \zeta_{\rm CR} \times 10$ [eV/s].

⇒ CRs are the most efficient heating source in dense molecular clouds.

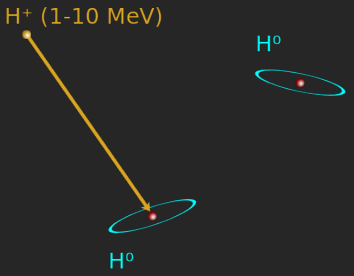

Cosmic-Ray (CR) heating

- Low-energy CRs (1–10 MeV) are the most numerous.
- They penetrate dense clouds where there are no UV photons.
- CR rate: $\boxed{\zeta_{\rm CR} \simeq (0.5 - 3) \times 10^{-16}\ {\rm s}^{-1}}$.

→ $\Gamma_{\rm CR} \simeq \zeta_{\rm CR} \times 10$ [eV/s].

⇒ CRs are the most efficient heating source in dense molecular clouds.

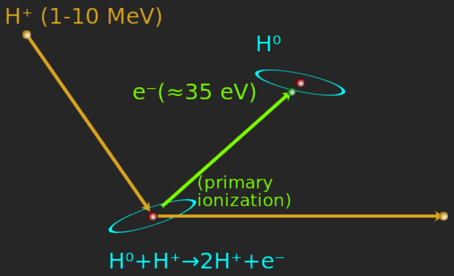

Cosmic-Ray (CR) heating

- Low-energy CRs (1–10 MeV) are the most numerous.
- They penetrate dense clouds where there are no UV photons.
- CR rate: $\boxed{\zeta_{\text{CR}} \simeq (0.5-3)\times10^{-16}\ \text{s}^{-1}}$.

→ $\Gamma_{\text{CR}} \simeq \zeta_{\text{CR}} \times 10$ [eV/s].

⇒ CRs are the most efficient heating source in dense molecular clouds.

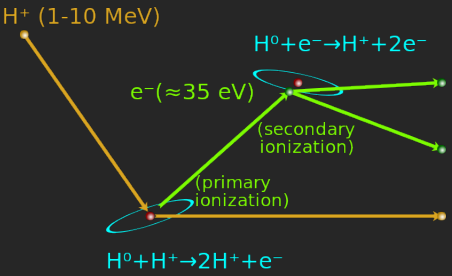

Cosmic-Ray (CR) heating

- Low-energy CRs (1–10 MeV) are the most numerous.
- They penetrate dense clouds where there are no UV photons.
- CR rate: $\boxed{\zeta_{\text{CR}} \simeq (0.5 - 3) \times 10^{-16}\ \text{s}^{-1}}$.

$\rightarrow$ $\Gamma_{\text{CR}} \simeq \zeta_{\text{CR}} \times 10$ [eV/s].

$\Rightarrow$ CRs are the most efficient heating source in dense molecular clouds.

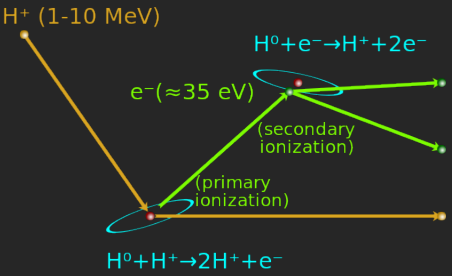

X-ray heating

Cosmic-Ray (CR) heating

- Low-energy CRs (1–10 MeV) are the most numerous.
- They penetrate dense clouds where there are no UV photons.
- CR rate: $\zeta_{CR} \simeq (0.5 - 3) \times 10^{-16}\ s^{-1}$.

→ $\Gamma_{CR} \simeq \zeta_{CR} \times 10$ [eV/s].

⇒ CRs are the most efficient heating source in dense molecular clouds.

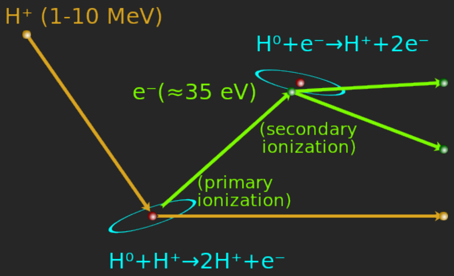

X-ray heating

- Similar interaction as cosmic rays but with lower energy.

Cosmic-Ray (CR) heating

- Low-energy CRs (1–10 MeV) are the most numerous.
- They penetrate dense clouds where there are no UV photons.
- CR rate: $\zeta_{\rm CR} \simeq (0.5-3)\times10^{-16}\ {\rm s}^{-1}$.

→ $\Gamma_{\rm CR} \simeq \zeta_{\rm CR} \times 10$ [eV/s].

⇒ CRs are the most efficient heating source in dense molecular clouds.

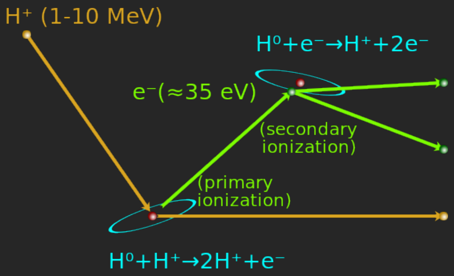

X-ray heating

- Similar interaction as cosmic rays but with lower energy.
- X-rays penetrate less deeply into clouds:

Cosmic-Ray (CR) heating

- Low-energy CRs (1–10 MeV) are the most numerous.
- They penetrate dense clouds where there are no UV photons.
- CR rate: $\zeta_{CR} \simeq (0.5 - 3) \times 10^{-16}\ \mathrm{s}^{-1}$.

→ $\Gamma_{CR} \simeq \zeta_{CR} \times 10$ [eV/s].

⇒ CRs are the most efficient heating source in dense molecular clouds.

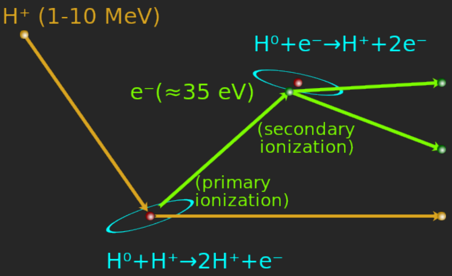

X-ray heating

- Similar interaction as cosmic rays but with lower energy.
- X-rays penetrate less deeply into clouds:
  Near bright X-ray sources: (binary, AGNs, *etc.*) → only regions where it dominates.

Cosmic-Ray (CR) heating

- Low-energy CRs (1–10 MeV) are the most numerous.
- They penetrate dense clouds where there are no UV photons.
- CR rate: $\boxed{\zeta_{CR} \simeq (0.5-3)\times 10^{-16}\ \text{s}^{-1}}$.

→ $\Gamma_{CR} \simeq \zeta_{CR} \times 10$ [eV/s].

⇒ CRs are the most efficient heating source in dense molecular clouds.

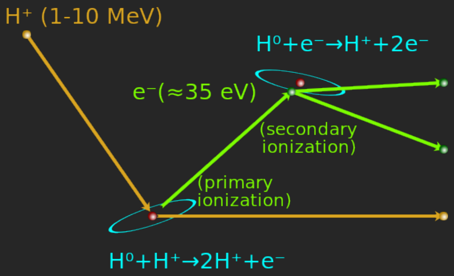

X-ray heating

- Similar interaction as cosmic rays but with lower energy.
- X-rays penetrate less deeply into clouds:

Near bright X-ray sources: (binary, AGNs, *etc.*) → only regions where it dominates.
Diffuse X-ray background: $\Gamma_{XR} \simeq 10^{-33}$ [W/H].

Cosmic-Ray (CR) heating

- Low-energy CRs (1–10 MeV) are the most numerous.
- They penetrate dense clouds where there are no UV photons.
- CR rate: $\boxed{\zeta_{CR} \simeq (0.5-3) \times 10^{-16}\ \text{s}^{-1}}$.

$\rightarrow$ $\Gamma_{CR} \simeq \zeta_{CR} \times 10$ [eV/s].

$\Rightarrow$ CRs are the most efficient heating source in dense molecular clouds.

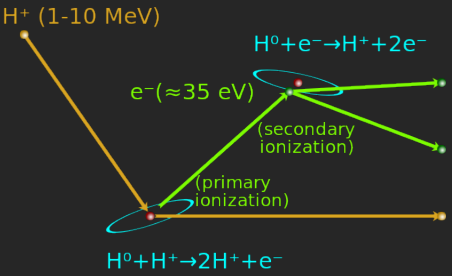

X-ray heating

- Similar interaction as cosmic rays but with lower energy.
- X-rays penetrate less deeply into clouds:

Near bright X-ray sources: (binary, AGNs, *etc.*) $\rightarrow$ only regions where it dominates.
Diffuse X-ray background: $\Gamma_{XR} \simeq 10^{-33}$ [W/H].

Shock Heating

Cosmic-Ray (CR) heating

- Low-energy CRs (1–10 MeV) are the most numerous.
- They penetrate dense clouds where there are no UV photons.
- CR rate: $\boxed{\zeta_{\rm CR} \simeq (0.5-3)\times 10^{-16}\ {\rm s}^{-1}}$.

→ $\Gamma_{\rm CR} \simeq \zeta_{\rm CR} \times 10$ [eV/s].

⇒ CRs are the most efficient heating source in dense molecular clouds.

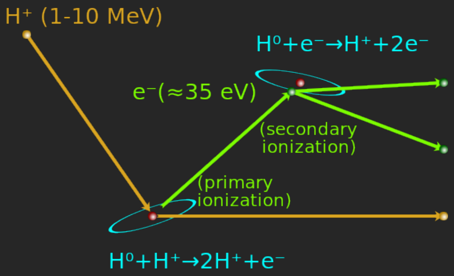

X-ray heating

- Similar interaction as cosmic rays but with lower energy.
- X-rays penetrate less deeply into clouds:

Near bright X-ray sources: (binary, AGNs, *etc.*) → only regions where it dominates.
Diffuse X-ray background: $\Gamma_{\rm XR} \simeq 10^{-33}$ [W/H].

Shock Heating

- $\Gamma_{\rm shock} \simeq 1/2 m_{\rm H} v_{\rm shock}^2 \times R_{\rm SN} \times f_{\rm V}$, w/ $v_{\rm shock} \simeq 300$ km/s, $R_{\rm SN} \simeq 1/(100\ {\rm year})$ & $f_{\rm V} \simeq 2\times 10^{-7}$.

Cosmic-Ray (CR) heating

- Low-energy CRs (1–10 MeV) are the most numerous.
- They penetrate dense clouds where there are no UV photons.
- CR rate: $\boxed{\zeta_{\rm CR} \simeq (0.5-3)\times 10^{-16}\ {\rm s}^{-1}}$.

$\rightarrow$ $\Gamma_{\rm CR} \simeq \zeta_{\rm CR} \times 10$ [eV/s].

$\Rightarrow$ CRs are the most efficient heating source in dense molecular clouds.

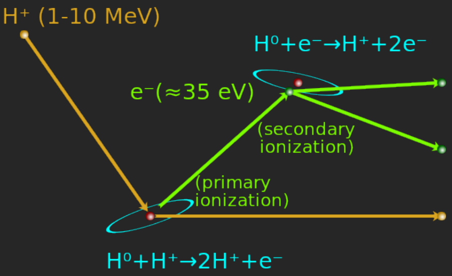

X-ray heating

- Similar interaction as cosmic rays but with lower energy.
- X-rays penetrate less deeply into clouds:

  Near bright X-ray sources: (binary, AGNs, *etc.*) $\rightarrow$ only regions where it dominates.
  Diffuse X-ray background: $\Gamma_{\rm XR} \simeq 10^{-33}$ [W/H].

Shock Heating

- $\Gamma_{\rm shock} \simeq 1/2 m_{\rm H} v_{\rm shock}^2 \times R_{\rm SN} \times f_V$, w/ $v_{\rm shock} \simeq 300$ km/s, $R_{\rm SN} \simeq 1/(100\ \text{year})$ & $f_V \simeq 2\times 10^{-7}$.

$\Rightarrow$ dominant heating process in the hot, intercloud, coronal gas.

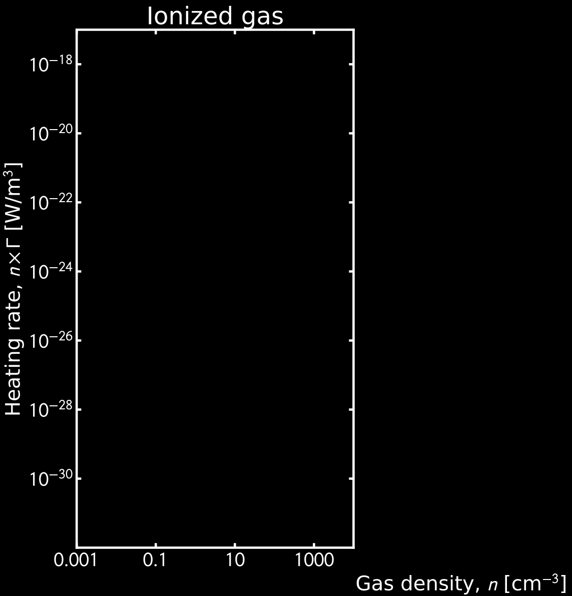
Ionized gas
Heating rate, n×Γ [W/m3]
10−18
10−20
10−22
10−24
10−26
10−28
10−30
0.001
0.1
10
1000
Gas density, n [cm−3]

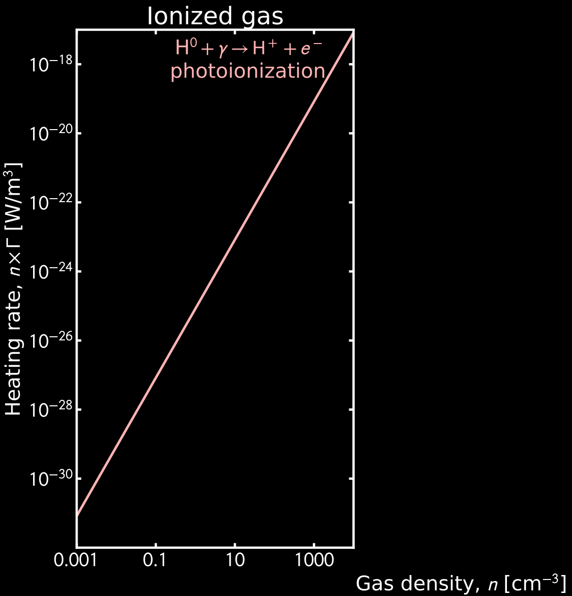
Ionized gas
$H^0 + \gamma \rightarrow H^+ + e^-$
photoionization
Heating rate, $n \times \Gamma$ [W/m^3]
10^{-18}
10^{-20}
10^{-22}
10^{-24}
10^{-26}
10^{-28}
10^{-30}
0.001
0.1
10
1000
Gas density, n [cm^{-3}]

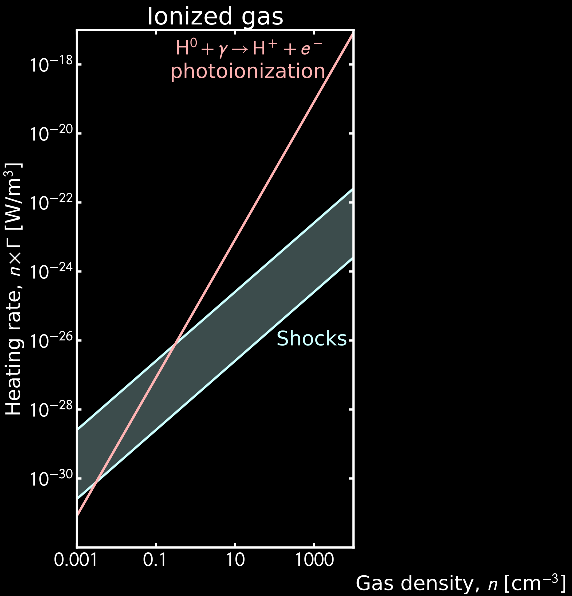

Ionized gas
H^0 + γ → H^+ + e^−
photoionization
Shocks
10^−18
10^−20
10^−22
10^−24
10^−26
10^−28
10^−30
Heating rate, n×Γ [W/m^3]
0.001
0.1
10
1000
Gas density, n [cm^−3]

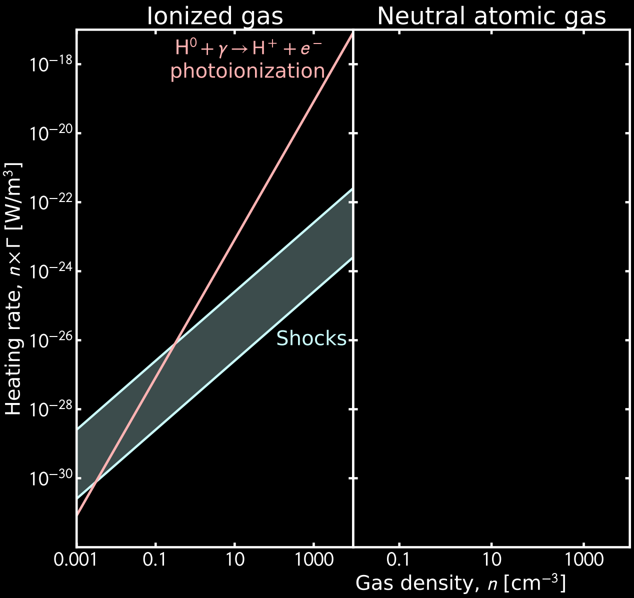
Ionized gas
Neutral atomic gas
$H^0 + \gamma \rightarrow H^+ + e^-$
photoionization
Shocks
Heating rate, $n \times \Gamma$ [W/m^3]
10^{-18}
10^{-20}
10^{-22}
10^{-24}
10^{-26}
10^{-28}
10^{-30}
0.001
0.1
10
1000
Gas density, n [cm^{-3}]

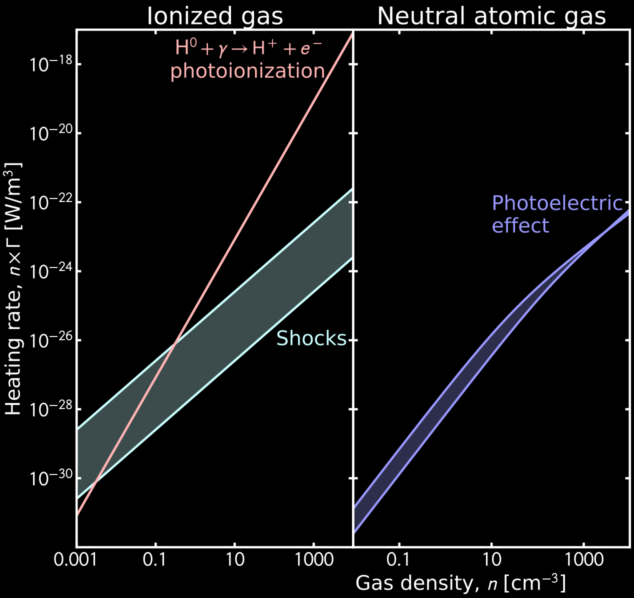
Ionized gas
Neutral atomic gas
$H^0 + \gamma \rightarrow H^+ + e^-$
photoionization
Shocks
Photoelectric
effect
Heating rate, $n \times \Gamma$ [W/m^3]
Gas density, n [cm^{-3}]
10^{-18}
10^{-20}
10^{-22}
10^{-24}
10^{-26}
10^{-28}
10^{-30}
0.001
0.1
10
1000

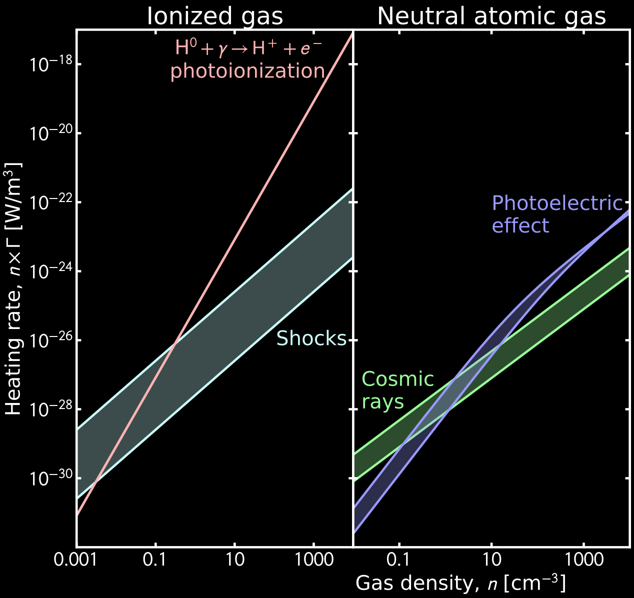
Ionized gas
Neutral atomic gas
$H^0 + \gamma \rightarrow H^+ + e^-$
photoionization
Shocks
Photoelectric
effect
Cosmic
rays
Heating rate, $n \times \Gamma$ [W/m^3]
10^{-18}
10^{-20}
10^{-22}
10^{-24}
10^{-26}
10^{-28}
10^{-30}
0.001
0.1
10
1000
0.1
10
1000
Gas density, n [cm^{-3}]

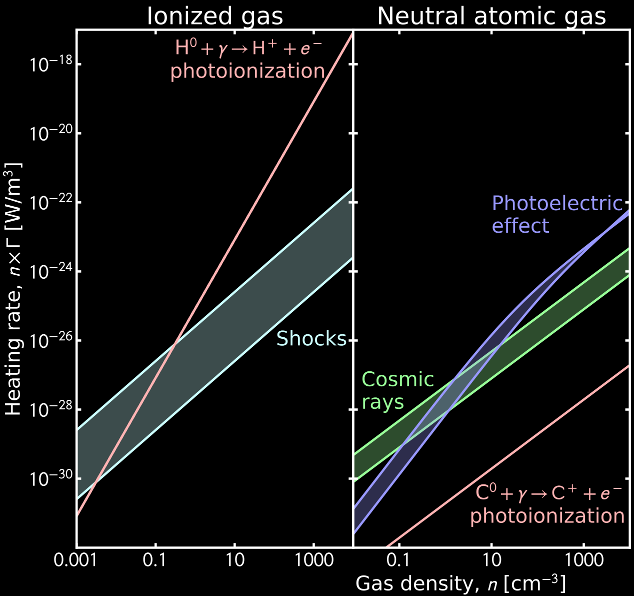
Ionized gas
Neutral atomic gas
$H^0 + \gamma \rightarrow H^+ + e^-$
photoionization
Shocks
Photoelectric
effect
Cosmic
rays
$C^0 + \gamma \rightarrow C^+ + e^-$
photoionization
Heating rate, $n \times \Gamma$ [W/m^3]
10^{-18}
10^{-20}
10^{-22}
10^{-24}
10^{-26}
10^{-28}
10^{-30}
0.001
0.1
10
1000
Gas density, n [cm^{-3}]

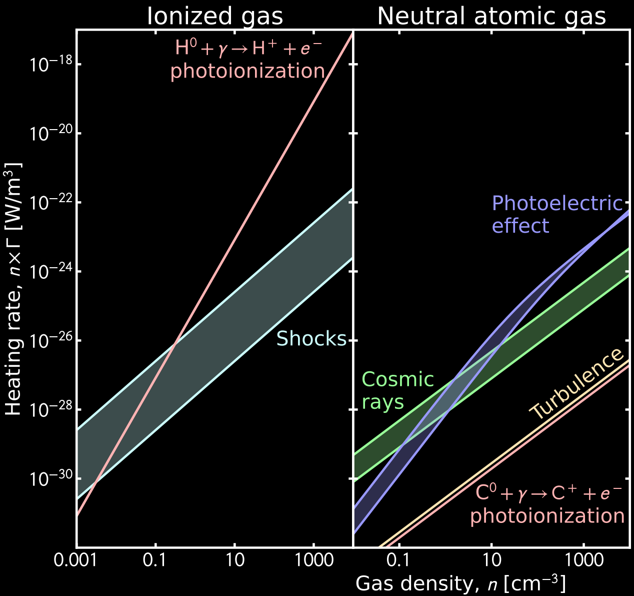
Ionized gas
Neutral atomic gas
$H^0 + \gamma \rightarrow H^+ + e^-$
photoionization
Shocks
Photoelectric
effect
Cosmic
rays
Turbulence
$C^0 + \gamma \rightarrow C^+ + e^-$
photoionization
Heating rate, $n \times \Gamma$ [W/m^3]
10^{-18}
10^{-20}
10^{-22}
10^{-24}
10^{-26}
10^{-28}
10^{-30}
0.001
0.1
10
1000
Gas density, n [cm^{-3}]

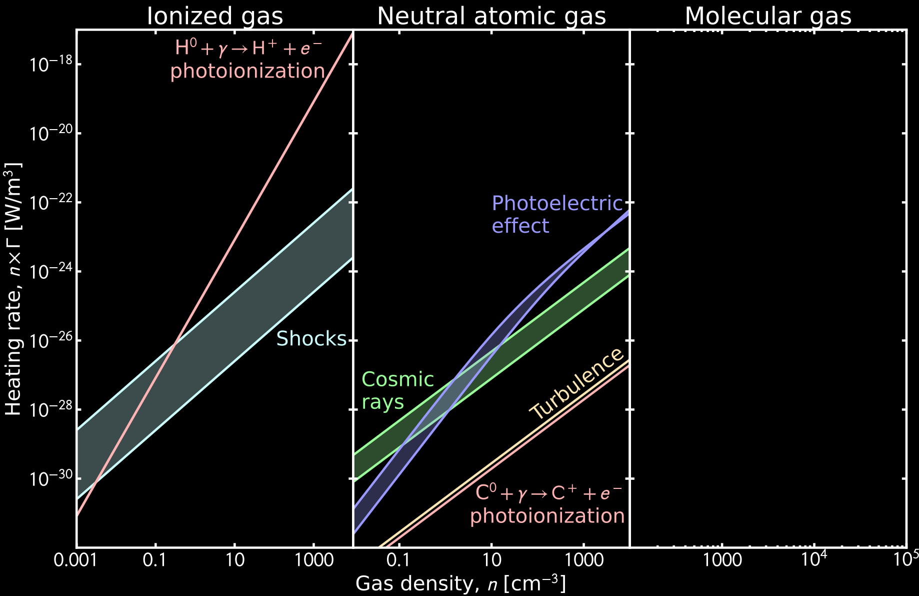
Ionized gas
Neutral atomic gas
Molecular gas
$H^0 + \gamma \rightarrow H^+ + e^-$
photoionization
Shocks
Photoelectric effect
Cosmic rays
Turbulence
$C^0 + \gamma \rightarrow C^+ + e^-$
photoionization
Heating rate, $n \times \Gamma$ [W/m^3]
10^{-18}
10^{-20}
10^{-22}
10^{-24}
10^{-26}
10^{-28}
10^{-30}
0.001
0.1
10
1000
0.1
10
1000
1000
10^4
10^5
Gas density, n [cm^{-3}]

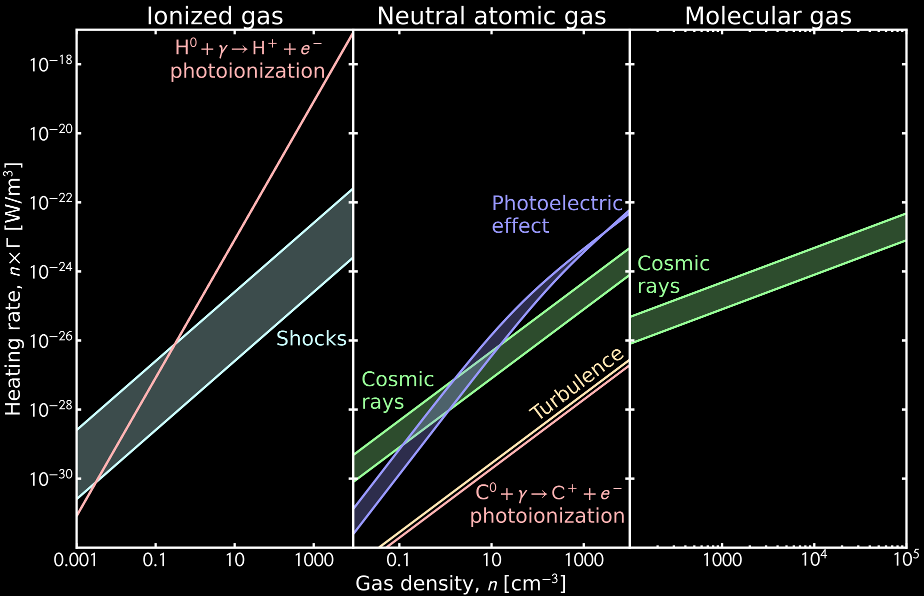
Ionized gas
Neutral atomic gas
Molecular gas
$H^0 + \gamma \rightarrow H^+ + e^-$
photoionization
Shocks
Photoelectric
effect
Cosmic
rays
Turbulence
$C^0 + \gamma \rightarrow C^+ + e^-$
photoionization
Cosmic
rays
Heating rate, $n \times \Gamma$ [W/m^3]
10^{-18}
10^{-20}
10^{-22}
10^{-24}
10^{-26}
10^{-28}
10^{-30}
0.001
0.1
10
1000
0.1
10
1000
1000
10^4
10^5
Gas density, n [cm^{-3}]

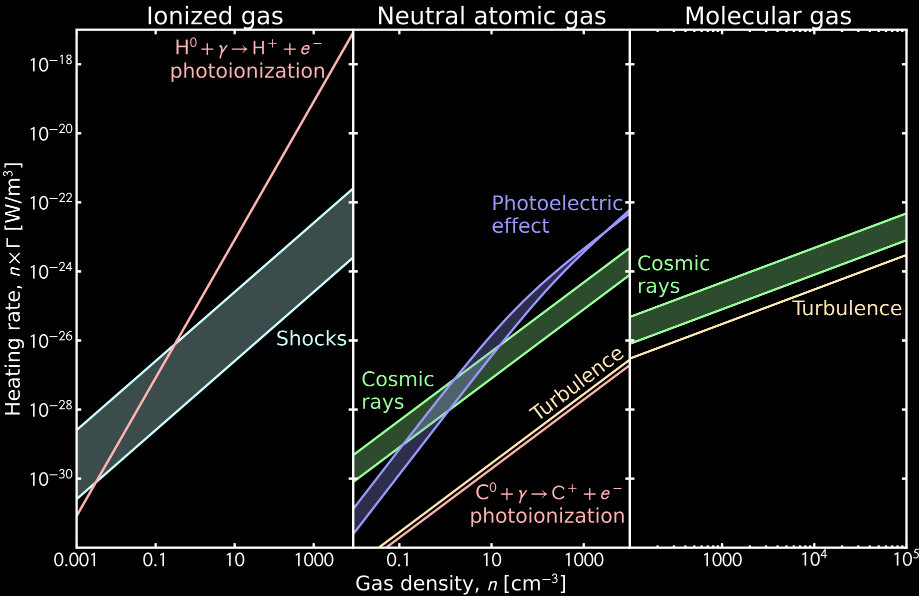
Ionized gas
Neutral atomic gas
Molecular gas
H^0 + γ → H$^+$ + e^-
photoionization
Shocks
Photoelectric
effect
Cosmic
rays
Turbulence
C^0 + γ → C$^+$ + e^-
photoionization
Cosmic
rays
Turbulence
Heating rate, $n \times \Gamma$ [W/m^3]
10^{-18}
10^{-20}
10^{-22}
10^{-24}
10^{-26}
10^{-28}
10^{-30}
0.001
0.1
10
1000
0.1
10
1000
1000
10^4
10^5
Gas density, n [cm^{-3}]

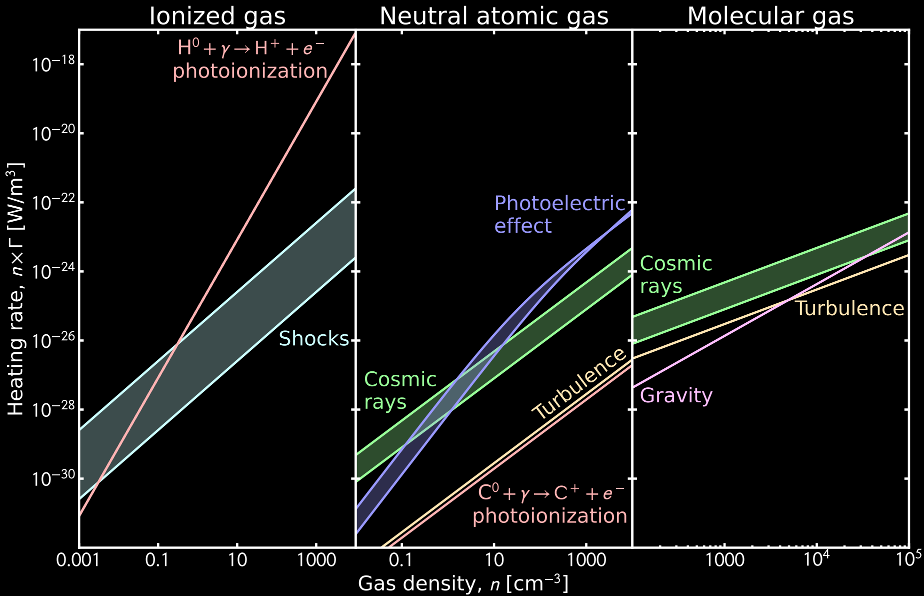

Ionized gas
Neutral atomic gas
Molecular gas
$H^0 + \gamma \rightarrow H^+ + e^-$ photoionization
Shocks
Photoelectric effect
Cosmic rays
Turbulence
$C^0 + \gamma \rightarrow C^+ + e^-$ photoionization
Cosmic rays
Turbulence
Gravity
Heating rate, $n \times \Gamma$ [W/m^3]
10^{-18}
10^{-20}
10^{-22}
10^{-24}
10^{-26}
10^{-28}
10^{-30}
Gas density, n [cm^{-3}]
0.001
0.1
10
1000
0.1
10
1000
1000
10^4
10^5

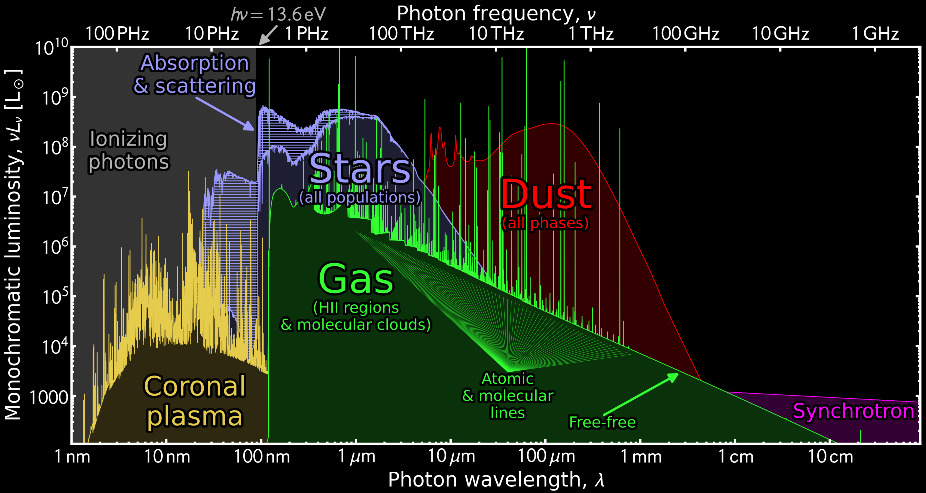

Photon frequency, ν
hν = 13.6 eV
100 PHz
10 PHz
1 PHz
100 THz
10 THz
1 THz
100 GHz
10 GHz
1 GHz
Monochromatic luminosity, νLν [L⊙]
10^10
10^9
10^8
10^7
10^6
10^5
10^4
1000
Absorption & scattering
Ionizing photons
Stars (all populations)
Dust (all phases)
Gas (HII regions & molecular clouds)
Coronal plasma
Atomic & molecular lines
Free-free
Synchrotron
1 nm
10 nm
100 nm
1 μm
10 μm
100 μm
1 mm
1 cm
10 cm
Photon wavelength, λ

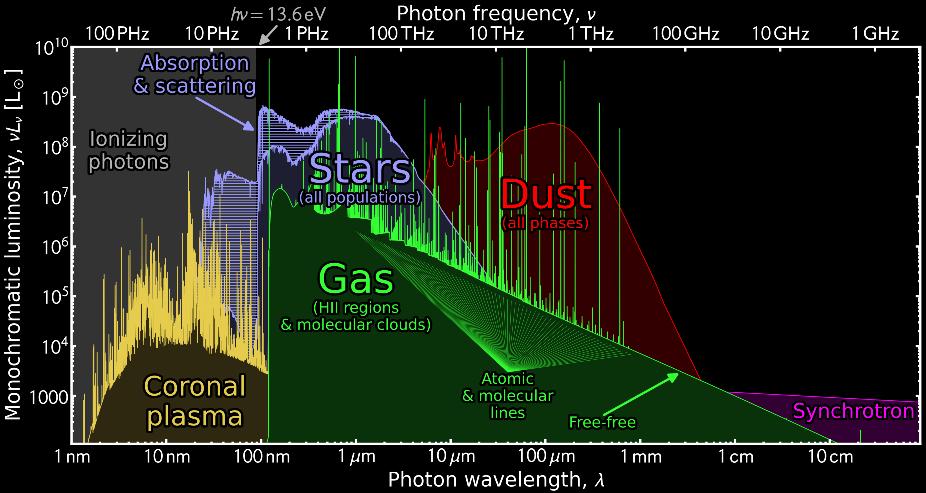

- Gas & dust are not thermalized (*e.g.* $T_{\rm gas}(\rm WNM) \simeq 10^4$ K *vs.* $T_{\rm dust}(\rm WNM) \simeq 18$ K).

Thermal Phases | Dust Cooling & Total ISM Cooling

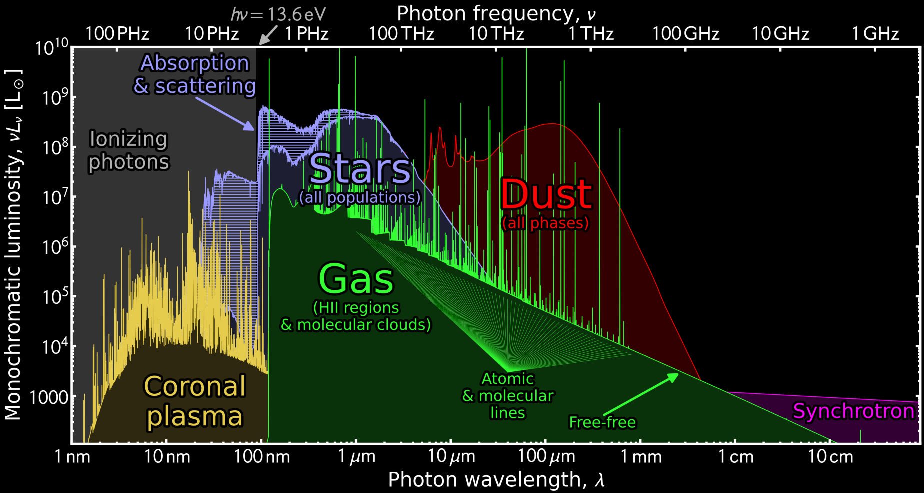

- Gas & dust are not thermalized (*e.g.* $T_{\text{gas}}(\text{WNM}) \simeq 10^4$ K *vs.* $T_{\text{dust}}(\text{WNM}) \simeq 18$ K).
- Dust dominates the energetic balance of the ISM: $L^{\text{cool}}_{\text{dust}} = L^{\text{abs}}_{\text{dust}} \simeq 30\,\%\ L_\star \Rightarrow L^{\text{cool}}_{\text{gas}} \simeq 1\,\%\ L^{\text{cool}}_{\text{dust}}$.

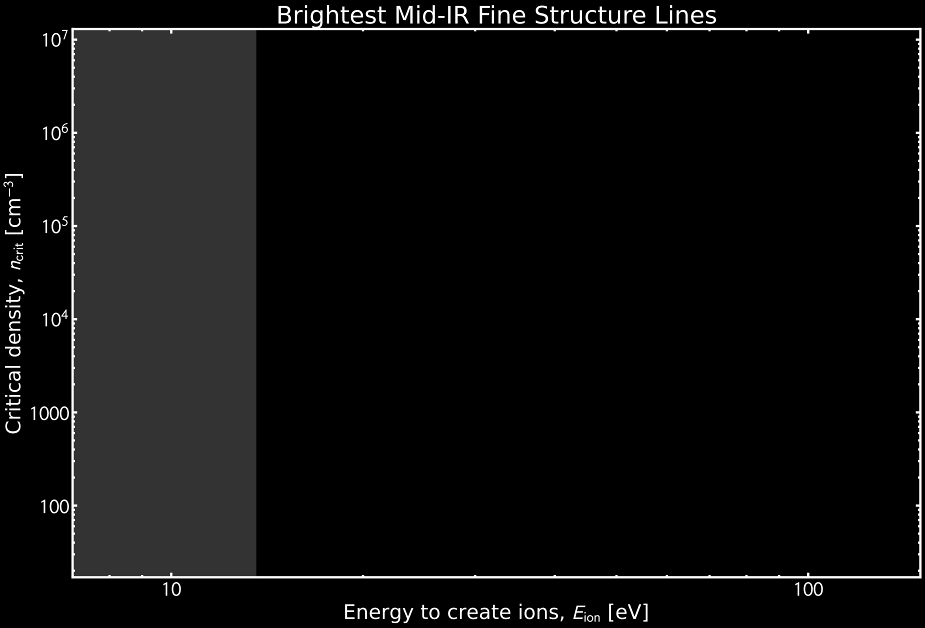
Brightest Mid-IR Fine Structure Lines
Critical density, n_{crit} [cm^{-3}]
10^7
10^6
10^5
10^4
1000
100
10
100
Energy to create ions, E_{ion} [eV]

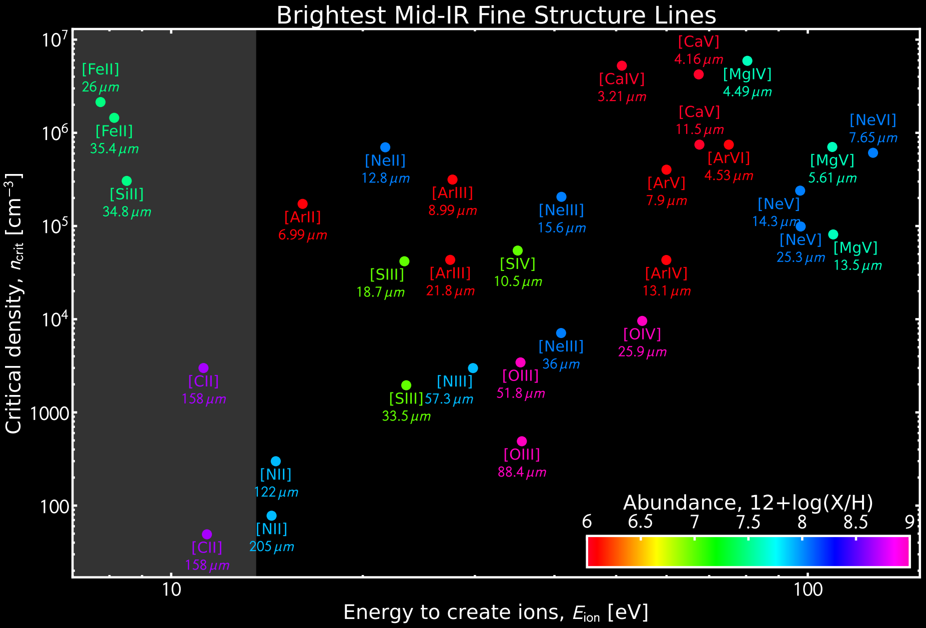
Brightest Mid-IR Fine Structure Lines
Critical density, n_{crit} [cm^{-3}]
Energy to create ions, E_{ion} [eV]
[FeII] 26 μm
[FeII] 35.4 μm
[SiII] 34.8 μm
[CII] 158 μm
[CII] 158 μm
[NII] 122 μm
[NII] 205 μm
[ArII] 6.99 μm
[NeII] 12.8 μm
[SIII] 18.7 μm
[SIII] 33.5 μm
[ArIII] 8.99 μm
[ArIII] 21.8 μm
[NIII] 57.3 μm
[SIV] 10.5 μm
[OIII] 51.8 μm
[OIII] 88.4 μm
[NeIII] 15.6 μm
[NeIII] 36 μm
[CaIV] 3.21 μm
[OIV] 25.9 μm
[CaV] 4.16 μm
[CaV] 11.5 μm
[ArV] 7.9 μm
[ArIV] 13.1 μm
[ArVI] 4.53 μm
[MgIV] 4.49 μm
[MgV] 5.61 μm
[MgV] 13.5 μm
[NeV] 14.3 μm
[NeV] 25.3 μm
[NeVI] 7.65 μm
Abundance, 12+log(X/H)
6 6.5 7 7.5 8 8.5 9

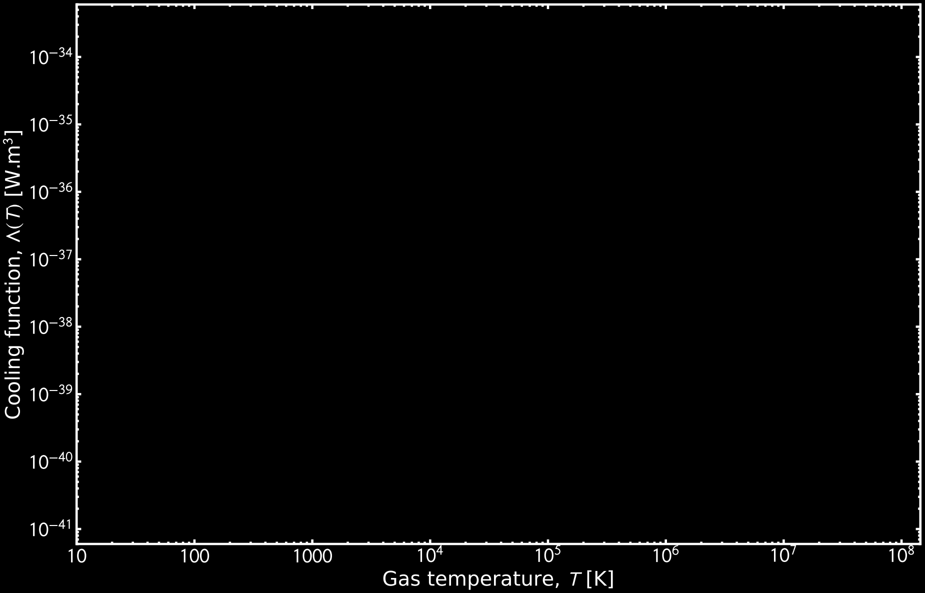

10^{-34}
10^{-35}
10^{-36}
10^{-37}
10^{-38}
10^{-39}
10^{-40}
10^{-41}
Cooling function, $\Lambda(T)$ [W.m^3]
10
100
1000
10^4
10^5
10^6
10^7
10^8
Gas temperature, T [K]

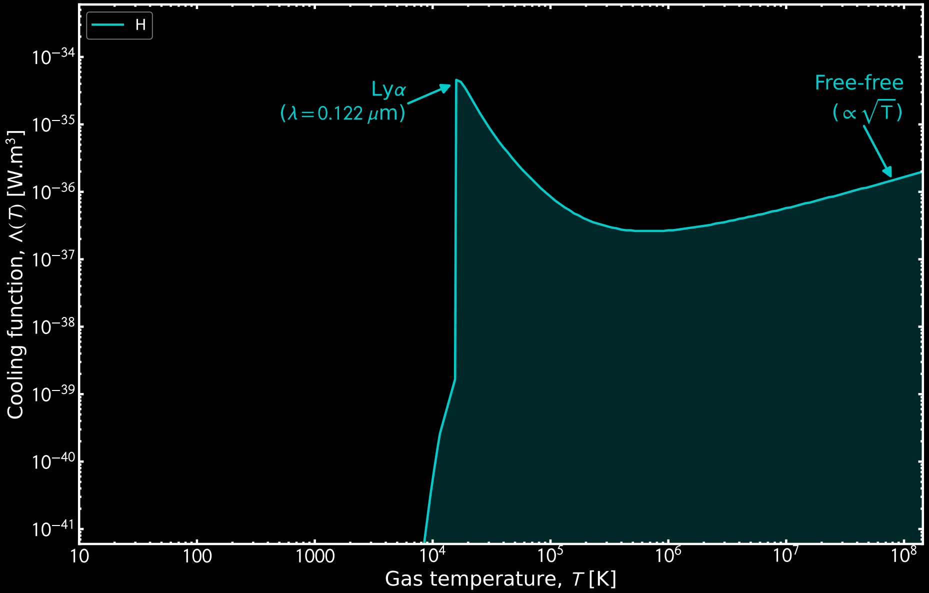

(Dalgarno & McCray, 1972; Schure et al., 2009; Wolfire et al., 1995, 2022)

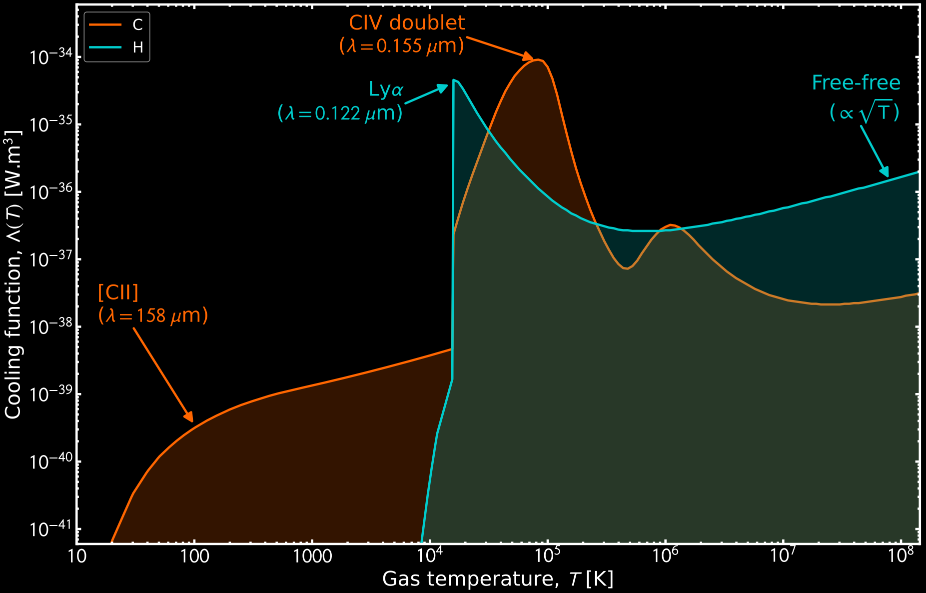

(Dalgarno & McCray, 1972; Schure et al., 2009; Wolfire et al., 1995, 2022)

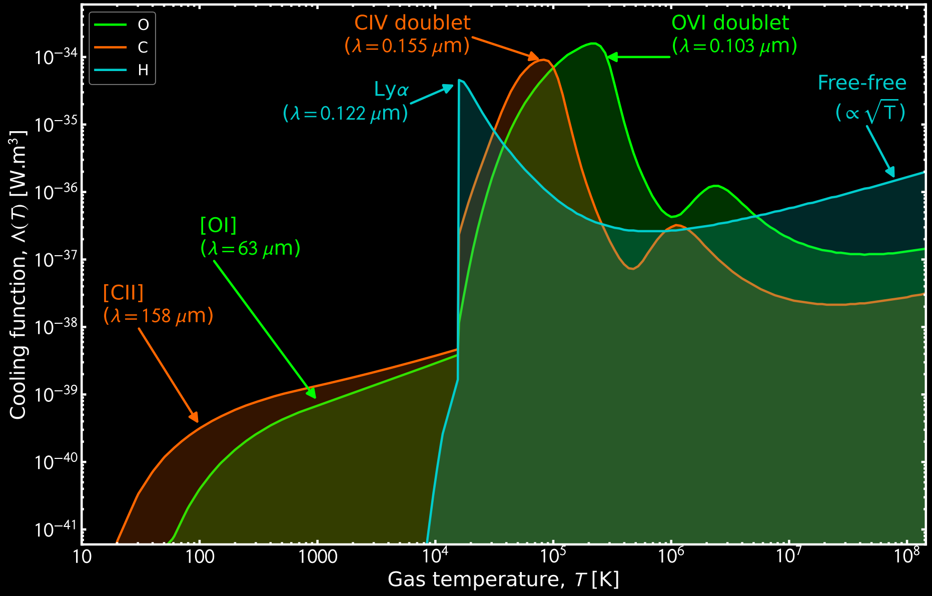

(Dalgarno & McCray, 1972; Schure et al., 2009; Wolfire et al., 1995, 2022)

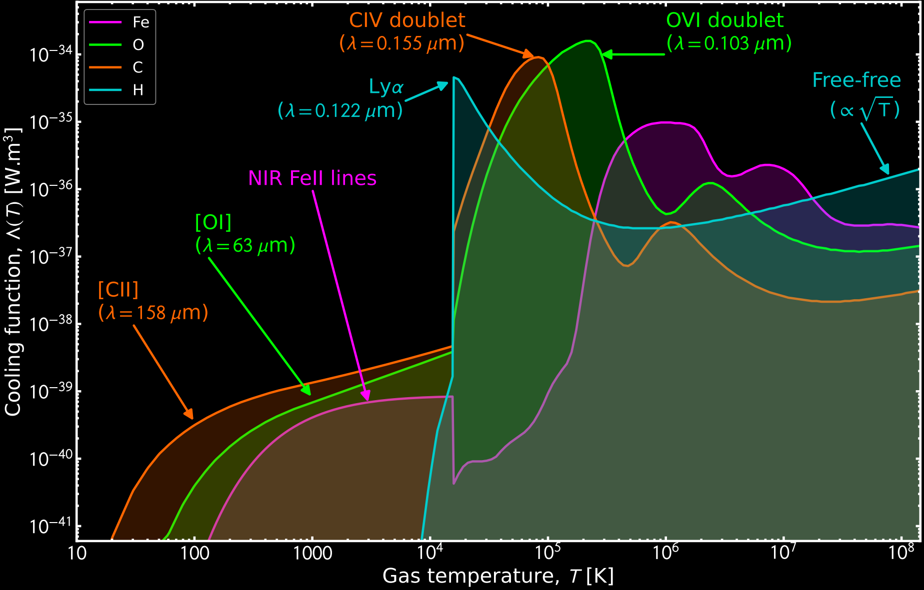

(Dalgarno & McCray, 1972; Schure et al., 2009; Wolfire et al., 1995, 2022)

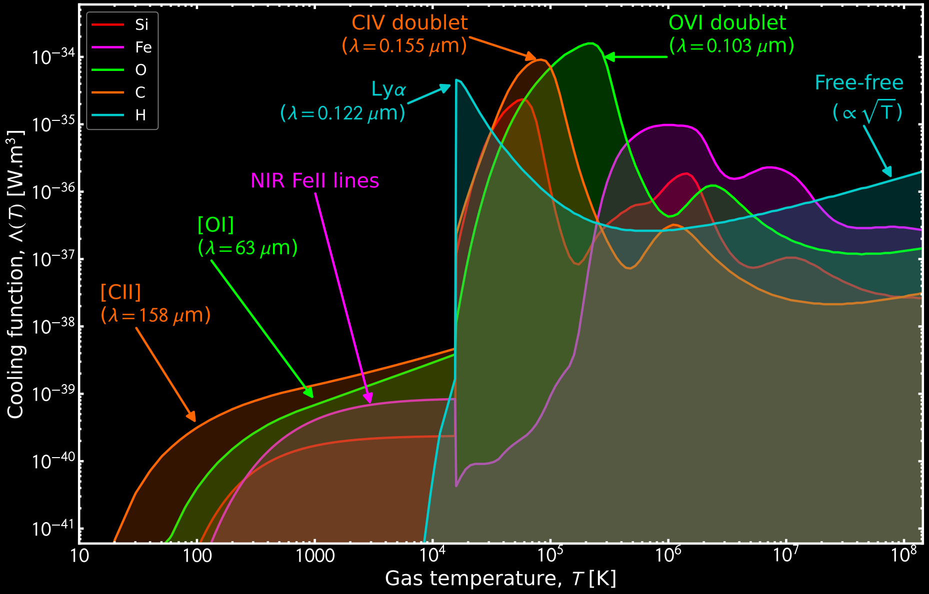

(Dalgarno & McCray, 1972; Schure et al., 2009; Wolfire et al., 1995, 2022)

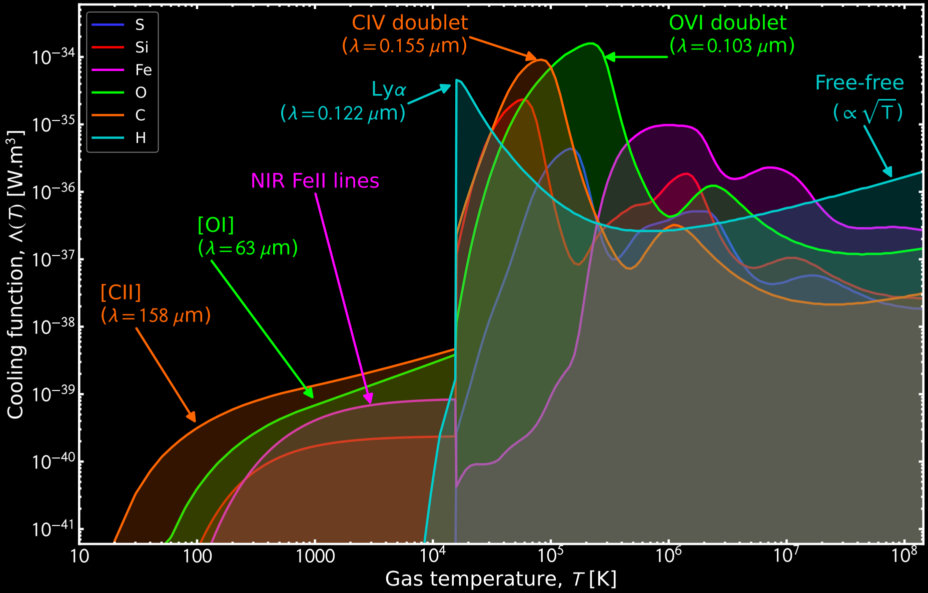

(Dalgarno & McCray, 1972; Schure et al., 2009; Wolfire et al., 1995, 2022)

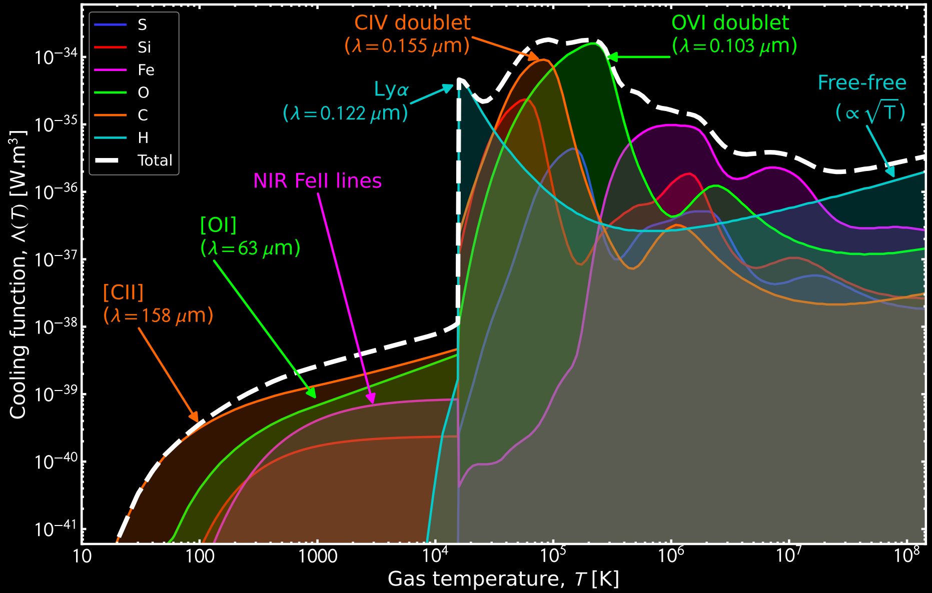

(Dalgarno & McCray, 1972; Schure et al., 2009; Wolfire et al., 1995, 2022)

Thermal balance: $n \times \Gamma = n^2 \times \Lambda(T)$

Thermal balance: $n \times \Gamma = n^2 \times \Lambda(T) \Rightarrow \frac{P}{k} = \frac{T \times \Gamma}{\Lambda(T)}$.

Thermal balance: $n \times \Gamma = n^2 \times \Lambda(T) \Rightarrow \frac{P}{k} = \frac{T \times \Gamma}{\Lambda(T)}$. **In the ISM:** $P/k \simeq 3000\ \mathrm{K.cm^{-3}}$.

Thermal balance: $n \times \Gamma = n^2 \times \Lambda(T) \Rightarrow \frac{P}{k} = \frac{T \times \Gamma}{\Lambda(T)}$. **In the ISM:** $P/k \simeq 3000\ \mathrm{K.cm^{-3}}$.

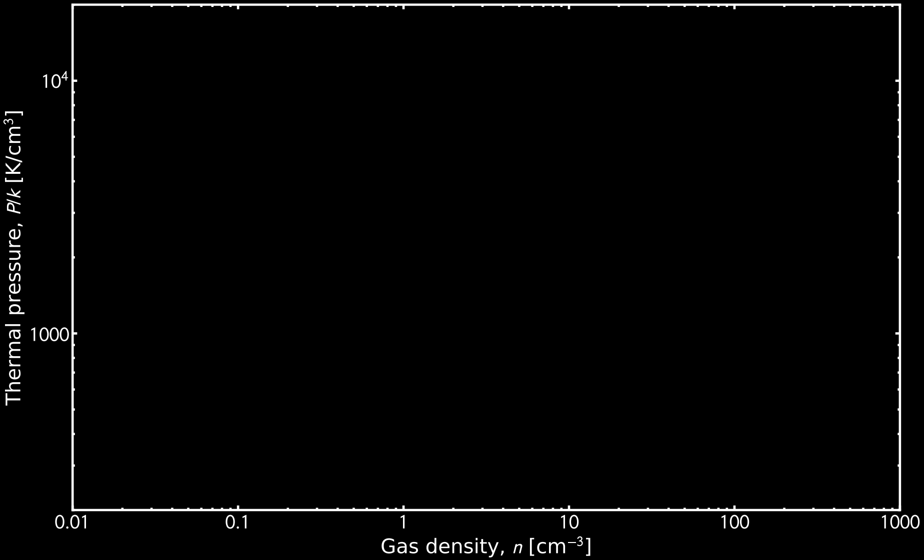

Thermal balance: $n \times \Gamma = n^2 \times \Lambda(T) \Rightarrow \dfrac{P}{k} = \dfrac{T \times \Gamma}{\Lambda(T)}$. **In the ISM:** $P/k \simeq 3000$ K.cm^{-3}.

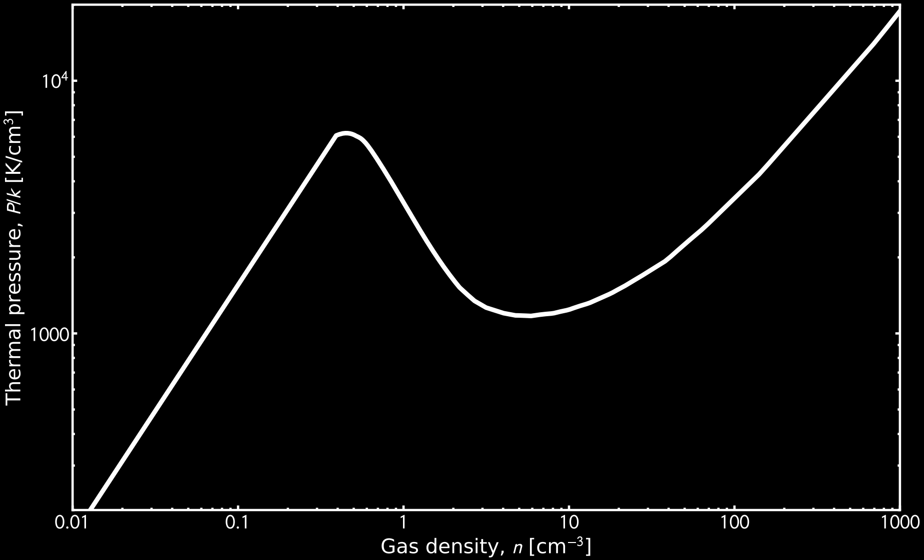

Thermal balance: $n \times \Gamma = n^2 \times \Lambda(T) \Rightarrow \frac{P}{k} = \frac{T \times \Gamma}{\Lambda(T)}$. **In the ISM:** $P/k \simeq 3000$ K.cm^{-3}.

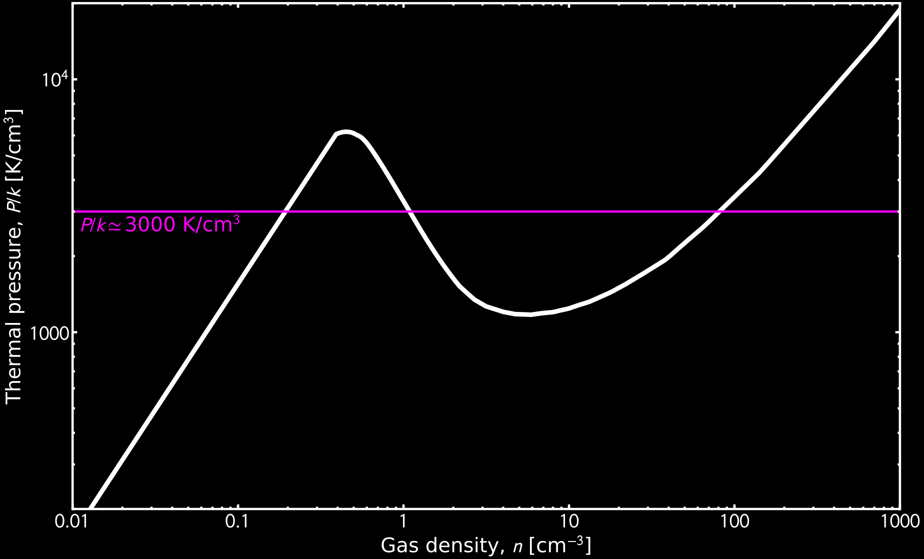

Thermal balance: $n \times \Gamma = n^2 \times \Lambda(T) \Rightarrow \frac{P}{k} = \frac{T \times \Gamma}{\Lambda(T)}$. **In the ISM:** $P/k \simeq 3000$ K.cm^{-3}.

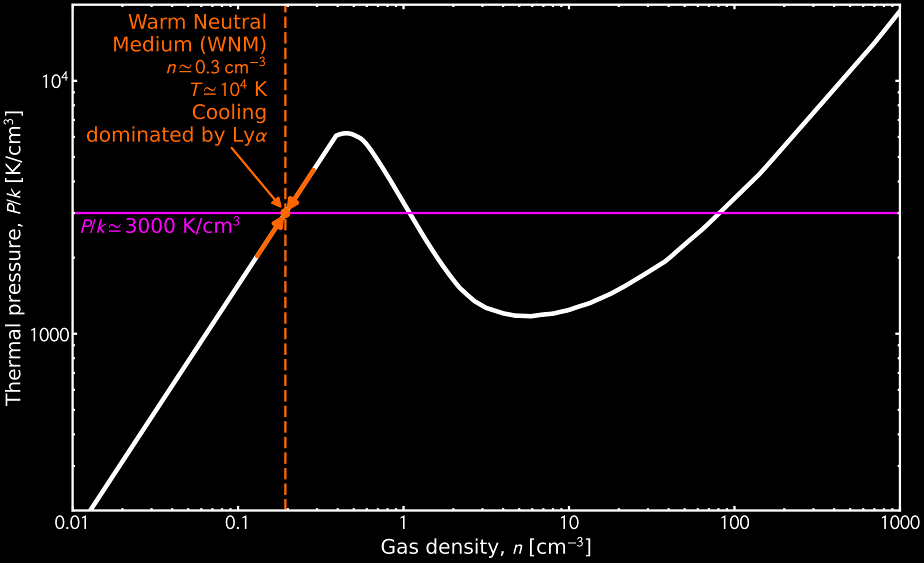

Thermal balance: $n \times \Gamma = n^2 \times \Lambda(T) \Rightarrow \frac{P}{k} = \frac{T \times \Gamma}{\Lambda(T)}$. **In the ISM:** $P/k \simeq 3000$ K.cm^{-3}.

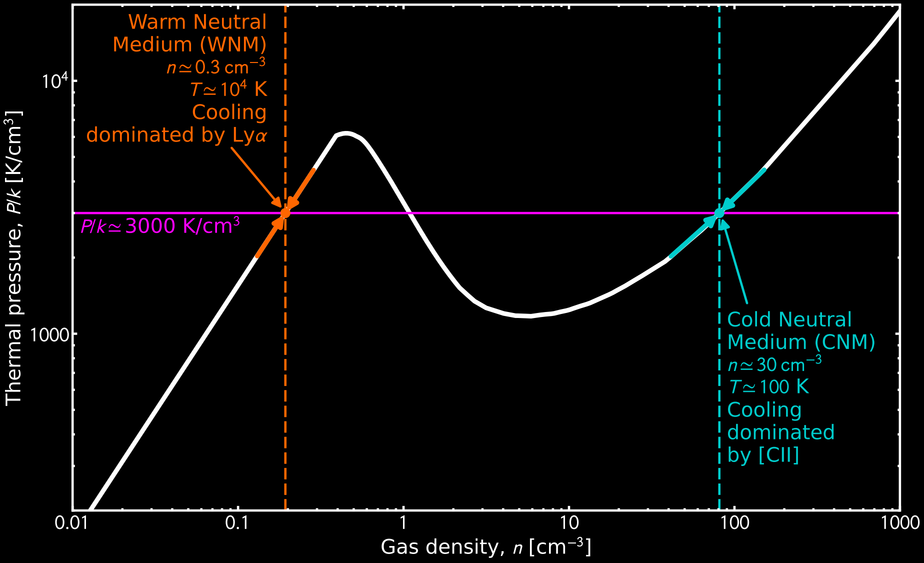

Thermal balance: $n \times \Gamma = n^2 \times \Lambda(T) \Rightarrow \frac{P}{k} = \frac{T \times \Gamma}{\Lambda(T)}$. **In the ISM:** $P/k \simeq 3000$ K.cm^{-3}.

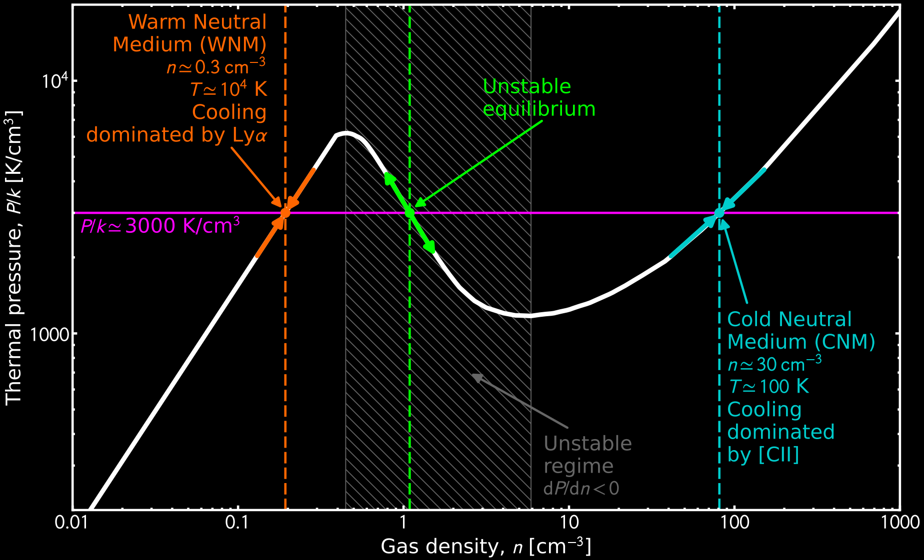

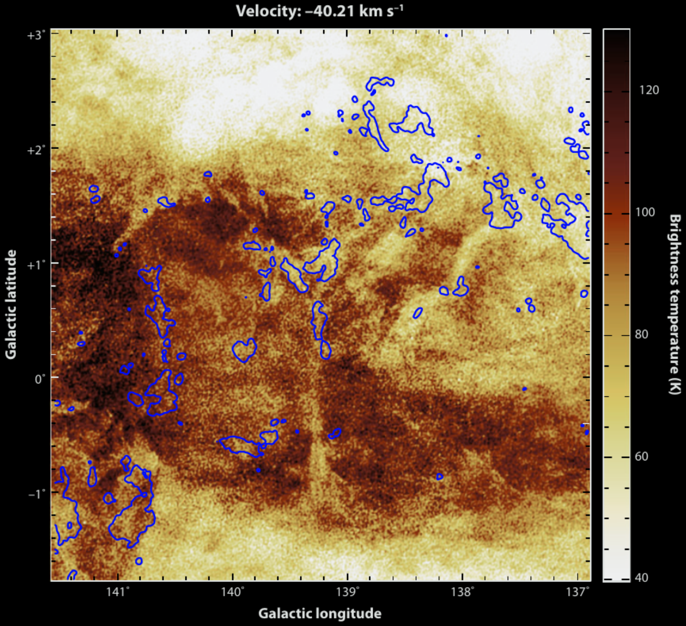

([H I]$_{21\,\mathrm{cm}}$ emission with CO contours; Kalberla & Kerp 2009)

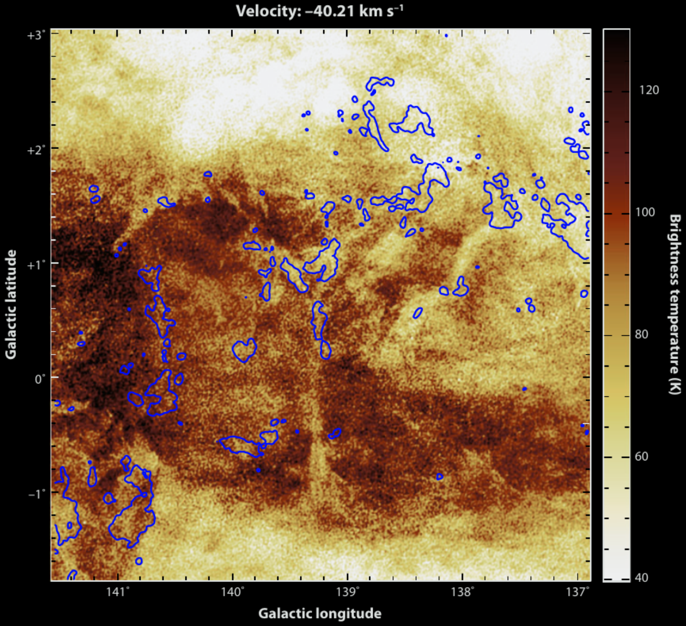

([H I]$_{21\,cm}$ emission with CO contours; Kalberla & Kerp 2009)

⇒ [H I]$_{21\,cm}$ CNM absorption in front of WNM [H I]$_{21\,cm}$ emission, without systematic association to CO.

Accounting for heating by shock & H^0 photoionization:

Accounting for heating by shock & H^0 photoionization:

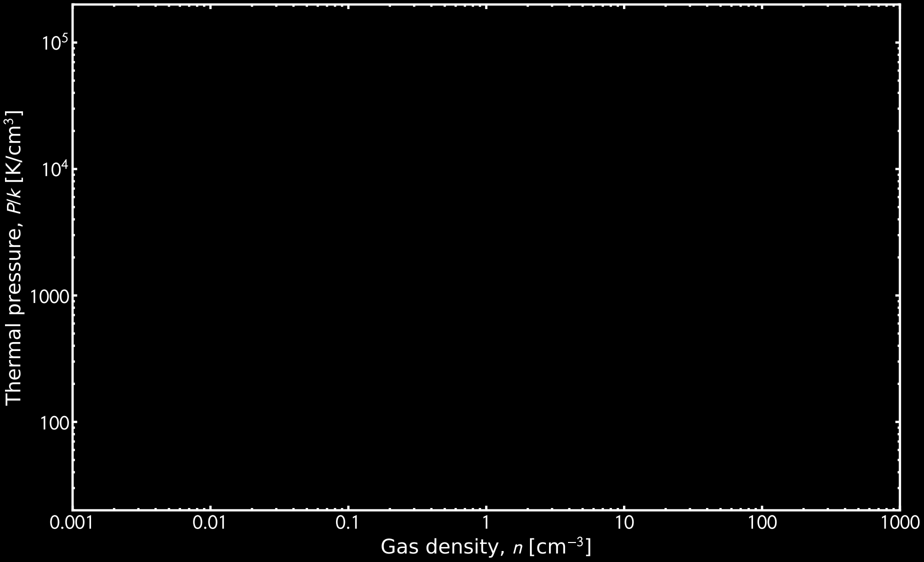

Accounting for heating by shock & H^0 photoionization:

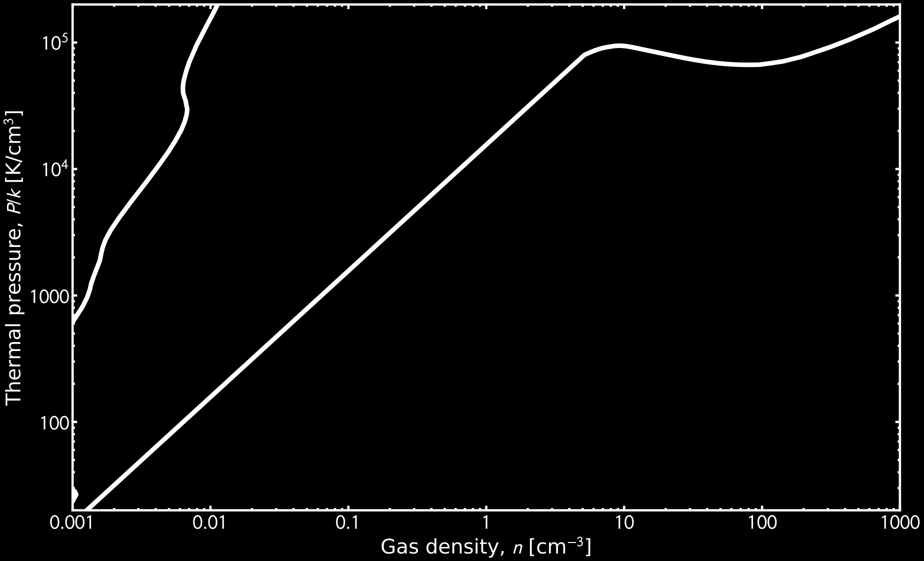

Accounting for heating by shock & H^0 photoionization:

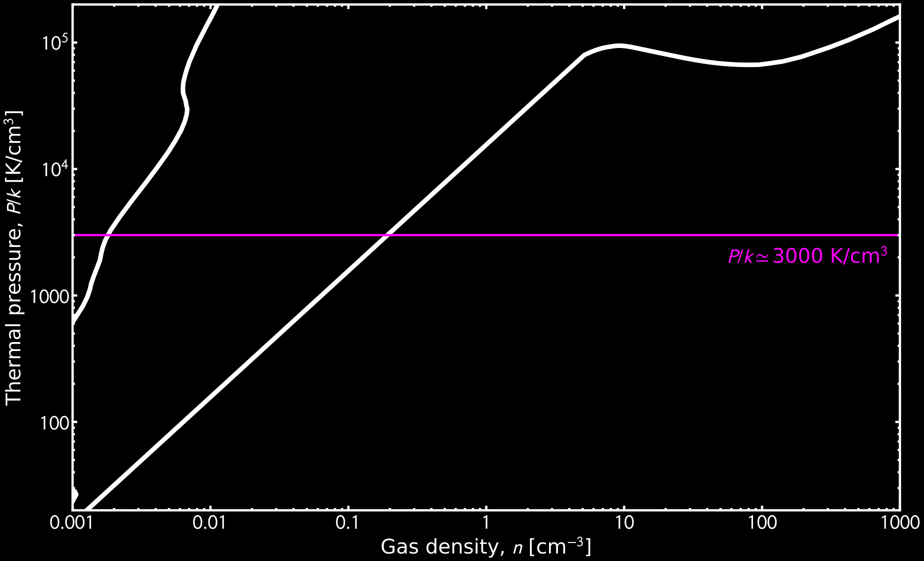

Accounting for heating by shock & H^0 photoionization:

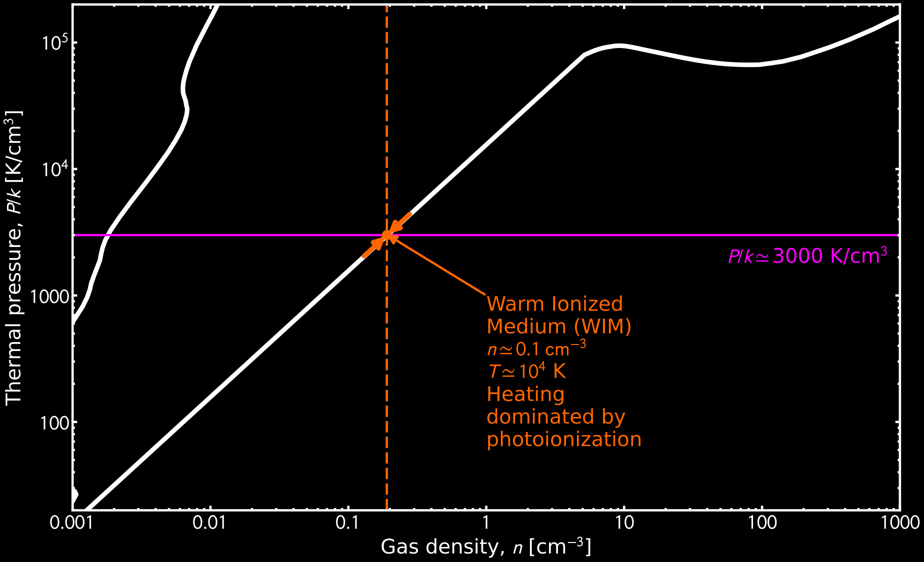

Accounting for heating by shock & H^0 photoionization:

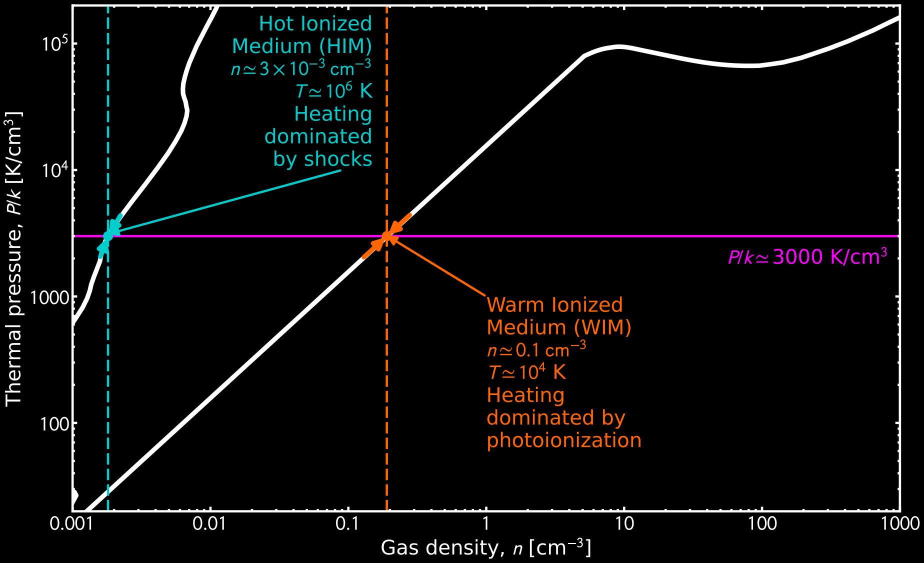

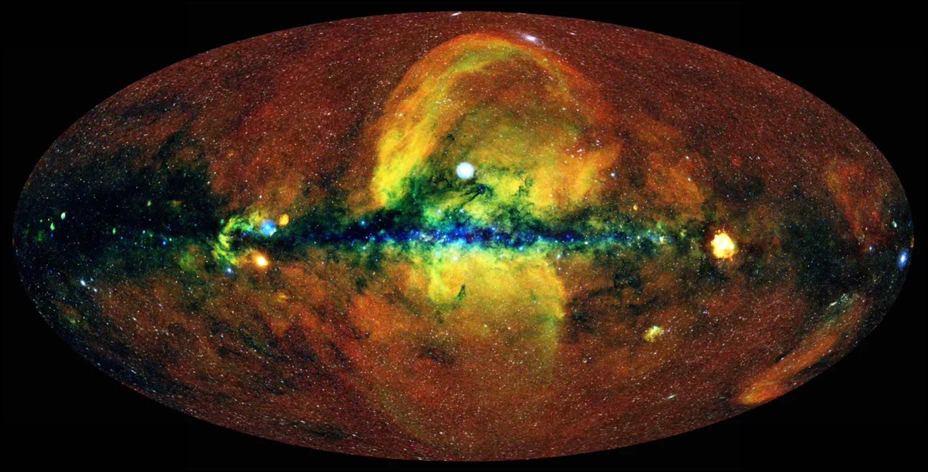

Credit: eRosita all-sky survey (0.3–0.6 keV / 0.6–1 keV / 1–2.3 keV); J. Sanders, H. Brunner & the eSASS team (MPE); E. Churazov, M. Gilfanov (on behalf of IKI).

Diffuse molecular clouds: $n(H_2) = 10^2 - 10^3\ cm^{-3}$ & $T = 40 - 100$ K.

Diffuse molecular clouds: $n(H_2) = 10^2 - 10^3\ \mathrm{cm}^{-3}$ & $T = 40 - 100$ K.

Dense molecular clouds: $n(H_2) = 10^3 - 10^6\ \mathrm{cm}^{-3}$ & $T = 20 - 50$ K.

Diffuse molecular clouds: $n(H_2) = 10^2 - 10^3$ cm^{-3} & $T = 40 - 100$ K.

Dense molecular clouds: $n(H_2) = 10^3 - 10^6$ cm^{-3} & $T = 20 - 50$ K.

Molecular cores: $n(H_2) = 10^6 - 10^7$ cm^{-3} & $T = 10 - 20$ K.

Diffuse molecular clouds: $n(H_2) = 10^2 - 10^3\ \text{cm}^{-3}$ & $T = 40 - 100$ K.

Dense molecular clouds: $n(H_2) = 10^3 - 10^6\ \text{cm}^{-3}$ & $T = 20 - 50$ K.

Molecular cores: $n(H_2) = 10^6 - 10^7\ \text{cm}^{-3}$ & $T = 10 - 20$ K.

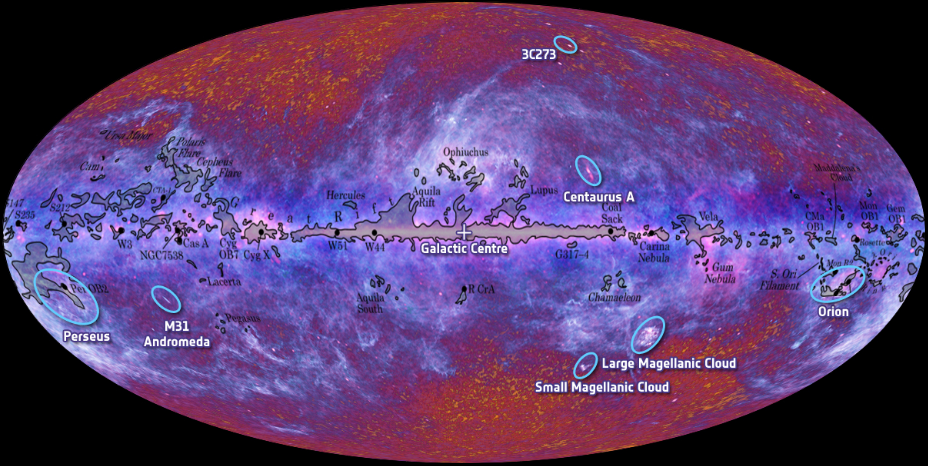

Credit: *Planck* image with $^{12}CO(J{=}1\rightarrow0)_{2.6mm}$ contours from Dame et al. (2001); ESA, HFI and LFI consortia.

Phase	Density [cm^{-3}]	Temperature [K]	Volume filling factor	Main heating	Main cooling

(Adapted from Tielens 2005 & Draine 2011)

Phase	Density [cm^{-3}]	Temperature [K]	Volume filling factor	Main heating	Main cooling
Hot Ionized Medium (HIM)	$\simeq 0.003$	$\simeq 10^6$	$\simeq 50\,\%$	Shocks	Free-free

(Adapted from Tielens 2005 & Draine 2011)

Phase	Density [cm^{-3}]	Temperature [K]	Volume filling factor	Main heating	Main cooling
Hot Ionized Medium (HIM)	$\simeq 0.003$	$\simeq 10^6$	$\simeq 50\,\%$	Shocks	Free-free
Warm Ionized Medium (WIM)	$\simeq 0.1$	$\simeq 10^4$	$\simeq 25\,\%$	Photoionization	Optical lines

(Adapted from Tielens 2005 & Draine 2011)

Phase	Density [cm^{-3}]	Temperature [K]	Volume filling factor	Main heating	Main cooling
Hot Ionized Medium (HIM)	$\simeq 0.003$	$\simeq 10^6$	$\simeq 50\,\%$	Shocks	Free-free
Warm Ionized Medium (WIM)	$\simeq 0.1$	$\simeq 10^4$	$\simeq 25\,\%$	Photoionization	Optical lines
Warm Neutral Medium (WNM)	$\simeq 0.3$	$\simeq 10^4$	$\simeq 30\,\%$	Photoelectric effect	Lyα

(Adapted from Tielens 2005 & Draine 2011)

Phase	Density [cm^{-3}]	Temperature [K]	Volume filling factor	Main heating	Main cooling
Hot Ionized Medium (HIM)	$\simeq 0.003$	$\simeq 10^6$	$\simeq 50\,\%$	Shocks	Free-free
Warm Ionized Medium (WIM)	$\simeq 0.1$	$\simeq 10^4$	$\simeq 25\,\%$	Photoionization	Optical lines
Warm Neutral Medium (WNM)	$\simeq 0.3$	$\simeq 10^4$	$\simeq 30\,\%$	Photoelectric effect	Lyα
Cold Neutral Medium (CNM)	$\simeq 30$	$\simeq 100$	$\simeq 1\,\%$	Photoelectric effect	$[\mathrm{C\,II}]_{158\mu m}$

(Adapted from Tielens 2005 & Draine 2011)

Thermal Phases | Summary of the Properties of the ISM Phases

Phase	Density [cm^{-3}]	Temperature [K]	Volume filling factor	Main heating	Main cooling
Hot Ionized Medium (HIM)	$\simeq 0.003$	$\simeq 10^6$	$\simeq 50\,\%$	Shocks	Free-free
Warm Ionized Medium (WIM)	$\simeq 0.1$	$\simeq 10^4$	$\simeq 25\,\%$	Photoionization	Optical lines
Warm Neutral Medium (WNM)	$\simeq 0.3$	$\simeq 10^4$	$\simeq 30\,\%$	Photoelectric effect	Lyα
Cold Neutral Medium (CNM)	$\simeq 30$	$\simeq 100$	$\simeq 1\,\%$	Photoelectric effect	$[\text{C II}]_{158\mu m}$
Molecular clouds	$10^2 - 10^6$	$10 - 50$	$\simeq 0.01\,\%$	Cosmic rays	CO lines

(Adapted from Tielens 2005 & Draine 2011)

Hot Ionized Medium
(HIM)

(adapted from P. van der Werf)

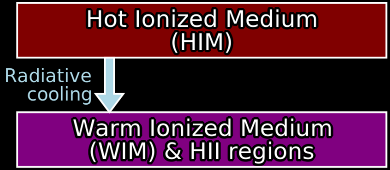

(adapted from P. van der Werf)

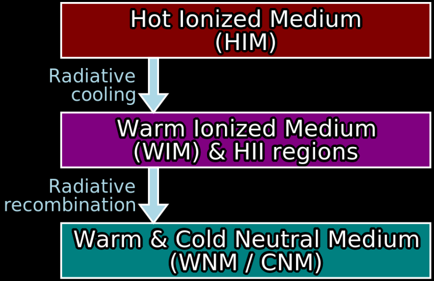

(adapted from P. van der Werf)

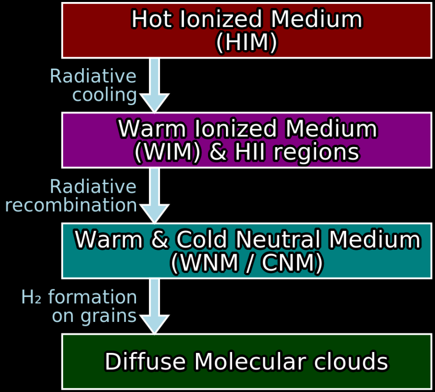

(adapted from P. van der Werf)

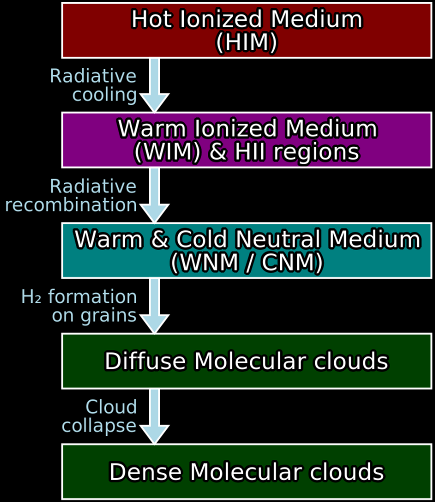

(adapted from P. van der Werf)

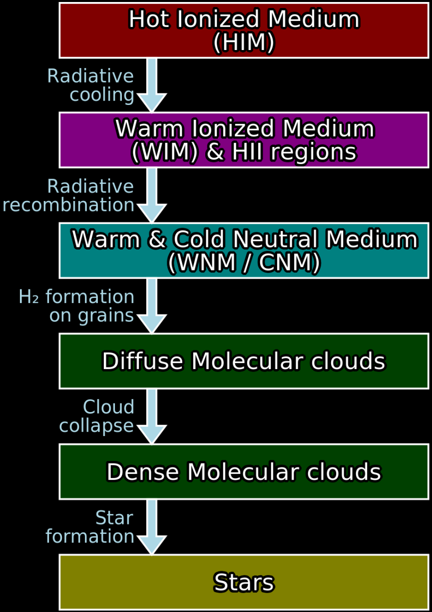

(adapted from P. van der Werf)

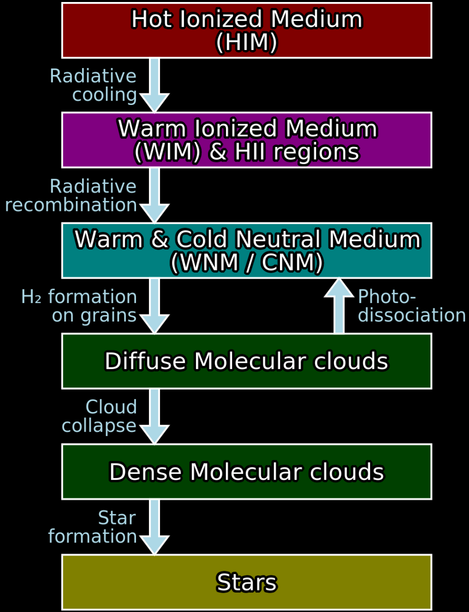

(adapted from P. van der Werf)

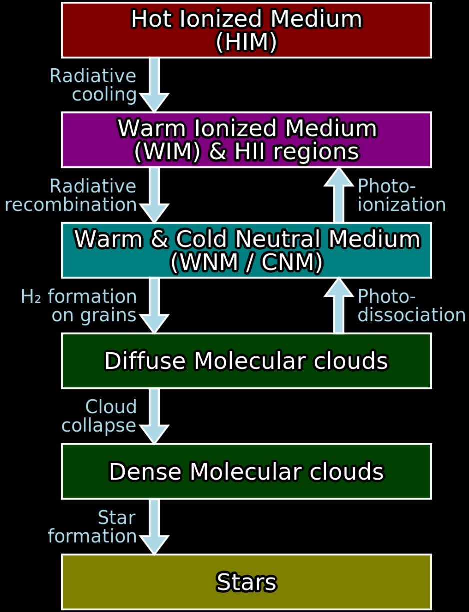

(adapted from P. van der Werf)

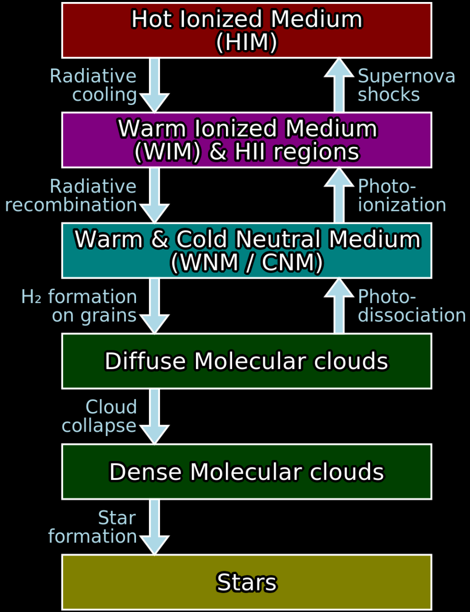

(adapted from P. van der Werf)

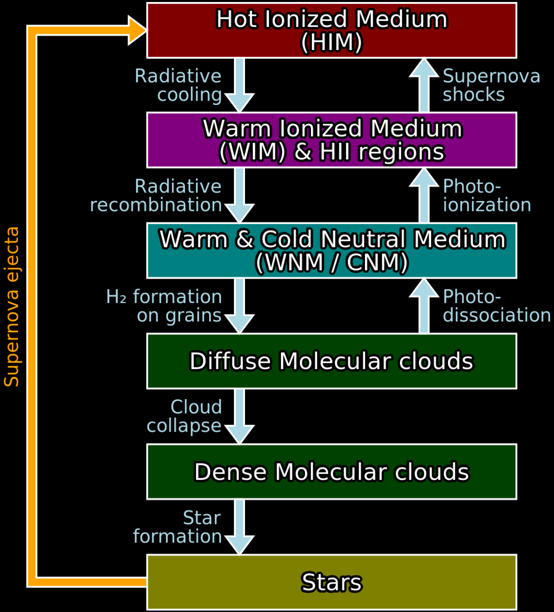

(adapted from P. van der Werf)

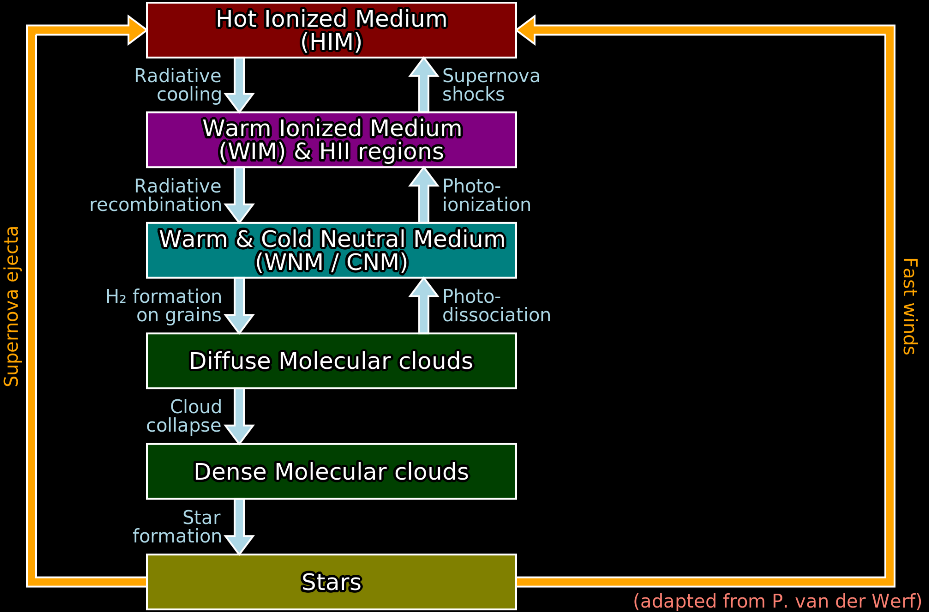

(adapted from P. van der Werf)

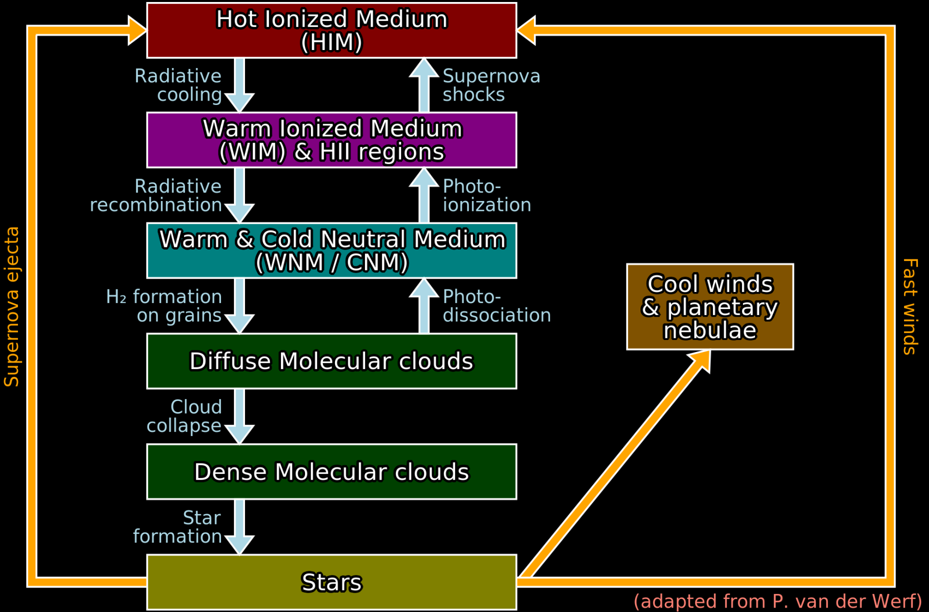

(adapted from P. van der Werf)

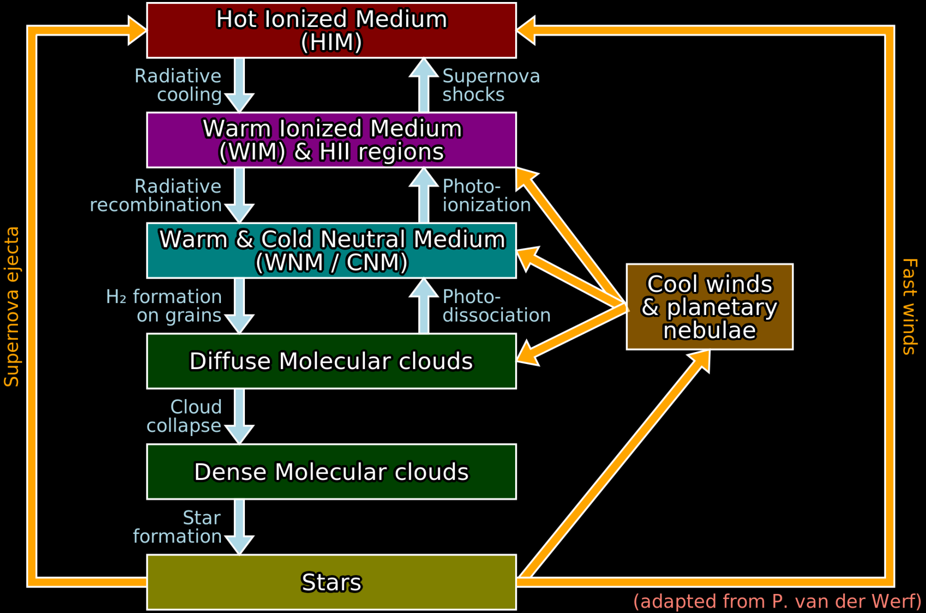

(adapted from P. van der Werf)

Outline of the Lecture

Spherical coordinate reminder

Spherical coordinate reminder

Solid angle: $d\Omega = \sin\theta d\theta d\phi$.

Spherical coordinate reminder

Solid angle: $\mathrm{d}\Omega = \sin\theta \mathrm{d}\theta \mathrm{d}\phi$. **Polar angle:** $0 \leq \theta < \pi$.

Spherical coordinate reminder

Solid angle: $\mathrm{d}\Omega = \sin\theta \mathrm{d}\theta \mathrm{d}\phi$. **Polar angle:** $0 \leq \theta < \pi$. **Azimuthal angle:** $0 \leq \phi < 2\pi$.

Spherical coordinate reminder

Solid angle: $\mathrm{d}\Omega = \sin\theta \mathrm{d}\theta \mathrm{d}\phi$. **Polar angle:** $0 \leq \theta < \pi$. **Azimuthal angle:** $0 \leq \phi < 2\pi$.

Specific & mean intensities

Spherical coordinate reminder

Solid angle: $d\Omega = \sin\theta d\theta d\phi$. **Polar angle:** $0 \leq \theta < \pi$. **Azimuthal angle:** $0 \leq \phi < 2\pi$.

Specific & mean intensities

Specific intensity: $I_\nu(\nu, \vec{r}, \theta, \phi) \equiv \dfrac{dE}{dt dA d\Omega d\nu}$.

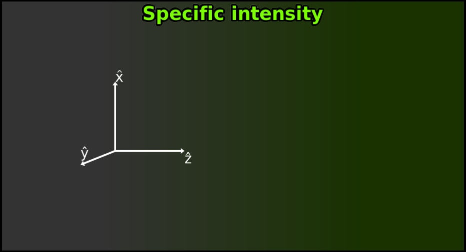

Spherical coordinate reminder

Solid angle: $\mathrm{d}\Omega = \sin\theta \mathrm{d}\theta \mathrm{d}\phi$. **Polar angle:** $0 \leq \theta < \pi$. **Azimuthal angle:** $0 \leq \phi < 2\pi$.

Specific & mean intensities

Specific intensity: $I_\nu(\nu, \vec{r}, \theta, \phi) \equiv \dfrac{\mathrm{d}E}{\mathrm{d}t\mathrm{d}A\mathrm{d}\Omega\mathrm{d}\nu}$.

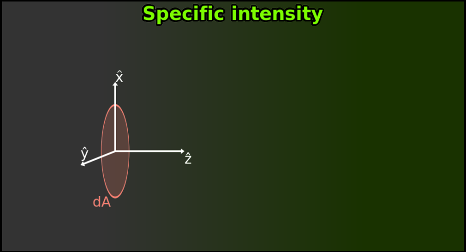

Spherical coordinate reminder

Solid angle: $d\Omega = \sin\theta d\theta d\phi$. **Polar angle:** $0 \leq \theta < \pi$. **Azimuthal angle:** $0 \leq \phi < 2\pi$.

Specific & mean intensities

Specific intensity: $I_\nu(\nu, \vec{r}, \theta, \phi) \equiv \frac{dE}{dt dA d\Omega d\nu}$.

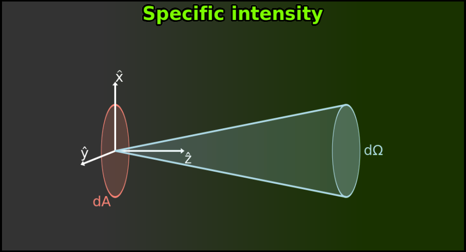

Spherical coordinate reminder

Solid angle: $\mathrm{d}\Omega = \sin\theta \mathrm{d}\theta \mathrm{d}\phi$. **Polar angle:** $0 \leq \theta < \pi$. **Azimuthal angle:** $0 \leq \phi < 2\pi$.

Specific & mean intensities

Specific intensity: $I_\nu(\nu, \vec{r}, \theta, \phi) \equiv \dfrac{\mathrm{d}E}{\mathrm{d}t\mathrm{d}A\mathrm{d}\Omega\mathrm{d}\nu}$.

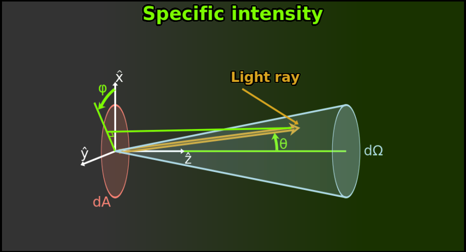

Spherical coordinate reminder

Solid angle: $\mathrm{d}\Omega = \sin\theta\mathrm{d}\theta\mathrm{d}\phi$. **Polar angle:** $0 \leq \theta < \pi$. **Azimuthal angle:** $0 \leq \phi < 2\pi$.

Specific & mean intensities

Specific intensity: $I_\nu(\nu, \vec{r}, \theta, \phi) \equiv \frac{\mathrm{d}E}{\mathrm{d}t\mathrm{d}A\mathrm{d}\Omega\mathrm{d}\nu}$.

Mean intensity: (0^{th} order moment of I_ν)

$$J_\nu(\nu, \vec{r}) \equiv \frac{1}{4\pi}\iint_\Omega I_\nu(\nu, \vec{r}, \theta, \phi)\,\mathrm{d}\Omega.$$

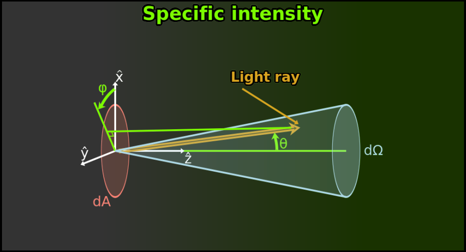

Spherical coordinate reminder

Solid angle: $d\Omega = \sin\theta d\theta d\phi$. **Polar angle:** $0 \leq \theta < \pi$. **Azimuthal angle:** $0 \leq \phi < 2\pi$.

Specific & mean intensities

Specific intensity: $I_\nu(\nu, \vec{r}, \theta, \phi) \equiv \frac{dE}{dt dA d\Omega d\nu}$.

Mean intensity: (0^{th} order moment of I_ν)

$$J_\nu(\nu, \vec{r}) \equiv \frac{1}{4\pi} \iint_\Omega I_\nu(\nu, \vec{r}, \theta, \phi)\, d\Omega.$$

Isotropic radiation $\Rightarrow I_\nu(\nu, \vec{r}) = J_\nu(\nu, \vec{r})$.

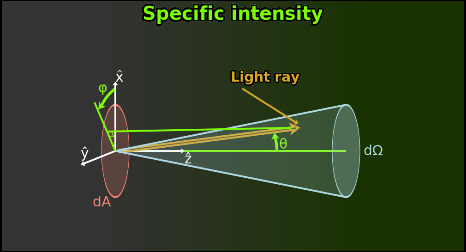

Spherical coordinate reminder

Solid angle: $d\Omega = \sin\theta d\theta d\phi$. **Polar angle:** $0 \leq \theta < \pi$. **Azimuthal angle:** $0 \leq \phi < 2\pi$.

Specific & mean intensities

Specific intensity: $I_\nu(\nu, \vec{r}, \theta, \phi) \equiv \frac{dE}{dt dA d\Omega d\nu}$.

Mean intensity: (0th order moment of I_ν)

$$J_\nu(\nu, \vec{r}) \equiv \frac{1}{4\pi} \iint_\Omega I_\nu(\nu, \vec{r}, \theta, \phi)\, d\Omega.$$

Isotropic radiation $\Rightarrow I_\nu(\nu, \vec{r}) = J_\nu(\nu, \vec{r})$.

The net flux

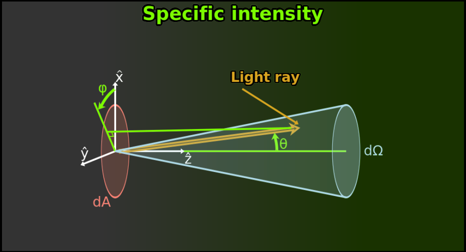

Spherical coordinate reminder

Solid angle: $\mathrm{d}\Omega = \sin\theta \mathrm{d}\theta \mathrm{d}\phi$. **Polar angle:** $0 \leq \theta < \pi$. **Azimuthal angle:** $0 \leq \phi < 2\pi$.

Specific & mean intensities

Specific intensity: $I_\nu(\nu, \vec{r}, \theta, \phi) \equiv \frac{\mathrm{d}E}{\mathrm{d}t \mathrm{d}A \mathrm{d}\Omega \mathrm{d}\nu}$.

Mean intensity: (0$^{\text{th}}$ order moment of I_ν)

$$J_\nu(\nu, \vec{r}) \equiv \frac{1}{4\pi} \iint_\Omega I_\nu(\nu, \vec{r}, \theta, \phi)\, \mathrm{d}\Omega.$$

Isotropic radiation $\Rightarrow I_\nu(\nu, \vec{r}) = J_\nu(\nu, \vec{r})$.

The net flux

Net monochromatic flux: (1$^{\text{st}}$ order moment of I_ν)

$$F_\nu(\nu, \vec{r}) \equiv \iint_\Omega I_\nu(\nu, \vec{r}, \theta, \phi) \cos\theta \, \mathrm{d}\Omega.$$

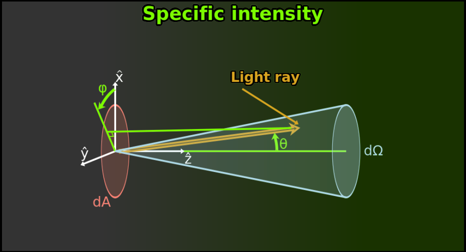

Spherical coordinate reminder

Solid angle: $d\Omega = \sin\theta d\theta d\phi$. **Polar angle:** $0 \leq \theta < \pi$. **Azimuthal angle:** $0 \leq \phi < 2\pi$.

Specific & mean intensities

Specific intensity: $I_\nu(\nu, \vec{r}, \theta, \phi) \equiv \frac{dE}{dt\,dA\,d\Omega\,d\nu}$.

Mean intensity: (0[th] order moment of I_ν)

$$J_\nu(\nu, \vec{r}) \equiv \frac{1}{4\pi} \iint_\Omega I_\nu(\nu, \vec{r}, \theta, \phi)\, d\Omega.$$

Isotropic radiation $\Rightarrow I_\nu(\nu, \vec{r}) = J_\nu(\nu, \vec{r})$.

The net flux

Net monochromatic flux: (1[st] order moment of I_ν)

$$F_\nu(\nu, \vec{r}) \equiv \iint_\Omega I_\nu(\nu, \vec{r}, \theta, \phi) \cos\theta\, d\Omega.$$

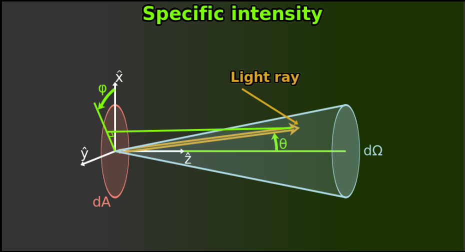

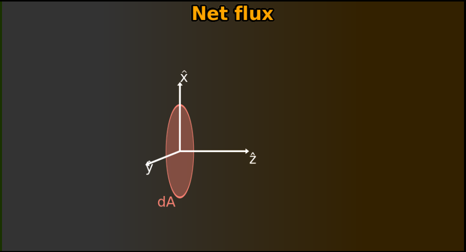

Spherical coordinate reminder

Solid angle: $d\Omega = \sin\theta d\theta d\phi$. **Polar angle:** $0 \leq \theta < \pi$. **Azimuthal angle:** $0 \leq \phi < 2\pi$.

Specific & mean intensities

Specific intensity: $I_\nu(\nu, \vec{r}, \theta, \phi) \equiv \frac{dE}{dt dA d\Omega d\nu}$.

Mean intensity: (0^{th} order moment of I_ν)

$$J_\nu(\nu, \vec{r}) \equiv \frac{1}{4\pi} \iint_\Omega I_\nu(\nu, \vec{r}, \theta, \phi)\, d\Omega.$$

Isotropic radiation $\Rightarrow I_\nu(\nu, \vec{r}) = J_\nu(\nu, \vec{r})$.

The net flux

Net monochromatic flux: (1^{st} order moment of I_ν)

$$F_\nu(\nu, \vec{r}) \equiv \iint_\Omega I_\nu(\nu, \vec{r}, \theta, \phi) \cos\theta\, d\Omega.$$

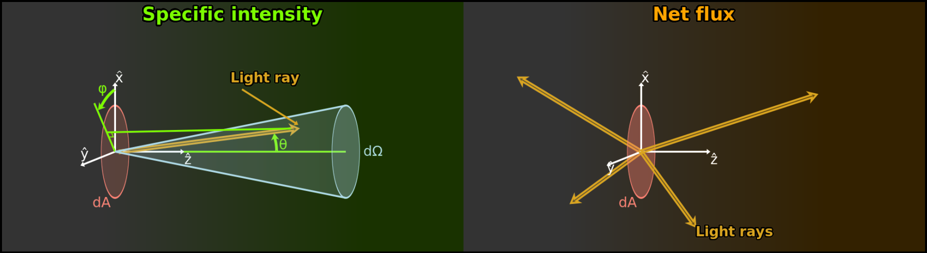

Spherical coordinate reminder

Solid angle: $d\Omega = \sin\theta d\theta d\phi$. **Polar angle:** $0 \leq \theta < \pi$. **Azimuthal angle:** $0 \leq \phi < 2\pi$.

Specific & mean intensities

Specific intensity: $I_\nu(\nu, \vec{r}, \theta, \phi) \equiv \frac{dE}{dt dA d\Omega d\nu}$.

Mean intensity: (0^{th} order moment of I_ν)

$$J_\nu(\nu, \vec{r}) \equiv \frac{1}{4\pi} \iint_\Omega I_\nu(\nu, \vec{r}, \theta, \phi)\, d\Omega.$$

Isotropic radiation $\Rightarrow I_\nu(\nu, \vec{r}) = J_\nu(\nu, \vec{r})$.

The net flux

Net monochromatic flux: (1^{st} order moment of I_ν)

$$F_\nu(\nu, \vec{r}) \equiv \iint_\Omega I_\nu(\nu, \vec{r}, \theta, \phi) \cos\theta\, d\Omega.$$

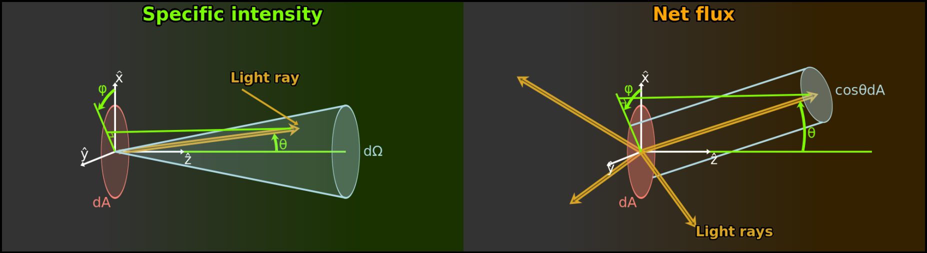

Spherical coordinate reminder

Solid angle: $\mathrm{d}\Omega = \sin\theta \mathrm{d}\theta \mathrm{d}\phi$. **Polar angle:** $0 \leq \theta < \pi$. **Azimuthal angle:** $0 \leq \phi < 2\pi$.

Specific & mean intensities

Specific intensity: $I_\nu(\nu, \vec{r}, \theta, \phi) \equiv \dfrac{\mathrm{d}E}{\mathrm{d}t \mathrm{d}A \mathrm{d}\Omega \mathrm{d}\nu}$.

Mean intensity: (0th order moment of I_ν)

$$J_\nu(\nu, \vec{r}) \equiv \frac{1}{4\pi} \iint_\Omega I_\nu(\nu, \vec{r}, \theta, \phi) \, \mathrm{d}\Omega.$$

Isotropic radiation $\Rightarrow I_\nu(\nu, \vec{r}) = J_\nu(\nu, \vec{r})$.

The net flux

Net monochromatic flux: (1st order moment of I_ν)

$$F_\nu(\nu, \vec{r}) \equiv \iint_\Omega I_\nu(\nu, \vec{r}, \theta, \phi) \cos\theta \, \mathrm{d}\Omega.$$

Isotropic case $\Rightarrow F_\nu(\nu, \vec{r}) = 0$.

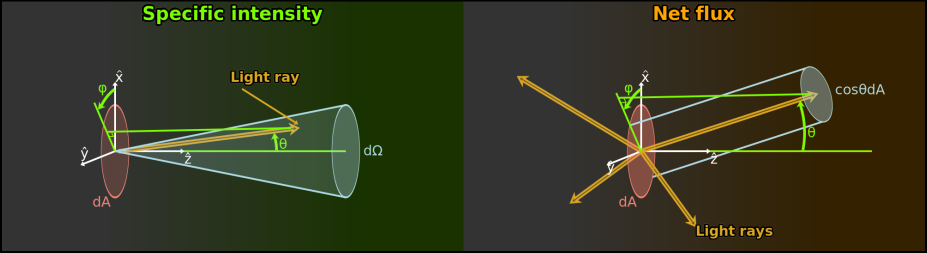

Transfer | The Specific Intensity & Its Moments (1/2)

Spherical coordinate reminder

Solid angle: $\mathrm{d}\Omega = \sin\theta \mathrm{d}\theta \mathrm{d}\phi$. **Polar angle:** $0 \leq \theta < \pi$. **Azimuthal angle:** $0 \leq \phi < 2\pi$.

Specific & mean intensities

Specific intensity: $I_\nu(\nu, \vec{r}, \theta, \phi) \equiv \frac{\mathrm{d}E}{\mathrm{d}t \mathrm{d}A \mathrm{d}\Omega \mathrm{d}\nu}$.

Mean intensity: (0th order moment of I_ν)

$$J_\nu(\nu, \vec{r}) \equiv \frac{1}{4\pi} \iint_\Omega I_\nu(\nu, \vec{r}, \theta, \phi) \, \mathrm{d}\Omega.$$

Isotropic radiation $\Rightarrow I_\nu(\nu, \vec{r}) = J_\nu(\nu, \vec{r})$.

The net flux

Net monochromatic flux: (1st order moment of I_ν)

$$F_\nu(\nu, \vec{r}) \equiv \iint_\Omega I_\nu(\nu, \vec{r}, \theta, \phi) \cos\theta \, \mathrm{d}\Omega.$$

Isotropic case $\Rightarrow F_\nu(\nu, \vec{r}) = 0$.

Hemispherical case $\Rightarrow F_\nu(\nu, \vec{r}) = \pi J_\nu(\nu, \vec{r})$.

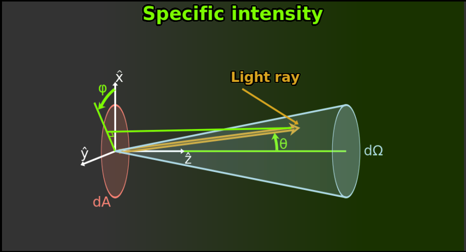

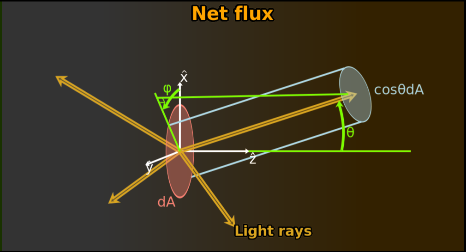

Radiation pressure

Radiation pressure

Momentum flux carried by a photon of frequency ν: $p = h\nu/c$.

Radiation pressure

Momentum flux carried by a photon of frequency ν: $p = h\nu/c$.

Radiation pressure: (2[nd] order moment of I_ν)

$$P_\nu \equiv \iint_\Omega I_\nu(\nu, \vec{r}, \theta, \phi) \cos^2\theta \, \mathrm{d}\Omega.$$

Radiation pressure

Momentum flux carried by a photon of frequency ν: $p = h\nu/c$.

Radiation pressure: (2^{nd} order moment of I_ν)

$$P_\nu \equiv \iint_\Omega I_\nu(\nu, \vec{r}, \theta, \phi) \cos^2\theta \, d\Omega.$$

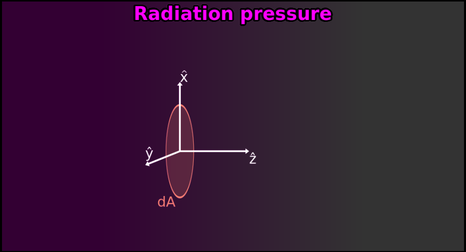

Radiation pressure

Momentum flux carried by a photon of frequency ν: $p = h\nu/c$.

Radiation pressure: (2nd order moment of I_ν)

$$P_\nu \equiv \iint_\Omega I_\nu(\nu, \vec{r}, \theta, \phi) \cos^2\theta \, \mathrm{d}\Omega.$$

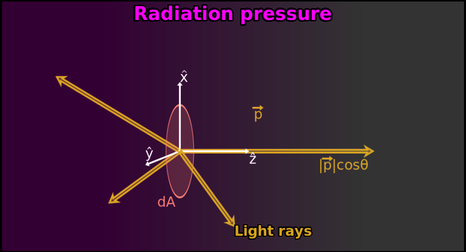

Radiation pressure

Momentum flux carried by a photon of frequency ν: $p = h\nu/c$.

Radiation pressure: (2^{nd} order moment of I_ν)

$$P_\nu \equiv \iint_\Omega I_\nu(\nu, \vec{r}, \theta, \phi) \cos^2\theta \, d\Omega.$$

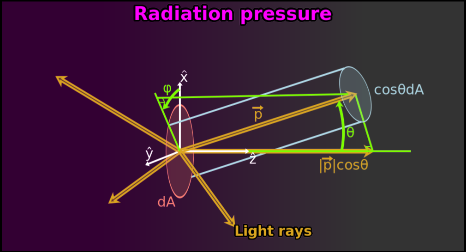

Radiation pressure

Momentum flux carried by a photon of frequency ν: $p = h\nu/c$.

Radiation pressure: (2nd order moment of I_ν)

$$P_\nu \equiv \iint_\Omega I_\nu(\nu, \vec{r}, \theta, \phi) \cos^2\theta \, \mathrm{d}\Omega.$$

Energy density

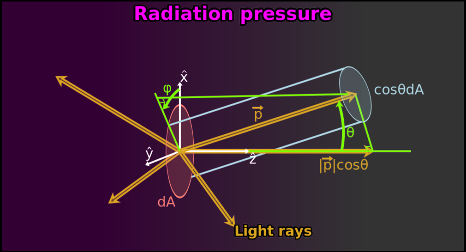

Radiation pressure

Momentum flux carried by a photon of frequency ν: $p = h\nu/c$.

Radiation pressure: (2^{nd} order moment of I_ν)

$$P_\nu \equiv \iint_\Omega I_\nu(\nu, \vec{r}, \theta, \phi) \cos^2\theta \, d\Omega.$$

Energy density

$$U_\nu(\nu, \vec{r}, \theta, \phi) \equiv \frac{dE}{dV d\Omega d\nu} = \frac{dE}{c dt dA d\Omega d\nu}$$

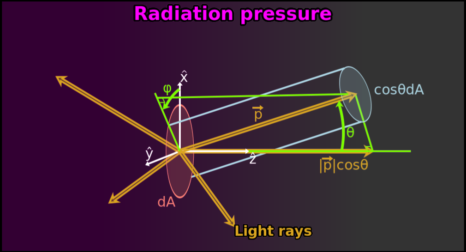

Radiation pressure

Momentum flux carried by a photon of frequency ν: $p = h\nu/c$.

Radiation pressure: (2nd order moment of I_ν)

$$P_\nu \equiv \iint_\Omega I_\nu(\nu,\vec{r},\theta,\phi)\cos^2\theta\,\mathrm{d}\Omega.$$

Energy density

$$U_\nu(\nu,\vec{r},\theta,\phi) \equiv \frac{\mathrm{d}E}{\mathrm{d}V\mathrm{d}\Omega\mathrm{d}\nu} = \frac{\mathrm{d}E}{c\mathrm{d}t\mathrm{d}A\mathrm{d}\Omega\mathrm{d}\nu}$$

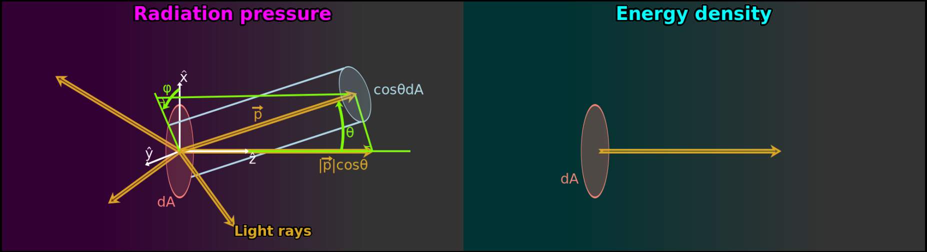

Radiation pressure

Momentum flux carried by a photon of frequency ν: $p = h\nu/c$.

Radiation pressure: (2^{nd} order moment of I_ν)

$$P_\nu \equiv \iint_\Omega I_\nu(\nu, \vec{r}, \theta, \phi) \cos^2\theta \, \mathrm{d}\Omega.$$

Energy density

$$U_\nu(\nu, \vec{r}, \theta, \phi) \equiv \frac{\mathrm{d}E}{\mathrm{d}V \mathrm{d}\Omega \mathrm{d}\nu} = \frac{\mathrm{d}E}{c\mathrm{d}t\mathrm{d}A\mathrm{d}\Omega\mathrm{d}\nu}$$

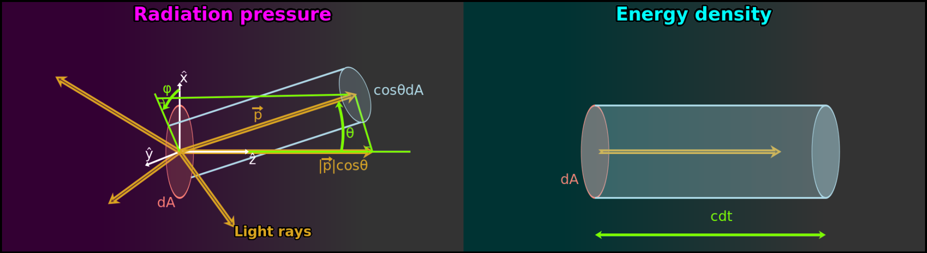

Radiation pressure

Momentum flux carried by a photon of frequency ν: $p = h\nu/c$.

Radiation pressure: (2[nd] order moment of I_ν)

$$P_\nu \equiv \iint_\Omega I_\nu(\nu, \vec{r}, \theta, \phi) \cos^2\theta \, d\Omega.$$

Energy density

$$U_\nu(\nu, \vec{r}, \theta, \phi) \equiv \frac{dE}{dV d\Omega d\nu} = \frac{dE}{c dt dA d\Omega d\nu}$$

$$\Rightarrow U_\nu(\nu, \vec{r}, \theta, \phi) = \frac{I_\nu(\nu, \vec{r}, \theta, \phi)}{c}.$$

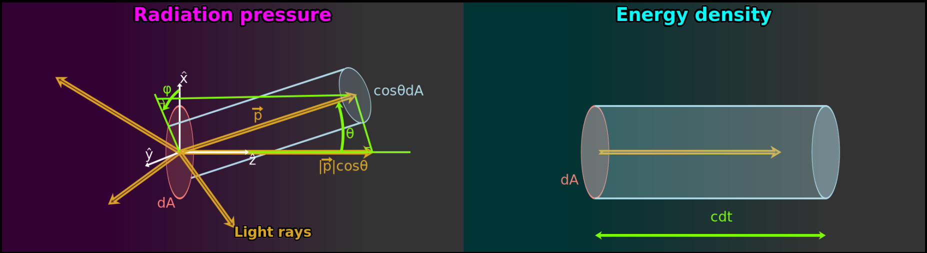

Emission & absorption coefficient

Radiation pressure

Momentum flux carried by a photon of frequency ν: $p = h\nu/c$.

Radiation pressure: (2nd order moment of I_ν)

$$P_\nu \equiv \iint_\Omega I_\nu(\nu, \vec{r}, \theta, \phi) \cos^2\theta \, \mathrm{d}\Omega.$$

Energy density

$$U_\nu(\nu, \vec{r}, \theta, \phi) \equiv \frac{\mathrm{d}E}{\mathrm{d}V \mathrm{d}\Omega \mathrm{d}\nu} = \frac{\mathrm{d}E}{c\mathrm{d}t\mathrm{d}A\mathrm{d}\Omega\mathrm{d}\nu}$$

$$\Rightarrow U_\nu(\nu, \vec{r}, \theta, \phi) = \frac{I_\nu(\nu, \vec{r}, \theta, \phi)}{c}.$$

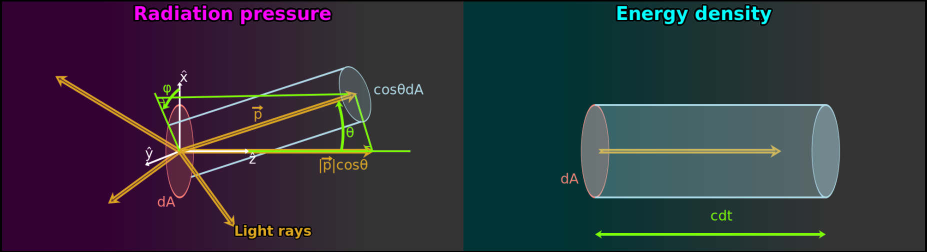

Emission & absorption coefficient

Emission coefficient:

$$j_\nu(\nu, \vec{r}, \theta, \phi) \equiv \frac{\mathrm{d}E_{\mathrm{em}}}{\mathrm{d}t\mathrm{d}V\mathrm{d}\Omega\mathrm{d}\nu}.$$

Radiation pressure

Momentum flux carried by a photon of frequency ν: $p = h\nu/c$.

Radiation pressure: (2nd order moment of I_ν)

$$P_\nu \equiv \iint_\Omega I_\nu(\nu, \vec{r}, \theta, \phi) \cos^2\theta \, d\Omega.$$

Energy density

$$U_\nu(\nu, \vec{r}, \theta, \phi) \equiv \frac{dE}{dV d\Omega d\nu} = \frac{dE}{c dt dA d\Omega d\nu}$$

$$\Rightarrow U_\nu(\nu, \vec{r}, \theta, \phi) = \frac{I_\nu(\nu, \vec{r}, \theta, \phi)}{c}.$$

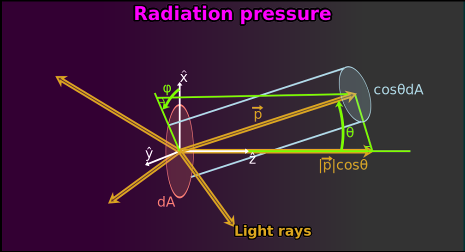

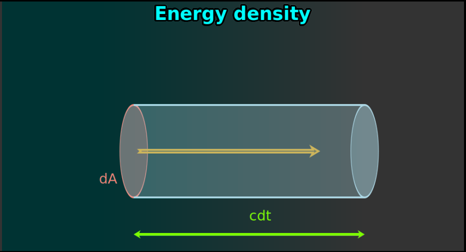

Emission & absorption coefficient

Emission coefficient:

$$j_\nu(\nu, \vec{r}, \theta, \phi) \equiv \frac{dE_{em}}{dt dV d\Omega d\nu}.$$

Extinction coefficient:

$$\alpha(\vec{r}, \nu) = \rho(\vec{r}) \times \kappa(\vec{r}, \nu).$$

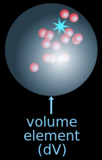

(Rybicky & Lightman, 1979; Steinacker et al., 2013)

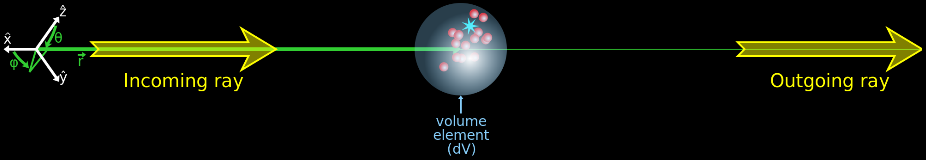

(Rybicky & Lightman, 1979; Steinacker et al., 2013)

$$\frac{\mathrm{d}I_\nu(\nu, \vec{r}, \theta, \phi)}{\mathrm{d}l} =$$

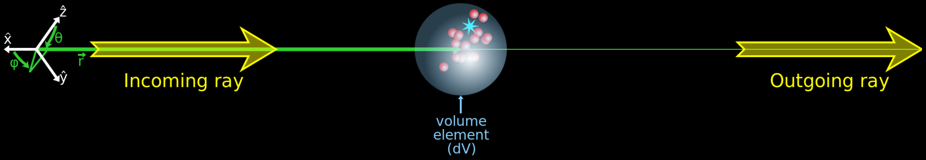

(Rybicky & Lightman, 1979; Steinacker et al., 2013)

$$\frac{\mathrm{d}I_\nu(\nu, \vec{r}, \theta, \phi)}{\mathrm{d}l} =$$

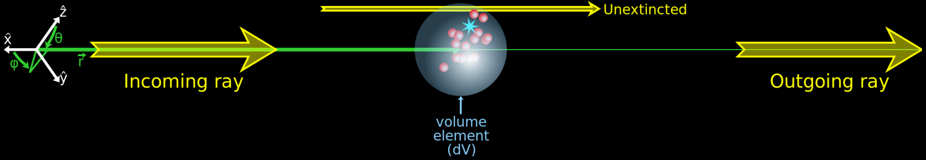

(Rybicky & Lightman, 1979; Steinacker et al., 2013)

$$\frac{\mathrm{d}I_\nu(\nu, \overrightarrow{r}, \theta, \phi)}{\mathrm{d}l} =$$

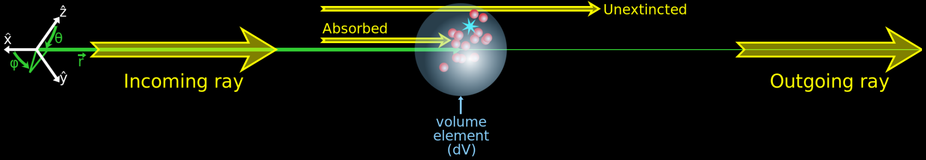

(Rybicky & Lightman, 1979; Steinacker et al., 2013)

$$\frac{\mathrm{d}I_\nu(\nu,\vec{r},\theta,\phi)}{\mathrm{d}l} = \underbrace{-\alpha_{\text{abs}}(\nu,\vec{r})I_\nu(\nu,\vec{r},\theta,\phi)}_{\text{absorption}}$$

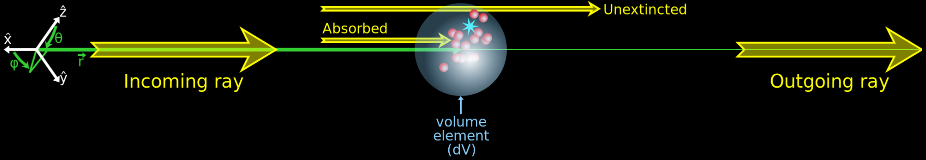

(Rybicky & Lightman, 1979; Steinacker et al., 2013)

$$\frac{\mathrm{d}I_\nu(\nu,\vec{r},\theta,\phi)}{\mathrm{d}l} = \underbrace{-\alpha_{\mathrm{abs}}(\nu,\vec{r})I_\nu(\nu,\vec{r},\theta,\phi)}_{\text{absorption}}$$

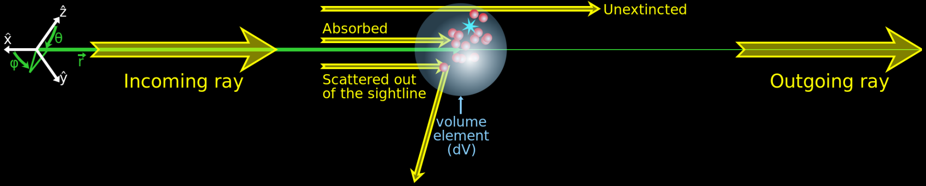

(Rybicky & Lightman, 1979; Steinacker et al., 2013)

$$\frac{dI_\nu(\nu,\vec{r},\theta,\phi)}{dl} = \underbrace{-\alpha_{\rm abs}(\nu,\vec{r})I_\nu(\nu,\vec{r},\theta,\phi)}_{\text{absorption}} \underbrace{-\alpha_{\rm sca}(\nu,\vec{r})I_\nu(\nu,\vec{r},\theta,\phi)}_{\text{scattering out of the sightline}}$$

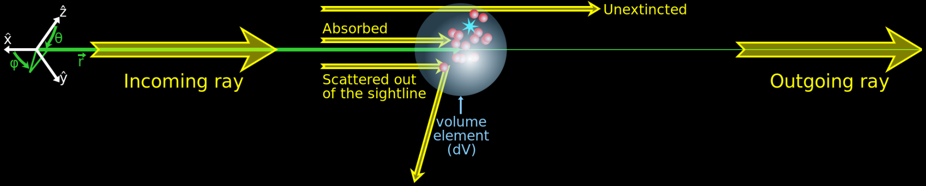

(Rybicky & Lightman, 1979; Steinacker et al., 2013)

$$\frac{\mathrm{d}I_\nu(\nu,\vec{r},\theta,\phi)}{\mathrm{d}l} = \underbrace{-\alpha_{\text{abs}}(\nu,\vec{r})I_\nu(\nu,\vec{r},\theta,\phi)}_{\text{absorption}} \underbrace{-\alpha_{\text{sca}}(\nu,\vec{r})I_\nu(\nu,\vec{r},\theta,\phi)}_{\text{scattering out of the sightline}}$$

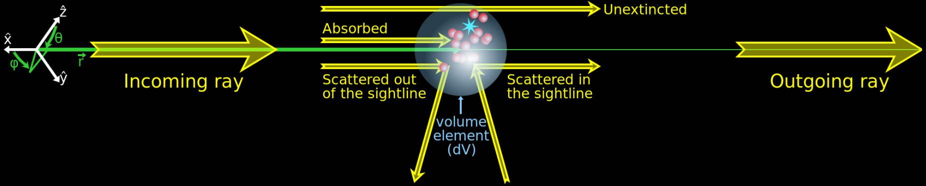

(Rybicky & Lightman, 1979; Steinacker et al., 2013)

$$\frac{\mathrm{d}I_\nu(\nu,\vec{r},\theta,\phi)}{\mathrm{d}l} = \underbrace{-\alpha_{\text{abs}}(\nu,\vec{r})I_\nu(\nu,\vec{r},\theta,\phi)}_{\text{absorption}} \underbrace{-\alpha_{\text{sca}}(\nu,\vec{r})I_\nu(\nu,\vec{r},\theta,\phi)}_{\text{scattering out of the sightline}}$$
$$\underbrace{+\alpha_{\text{sca}}(\nu,\vec{r})2\pi\int_{-1}^{1}\Phi(\cos\theta',\nu)I_\nu(\nu,\vec{r},\theta(\theta'),\phi(\theta'))\,\mathrm{d}\cos\theta'}_{\text{scattering in the sightline}}$$

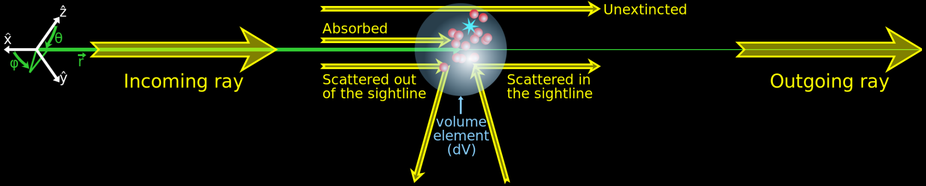

(Rybicky & Lightman, 1979; Steinacker et al., 2013)

$$\frac{dI_\nu(\nu,\vec{r},\theta,\phi)}{dl} = \underbrace{-\alpha_{\rm abs}(\nu,\vec{r})I_\nu(\nu,\vec{r},\theta,\phi)}_{\text{absorption}} \underbrace{-\alpha_{\rm sca}(\nu,\vec{r})I_\nu(\nu,\vec{r},\theta,\phi)}_{\text{scattering out of the sightline}}$$
$$\underbrace{+\alpha_{\rm sca}(\nu,\vec{r})2\pi\int_{-1}^{1}\Phi(\cos\theta',\nu)I_\nu(\nu,\vec{r},\theta(\theta'),\phi(\theta'))\,d\cos\theta'}_{\text{scattering in the sightline}}$$

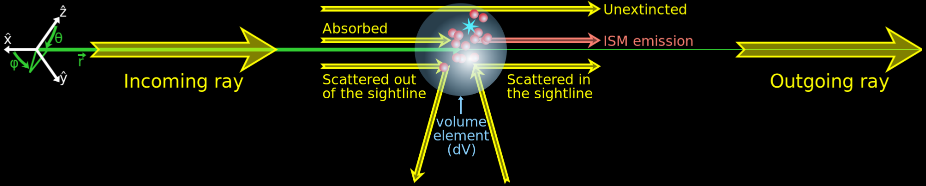

(Rybicky & Lightman, 1979; Steinacker et al., 2013)

$$\frac{\mathrm{d}I_\nu(\nu,\vec{r},\theta,\phi)}{\mathrm{d}l} = \underbrace{-\alpha_{\mathrm{abs}}(\nu,\vec{r})I_\nu(\nu,\vec{r},\theta,\phi)}_{\text{absorption}} \underbrace{-\alpha_{\mathrm{sca}}(\nu,\vec{r})I_\nu(\nu,\vec{r},\theta,\phi)}_{\text{scattering out of the sightline}}$$

$$+\underbrace{\alpha_{\mathrm{sca}}(\nu,\vec{r})2\pi\int_{-1}^{1}\Phi(\cos\theta',\nu)I_\nu(\nu,\vec{r},\theta(\theta'),\phi(\theta'))\,\mathrm{d}\cos\theta'}_{\text{scattering in the sightline}}$$

$$+\underbrace{j_\nu^{\mathrm{ISM}}(\nu,\vec{r})}_{\text{ISM emission}}$$

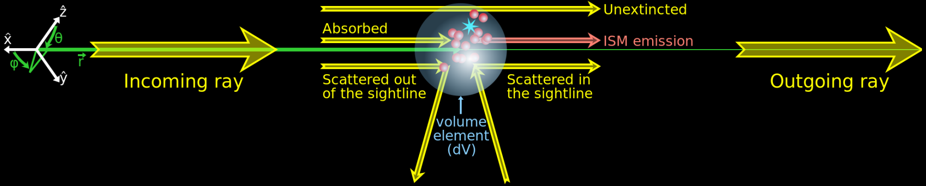

(Rybicky & Lightman, 1979; Steinacker et al., 2013)

$$\frac{\mathrm{d}I_\nu(\nu,\vec{r},\theta,\phi)}{\mathrm{d}l} = \underbrace{-\alpha_{\mathrm{abs}}(\nu,\vec{r})I_\nu(\nu,\vec{r},\theta,\phi)}_{\text{absorption}} \underbrace{-\alpha_{\mathrm{sca}}(\nu,\vec{r})I_\nu(\nu,\vec{r},\theta,\phi)}_{\text{scattering out of the sightline}}$$

$$+\underbrace{\alpha_{\mathrm{sca}}(\nu,\vec{r})2\pi\int_{-1}^{1}\Phi(\cos\theta',\nu)I_\nu(\nu,\vec{r},\theta(\theta'),\phi(\theta'))\,\mathrm{d}\cos\theta'}_{\text{scattering in the sightline}}$$

$$+\underbrace{j_\nu^{\mathrm{ISM}}(\nu,\vec{r})}_{\text{ISM emission}}$$

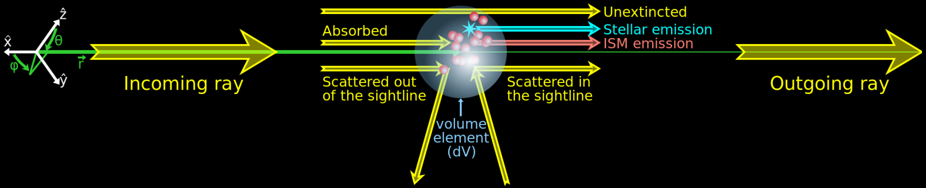

(Rybicky & Lightman, 1979; Steinacker et al., 2013)

$$\frac{dI_\nu(\nu,\vec{r},\theta,\phi)}{dl} = \underbrace{-\alpha_{\text{abs}}(\nu,\vec{r})I_\nu(\nu,\vec{r},\theta,\phi)}_{\text{absorption}} \underbrace{-\alpha_{\text{sca}}(\nu,\vec{r})I_\nu(\nu,\vec{r},\theta,\phi)}_{\text{scattering out of the sightline}}$$
$$\underbrace{+\alpha_{\text{sca}}(\nu,\vec{r})2\pi\int_{-1}^{1}\Phi(\cos\theta',\nu)I_\nu(\nu,\vec{r},\theta(\theta'),\phi(\theta'))\,d\cos\theta'}_{\text{scattering in the sightline}}$$
$$+\underbrace{j_\nu^{\text{ISM}}(\nu,\vec{r})}_{\text{ISM emission}}+\underbrace{j_\nu^{\star}(\nu,\vec{r})}_{\text{stellar emission}}.$$

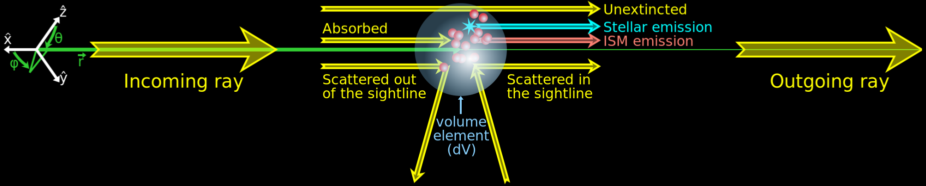

(Rybicky & Lightman, 1979; Steinacker et al., 2013)

$$\frac{\mathrm{d}I_\nu(\nu,\vec{r},\theta,\phi)}{\mathrm{d}l} = \underbrace{-\alpha_{\mathrm{abs}}(\nu,\vec{r})I_\nu(\nu,\vec{r},\theta,\phi)}_{\text{absorption}} \underbrace{-\alpha_{\mathrm{sca}}(\nu,\vec{r})I_\nu(\nu,\vec{r},\theta,\phi)}_{\text{scattering out of the sightline}}$$
$$\underbrace{+\alpha_{\mathrm{sca}}(\nu,\vec{r})2\pi\int_{-1}^{1}\Phi(\cos\theta',\nu)I_\nu(\nu,\vec{r},\theta(\theta'),\phi(\theta'))\,\mathrm{d}\cos\theta'}_{\text{scattering in the sightline}}$$
$$+\underbrace{j_\nu^{\mathrm{ISM}}(\nu,\vec{r})}_{\text{ISM emission}}+\underbrace{j_\nu^{\star}(\nu,\vec{r})}_{\text{stellar emission}}.$$

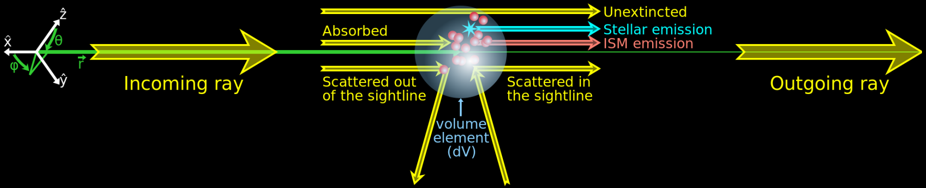

Solve this $\forall\ \theta,\ \forall\ \phi,\ \forall\ \vec{r},\ \forall\ \nu$

(Rybicky & Lightman, 1979; Steinacker et al., 2013)

$$\frac{\mathrm{d}I_\nu(\nu,\vec{r},\theta,\phi)}{\mathrm{d}l} = \underbrace{-\,\alpha_{\mathrm{abs}}(\nu,\vec{r})I_\nu(\nu,\vec{r},\theta,\phi)}_{\text{absorption}}\ \underbrace{-\,\alpha_{\mathrm{sca}}(\nu,\vec{r})I_\nu(\nu,\vec{r},\theta,\phi)}_{\text{scattering out of the sightline}}$$

$$+\underbrace{\alpha_{\mathrm{sca}}(\nu,\vec{r})2\pi\int_{-1}^{1}\Phi(\cos\theta',\nu)I_\nu(\nu,\vec{r},\theta(\theta'),\phi(\theta'))\,\mathrm{d}\cos\theta'}_{\text{scattering in the sightline}}$$

$$+\underbrace{j_\nu^{\mathrm{ISM}}(\nu,\vec{r})}_{\text{ISM emission}}+\underbrace{j_\nu^{\star}(\nu,\vec{r})}_{\text{stellar emission}}\ .$$

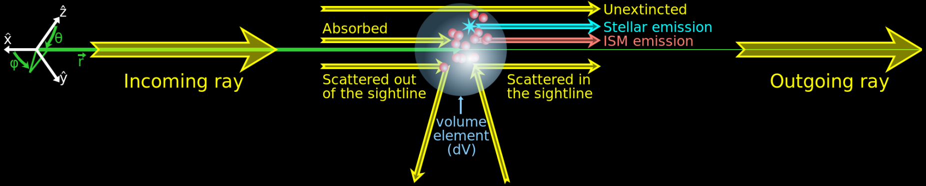

Solve this $\forall\ \theta$, $\forall\ \phi$, $\forall\ \vec{r}$, $\forall\ \nu \Rightarrow$ numerically intensive.

(Rybicky & Lightman, 1979; Steinacker et al., 2013)

The optical depth along a sightline

The optical depth along a sightline

Along a given sightline, l:

The optical depth along a sightline

Along a given sightline, l:

$$\mathrm{d}\tau(\nu,l) = \alpha(\nu,l)\,\mathrm{d}l$$

The optical depth along a sightline

Along a given sightline, l:

$$\mathrm{d}\tau(\nu,l) = \alpha(\nu,l)\,\mathrm{d}l = \underbrace{\rho(l)}_{\text{specific mass}} \times \underbrace{\kappa(\nu,l)}_{\text{opacity}}\,\mathrm{d}l$$

The optical depth along a sightline

Along a given sightline, l:

$$d\tau(\nu, l) = \alpha(\nu, l)\,dl = \underbrace{\rho(l)}_{\text{specific mass}} \times \underbrace{\kappa(\nu, l)}_{\text{opacity}}\,dl$$

$$\Rightarrow \boxed{\tau(\nu, l) = \int_0^l \rho(l') \times \kappa(\nu, l')\,dl'}.$$

The optical depth along a sightline

Along a given sightline, l:

$$d\tau(\nu,l) = \alpha(\nu,l)\,dl = \underbrace{\rho(l)}_{\text{specific mass}} \times \underbrace{\kappa(\nu,l)}_{\text{opacity}}\,dl$$

$$\Rightarrow \boxed{\tau(\nu,l) = \int_0^l \rho(l') \times \kappa(\nu,l')\,dl'}.$$

The mean free path of a photon

The optical depth along a sightline

Along a given sightline, l:

$$\mathrm{d}\tau(\nu,l) = \alpha(\nu,l)\,\mathrm{d}l = \underbrace{\rho(l)}_{\text{specific mass}} \times \underbrace{\kappa(\nu,l)}_{\text{opacity}}\,\mathrm{d}l$$

$$\Rightarrow \boxed{\tau(\nu,l) = \int_0^l \rho(l') \times \kappa(\nu,l')\,\mathrm{d}l'}.$$

The mean free path of a photon

$$l_{\text{mean}}(\nu,\vec{r}) = \frac{1}{\alpha(\nu,\vec{r})} = \frac{1}{\rho(\vec{r})\kappa(\nu,\vec{r})}$$

The optical depth along a sightline

Along a given sightline, l:

$$\mathrm{d}\tau(\nu,l) = \alpha(\nu,l)\,\mathrm{d}l = \underbrace{\rho(l)}_{\text{specific mass}} \times \underbrace{\kappa(\nu,l)}_{\text{opacity}}\,\mathrm{d}l$$

$$\Rightarrow \boxed{\tau(\nu,l) = \int_0^l \rho(l') \times \kappa(\nu,l')\,\mathrm{d}l'}.$$

The mean free path of a photon

$$l_{\text{mean}}(\nu,\vec{r}) = \frac{1}{\alpha(\nu,\vec{r})} = \frac{1}{\rho(\vec{r})\kappa(\nu,\vec{r})}$$

- $\tau \ll 1 \Rightarrow$ "*optically-thin*".

The optical depth along a sightline

Along a given sightline, l:

$$d\tau(\nu,l) = \alpha(\nu,l)\,dl = \underbrace{\rho(l)}_{\text{specific mass}} \times \underbrace{\kappa(\nu,l)}_{\text{opacity}}\,dl$$

$$\Rightarrow \boxed{\tau(\nu,l) = \int_0^l \rho(l') \times \kappa(\nu,l')\,dl'}.$$

The mean free path of a photon

$$l_{\text{mean}}(\nu,\vec{r}) = \frac{1}{\alpha(\nu,\vec{r})} = \frac{1}{\rho(\vec{r})\kappa(\nu,\vec{r})}$$

- $\tau \ll 1 \Rightarrow$ "*optically-thin*".
- $\tau = 1 \Rightarrow l = l_{\text{mean}}$.

The optical depth along a sightline

Along a given sightline, l:

$$d\tau(\nu,l) = \alpha(\nu,l)\,dl = \underbrace{\rho(l)}_{\text{specific mass}} \times \underbrace{\kappa(\nu,l)}_{\text{opacity}}\,dl$$

$$\Rightarrow \boxed{\tau(\nu,l) = \int_0^l \rho(l') \times \kappa(\nu,l')\,dl'}.$$

The mean free path of a photon

$$l_{\text{mean}}(\nu,\vec{r}) = \frac{1}{\alpha(\nu,\vec{r})} = \frac{1}{\rho(\vec{r})\kappa(\nu,\vec{r})}$$

- $\tau \ll 1 \Rightarrow$ "*optically-thin*".
- $\tau = 1 \Rightarrow l = l_{\text{mean}}$.
- $\tau \gg 1 \Rightarrow$ "*optically-thick*".

The optical depth along a sightline

Along a given sightline, l:

$$d\tau(\nu,l) = \alpha(\nu,l)\,dl = \underbrace{\rho(l)}_{\text{specific mass}} \times \underbrace{\kappa(\nu,l)}_{\text{opacity}}\,dl$$

$$\Rightarrow \boxed{\tau(\nu,l) = \int_0^l \rho(l') \times \kappa(\nu,l')\,dl'}.$$

The mean free path of a photon

$$l_{\text{mean}}(\nu,\vec{r}) = \frac{1}{\alpha(\nu,\vec{r})} = \frac{1}{\rho(\vec{r})\kappa(\nu,\vec{r})}$$

- $\tau \ll 1 \Rightarrow$ "*optically-thin*".
- $\tau = 1 \Rightarrow l = l_{\text{mean}}$.
- $\tau \gg 1 \Rightarrow$ "*optically-thick*".

The visible / near-IR mean free path for the different ISM phases

HIM	WNM	CNM	Molecular clouds
$n_{\text{H}} = 0.003\text{ cm}^{-3}$	$n_{\text{H}} = 0.3\text{ cm}^{-3}$	$n_{\text{H}} = 30\text{ cm}^{-3}$	$n_{\text{H}} = 10^4\text{ cm}^{-3}$

The optical depth along a sightline

Along a given sightline, l:

$$\mathrm{d}\tau(\nu,l) = \alpha(\nu,l)\,\mathrm{d}l = \underbrace{\rho(l)}_{\text{specific mass}} \times \underbrace{\kappa(\nu,l)}_{\text{opacity}}\,\mathrm{d}l$$

$$\Rightarrow \boxed{\tau(\nu,l) = \int_0^l \rho(l') \times \kappa(\nu,l')\,\mathrm{d}l'}.$$

The mean free path of a photon

$$l_{\text{mean}}(\nu,\vec{r}) = \frac{1}{\alpha(\nu,\vec{r})} = \frac{1}{\rho(\vec{r})\kappa(\nu,\vec{r})}$$

- $\tau \ll 1 \Rightarrow$ "*optically-thin*".
- $\tau = 1 \Rightarrow l = l_{\text{mean}}$.
- $\tau \gg 1 \Rightarrow$ "*optically-thick*".

The visible / near-IR mean free path for the different ISM phases

	HIM $n_{\text{H}} = 0.003\ \text{cm}^{-3}$	WNM $n_{\text{H}} = 0.3\ \text{cm}^{-3}$	CNM $n_{\text{H}} = 30\ \text{cm}^{-3}$	Molecular clouds $n_{\text{H}} = 10^4\ \text{cm}^{-3}$
$l_{\text{mean}}(U)$	139 kpc	1.39 kpc	13.9 pc	0.0417 pc

The optical depth along a sightline

Along a given sightline, l:

$$d\tau(\nu,l) = \alpha(\nu,l)\,dl = \underbrace{\rho(l)}_{\text{specific mass}} \times \underbrace{\kappa(\nu,l)}_{\text{opacity}}\,dl$$

$$\Rightarrow \boxed{\tau(\nu,l) = \int_0^l \rho(l') \times \kappa(\nu,l')\,dl'}.$$

The mean free path of a photon

$$l_{\text{mean}}(\nu,\vec{r}) = \frac{1}{\alpha(\nu,\vec{r})} = \frac{1}{\rho(\vec{r})\kappa(\nu,\vec{r})}$$

- $\tau \ll 1 \Rightarrow$ "*optically-thin*".
- $\tau = 1 \Rightarrow l = l_{\text{mean}}$.
- $\tau \gg 1 \Rightarrow$ "*optically-thick*".

The visible / near-IR mean free path for the different ISM phases

	HIM $n_H = 0.003$ cm^{-3}	WNM $n_H = 0.3$ cm^{-3}	CNM $n_H = 30$ cm^{-3}	Molecular clouds $n_H = 10^4$ cm^{-3}
$l_{\text{mean}}(U)$	139 kpc	1.39 kpc	13.9 pc	0.0417 pc
$l_{\text{mean}}(B)$	177 kpc	1.77 kpc	17.7 pc	0.0532 pc

The optical depth along a sightline

Along a given sightline, l:

$$d\tau(\nu,l) = \alpha(\nu,l)\,dl = \underbrace{\rho(l)}_{\text{specific mass}} \times \underbrace{\kappa(\nu,l)}_{\text{opacity}}\,dl$$

$$\Rightarrow \boxed{\tau(\nu,l) = \int_0^l \rho(l') \times \kappa(\nu,l')\,dl'}.$$

The mean free path of a photon

$$l_{\text{mean}}(\nu,\vec{r}) = \frac{1}{\alpha(\nu,\vec{r})} = \frac{1}{\rho(\vec{r})\kappa(\nu,\vec{r})}$$

- $\tau \ll 1 \Rightarrow$ "*optically-thin*".
- $\tau = 1 \Rightarrow l = l_{\text{mean}}$.
- $\tau \gg 1 \Rightarrow$ "*optically-thick*".

The visible / near-IR mean free path for the different ISM phases

	HIM $n_H = 0.003$ cm^{-3}	WNM $n_H = 0.3$ cm^{-3}	CNM $n_H = 30$ cm^{-3}	Molecular clouds $n_H = 10^4$ cm^{-3}
$l_{\text{mean}}(U)$	139 kpc	1.39 kpc	13.9 pc	0.0417 pc
$l_{\text{mean}}(B)$	177 kpc	1.77 kpc	17.7 pc	0.0532 pc
$l_{\text{mean}}(V)$	223 kpc	2.23 kpc	22.3 pc	0.0669 pc

The optical depth along a sightline

Along a given sightline, l:

$$d\tau(\nu,l) = \alpha(\nu,l)\,dl = \underbrace{\rho(l)}_{\text{specific mass}} \times \underbrace{\kappa(\nu,l)}_{\text{opacity}}\,dl$$

$$\Rightarrow \boxed{\tau(\nu,l) = \int_0^l \rho(l') \times \kappa(\nu,l')\,dl'}.$$

The mean free path of a photon

$$l_{\rm mean}(\nu,\vec{r}) = \frac{1}{\alpha(\nu,\vec{r})} = \frac{1}{\rho(\vec{r})\kappa(\nu,\vec{r})}$$

- $\tau \ll 1 \Rightarrow$ "*optically-thin*".
- $\tau = 1 \Rightarrow l = l_{\rm mean}$.
- $\tau \gg 1 \Rightarrow$ "*optically-thick*".

The visible / near-IR mean free path for the different ISM phases

	HIM $n_H = 0.003$ cm^{-3}	WNM $n_H = 0.3$ cm^{-3}	CNM $n_H = 30$ cm^{-3}	Molecular clouds $n_H = 10^4$ cm^{-3}
$l_{\rm mean}(U)$	139 kpc	1.39 kpc	13.9 pc	0.0417 pc
$l_{\rm mean}(B)$	177 kpc	1.77 kpc	17.7 pc	0.0532 pc
$l_{\rm mean}(V)$	223 kpc	2.23 kpc	22.3 pc	0.0669 pc
$l_{\rm mean}(R)$	275 kpc	2.75 kpc	27.5 pc	0.0824 pc

The optical depth along a sightline

Along a given sightline, l:

$$d\tau(\nu,l) = \alpha(\nu,l)\,dl = \underbrace{\rho(l)}_{\text{specific mass}} \times \underbrace{\kappa(\nu,l)}_{\text{opacity}}\,dl$$

$$\Rightarrow \boxed{\tau(\nu,l) = \int_0^l \rho(l') \times \kappa(\nu,l')\,dl'}.$$

The mean free path of a photon

$$l_{\text{mean}}(\nu,\vec{r}) = \frac{1}{\alpha(\nu,\vec{r})} = \frac{1}{\rho(\vec{r})\kappa(\nu,\vec{r})}$$

- $\tau \ll 1 \Rightarrow$ "*optically-thin*".
- $\tau = 1 \Rightarrow l = l_{\text{mean}}$.
- $\tau \gg 1 \Rightarrow$ "*optically-thick*".

The visible / near-IR mean free path for the different ISM phases

	HIM $n_H = 0.003\text{ cm}^{-3}$	WNM $n_H = 0.3\text{ cm}^{-3}$	CNM $n_H = 30\text{ cm}^{-3}$	Molecular clouds $n_H = 10^4\text{ cm}^{-3}$
$l_{\text{mean}}(U)$	139 kpc	1.39 kpc	13.9 pc	0.0417 pc
$l_{\text{mean}}(B)$	177 kpc	1.77 kpc	17.7 pc	0.0532 pc
$l_{\text{mean}}(V)$	223 kpc	2.23 kpc	22.3 pc	0.0669 pc
$l_{\text{mean}}(R)$	275 kpc	2.75 kpc	27.5 pc	0.0824 pc
$l_{\text{mean}}(I)$	358 pc	3.58 kpc	35.8 pc	0.107 pc

The optical depth along a sightline

Along a given sightline, l:

$$d\tau(\nu,l) = \alpha(\nu,l)\,dl = \underbrace{\rho(l)}_{\text{specific mass}} \times \underbrace{\kappa(\nu,l)}_{\text{opacity}}\,dl$$

$$\Rightarrow \boxed{\tau(\nu,l) = \int_0^l \rho(l')\times\kappa(\nu,l')\,dl'}.$$

The mean free path of a photon

$$l_{\text{mean}}(\nu,\vec{r}) = \frac{1}{\alpha(\nu,\vec{r})} = \frac{1}{\rho(\vec{r})\kappa(\nu,\vec{r})}$$

- $\tau \ll 1 \Rightarrow$ "*optically-thin*".
- $\tau = 1 \Rightarrow l = l_{\text{mean}}$.
- $\tau \gg 1 \Rightarrow$ "*optically-thick*".

The visible / near-IR mean free path for the different ISM phases

	HIM $n_H = 0.003\ \text{cm}^{-3}$	WNM $n_H = 0.3\ \text{cm}^{-3}$	CNM $n_H = 30\ \text{cm}^{-3}$	Molecular clouds $n_H = 10^4\ \text{cm}^{-3}$
$l_{\text{mean}}(U)$	139 kpc	1.39 kpc	13.9 pc	0.0417 pc
$l_{\text{mean}}(B)$	177 kpc	1.77 kpc	17.7 pc	0.0532 pc
$l_{\text{mean}}(V)$	223 kpc	2.23 kpc	22.3 pc	0.0669 pc
$l_{\text{mean}}(R)$	275 kpc	2.75 kpc	27.5 pc	0.0824 pc
$l_{\text{mean}}(I)$	358 pc	3.58 kpc	35.8 pc	0.107 pc
$l_{\text{mean}}(J)$	691 kpc	6.91 kpc	69.1 pc	0.207 pc

The optical depth along a sightline

Along a given sightline, l:

$$d\tau(\nu,l) = \alpha(\nu,l)\,dl = \underbrace{\rho(l)}_{\text{specific mass}} \times \underbrace{\kappa(\nu,l)}_{\text{opacity}}\,dl$$

$$\Rightarrow \boxed{\tau(\nu,l) = \int_0^l \rho(l') \times \kappa(\nu,l')\,dl'}.$$

The mean free path of a photon

$$l_{\text{mean}}(\nu,\vec{r}) = \frac{1}{\alpha(\nu,\vec{r})} = \frac{1}{\rho(\vec{r})\kappa(\nu,\vec{r})}$$

- $\tau \ll 1 \Rightarrow$ "*optically-thin*".
- $\tau = 1 \Rightarrow l = l_{\text{mean}}$.
- $\tau \gg 1 \Rightarrow$ "*optically-thick*".

The visible / near-IR mean free path for the different ISM phases

	HIM $n_{\text{H}} = 0.003\text{ cm}^{-3}$	WNM $n_{\text{H}} = 0.3\text{ cm}^{-3}$	CNM $n_{\text{H}} = 30\text{ cm}^{-3}$	Molecular clouds $n_{\text{H}} = 10^4\text{ cm}^{-3}$
$l_{\text{mean}}(U)$	139 kpc	1.39 kpc	13.9 pc	0.0417 pc
$l_{\text{mean}}(B)$	177 kpc	1.77 kpc	17.7 pc	0.0532 pc
$l_{\text{mean}}(V)$	223 kpc	2.23 kpc	22.3 pc	0.0669 pc
$l_{\text{mean}}(R)$	275 kpc	2.75 kpc	27.5 pc	0.0824 pc
$l_{\text{mean}}(I)$	358 pc	3.58 kpc	35.8 pc	0.107 pc
$l_{\text{mean}}(J)$	691 kpc	6.91 kpc	69.1 pc	0.207 pc
$l_{\text{mean}}(H)$	1021 kpc	10.2 kpc	102 pc	0.306 pc

The optical depth along a sightline

Along a given sightline, l:

$$d\tau(\nu,l) = \alpha(\nu,l)\,dl = \underbrace{\rho(l)}_{\text{specific mass}} \times \underbrace{\kappa(\nu,l)}_{\text{opacity}}\,dl$$

$$\Rightarrow \boxed{\tau(\nu,l) = \int_0^l \rho(l') \times \kappa(\nu,l')\,dl'}.$$

The mean free path of a photon

$$l_{\text{mean}}(\nu,\vec{r}) = \frac{1}{\alpha(\nu,\vec{r})} = \frac{1}{\rho(\vec{r})\kappa(\nu,\vec{r})}$$

- $\tau \ll 1 \Rightarrow$ "*optically-thin*".
- $\tau = 1 \Rightarrow l = l_{\text{mean}}$.
- $\tau \gg 1 \Rightarrow$ "*optically-thick*".

The visible / near-IR mean free path for the different ISM phases

	HIM $n_H = 0.003\text{ cm}^{-3}$	**WNM** $n_H = 0.3\text{ cm}^{-3}$	**CNM** $n_H = 30\text{ cm}^{-3}$	**Molecular clouds** $n_H = 10^4\text{ cm}^{-3}$
$l_{\text{mean}}(U)$	139 kpc	1.39 kpc	13.9 pc	0.0417 pc
$l_{\text{mean}}(B)$	177 kpc	1.77 kpc	17.7 pc	0.0532 pc
$l_{\text{mean}}(V)$	223 kpc	2.23 kpc	22.3 pc	0.0669 pc
$l_{\text{mean}}(R)$	275 kpc	2.75 kpc	27.5 pc	0.0824 pc
$l_{\text{mean}}(I)$	358 pc	3.58 kpc	35.8 pc	0.107 pc
$l_{\text{mean}}(J)$	691 kpc	6.91 kpc	69.1 pc	0.207 pc
$l_{\text{mean}}(H)$	1021 kpc	10.2 kpc	102 pc	0.306 pc
$l_{\text{mean}}(K)$	1734 kpc	17.3 kpc	173 pc	0.52 pc

(Rybicky & Lightman, 1979)

Transfer equation: $\frac{\mathrm{d}I_\nu}{\mathrm{d}r} = 0$

(Rybicky & Lightman, 1979)

Transfer equation: $\frac{\mathrm{d}I_\nu}{\mathrm{d}r} = 0 \Rightarrow I_\nu(R_\star) = I_\nu(r) = B_\nu(T_\star)$

(Rybicky & Lightman, 1979)

Transfer equation: $\frac{\mathrm{d}I_\nu}{\mathrm{d}r} = 0 \Rightarrow I_\nu(R_\star) = I_\nu(r) = B_\nu(T_\star) \leftarrow$ energy conservation.

(Rybicky & Lightman, 1979)

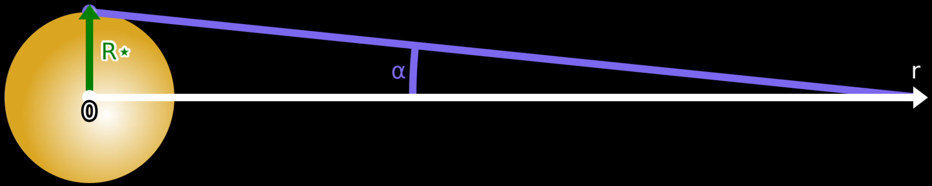

Transfer equation: $\frac{dI_\nu}{dr} = 0 \Rightarrow I_\nu(R_\star) = I_\nu(r) = B_\nu(T_\star) \leftarrow$ energy conservation.

(Rybicky & Lightman, 1979)

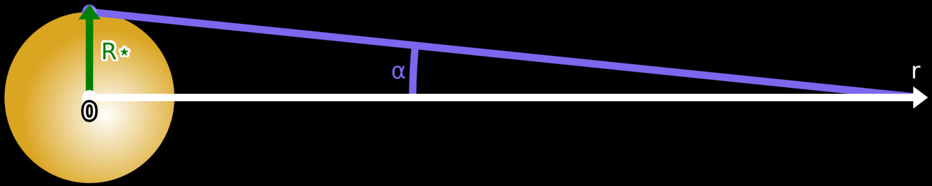

Transfer equation: $\frac{dI_\nu}{dr} = 0 \Rightarrow I_\nu(R_\star) = I_\nu(r) = B_\nu(T_\star) \leftarrow$ energy conservation.

Angular size at distance r: $\sin\alpha = \frac{R_\star}{r}$.

(Rybicky & Lightman, 1979)

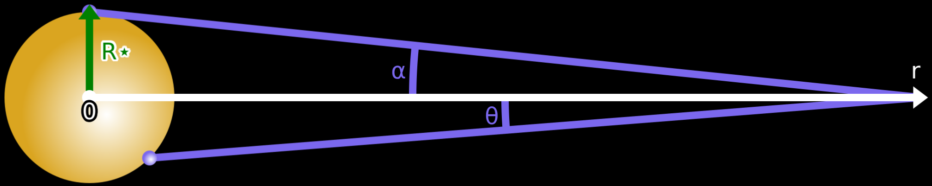

Transfer equation: $\frac{dI_\nu}{dr} = 0 \Rightarrow I_\nu(R_\star) = I_\nu(r) = B_\nu(T_\star) \leftarrow$ energy conservation.

Angular size at distance r: $\sin\alpha = \frac{R_\star}{r}$.

(Rybicky & Lightman, 1979)

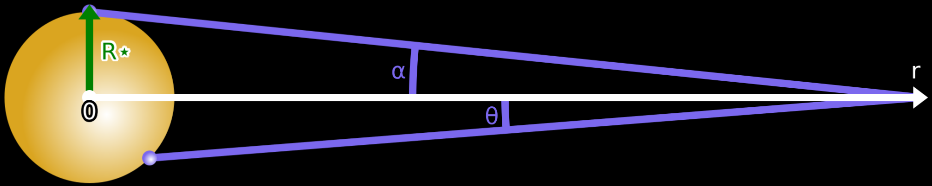

Transfer equation: $\frac{\mathrm{d}I_\nu}{\mathrm{d}r} = 0 \Rightarrow I_\nu(R_\star) = I_\nu(r) = B_\nu(T_\star) \leftarrow$ energy conservation.

Angular size at distance r: $\sin\alpha = \frac{R_\star}{r}$.

Flux at r: $F_\nu(r) = \int_0^{2\pi}\int_0^{\alpha} I_\nu \cos\theta \,\mathrm{d}\theta\,\mathrm{d}\phi$

(Rybicky & Lightman, 1979)

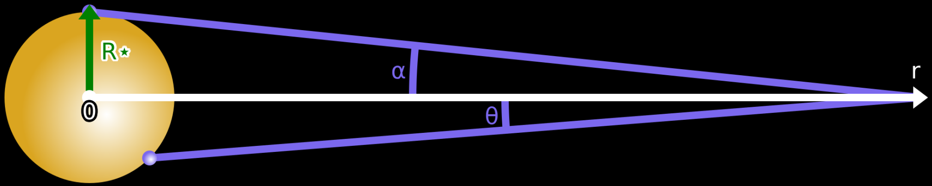

Transfer equation: $\frac{\mathrm{d}I_\nu}{\mathrm{d}r} = 0 \Rightarrow I_\nu(R_\star) = I_\nu(r) = B_\nu(T_\star) \leftarrow$ energy conservation.

Angular size at distance r: $\sin\alpha = \frac{R_\star}{r}$.

Flux at r: $F_\nu(r) = \int_0^{2\pi}\int_0^{\alpha} I_\nu \cos\theta \, \mathrm{d}\theta \, \mathrm{d}\phi = 2\pi B_\nu(T_\star)\int_0^{\alpha} \cos\theta \sin\theta \mathrm{d}\theta$

(Rybicky & Lightman, 1979)

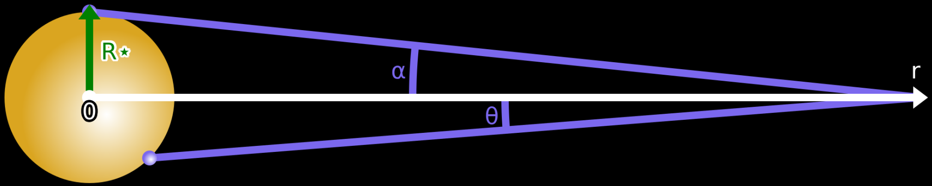

Transfer equation: $\frac{dI_\nu}{dr} = 0 \Rightarrow I_\nu(R_\star) = I_\nu(r) = B_\nu(T_\star) \leftarrow$ energy conservation.

Angular size at distance r: $\sin\alpha = \frac{R_\star}{r}$.

Flux at r: $F_\nu(r) = \int_0^{2\pi}\int_0^{\alpha} I_\nu \cos\theta \, d\theta \, d\phi = 2\pi B_\nu(T_\star)\int_0^{\alpha}\cos\theta\sin\theta d\theta = \pi B_\nu(T_\star)\sin^2\alpha$

(Rybicky & Lightman, 1979)

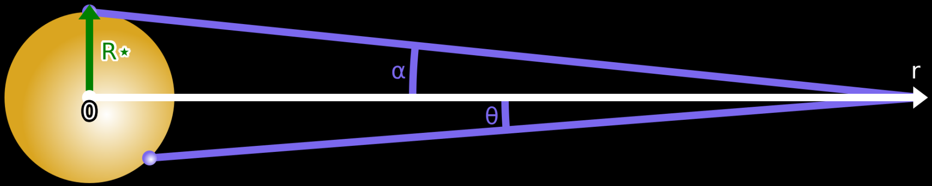

Transfer equation: $\frac{\mathrm{d}I_\nu}{\mathrm{d}r} = 0 \Rightarrow I_\nu(R_\star) = I_\nu(r) = B_\nu(T_\star) \leftarrow$ energy conservation.

Angular size at distance r: $\sin\alpha = \frac{R_\star}{r}$.

Flux at r: $F_\nu(r) = \int_0^{2\pi}\int_0^{\alpha} I_\nu \cos\theta \,\mathrm{d}\theta\,\mathrm{d}\phi = 2\pi B_\nu(T_\star)\int_0^{\alpha}\cos\theta\sin\theta\mathrm{d}\theta = \pi B_\nu(T_\star)\sin^2\alpha$

$$\Rightarrow \boxed{F_\nu(r) = \pi B_\nu(T_\star)\left(\frac{R_\star}{r}\right)^2}.$$

(Rybicky & Lightman, 1979)

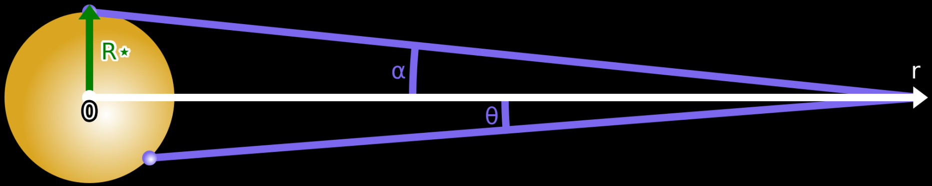

Transfer equation: $\frac{\mathrm{d}I_\nu}{\mathrm{d}r} = 0 \Rightarrow I_\nu(R_\star) = I_\nu(r) = B_\nu(T_\star) \leftarrow$ energy conservation.

Angular size at distance r: $\sin\alpha = \frac{R_\star}{r}$.

Flux at r: $F_\nu(r) \;=\; \int_0^{2\pi}\int_0^{\alpha} I_\nu \cos\theta \,\mathrm{d}\theta\,\mathrm{d}\phi \;=\; 2\pi B_\nu(T_\star)\int_0^{\alpha}\cos\theta\sin\theta\mathrm{d}\theta \;=\; \pi B_\nu(T_\star)\sin^2\alpha$

$$\Rightarrow \boxed{F_\nu(r) = \pi B_\nu(T_\star)\left(\frac{R_\star}{r}\right)^2}.$$

Consistency check: $F_\nu(R_\star) = \pi B_\nu(T_\star)$

(Rybicky & Lightman, 1979)

Emission only

Transfer | Analytical Solutions: Emission or Absorption

Emission only

Emission only

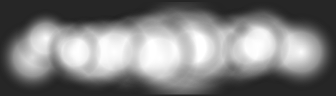

Hypothesis: homogeneous dust cloud of grains at thermal equilibrium, $T = T_{\mathrm{d}}$, with opacity κ.

Emission only

Hypothesis: homogeneous dust cloud of grains at thermal equilibrium, $T = T_{\rm d}$, with opacity κ.

Emission only

Hypothesis: homogeneous dust cloud of grains at thermal equilibrium, $T = T_{\rm d}$, with opacity κ.

Transfer equation: $\frac{{\rm d}I_\nu}{{\rm d}l} = \rho(l)\kappa B_\nu(T_{\rm d})$.

Emission only

Hypothesis: homogeneous dust cloud of grains at thermal equilibrium, $T = T_{\rm d}$, with opacity κ.

Transfer equation: $\dfrac{{\rm d}I_\nu}{{\rm d}l} = \rho(l)\kappa B_\nu(T_{\rm d})$.

Surface brightness: $I_\nu(L) = \kappa B_\nu(T_{\rm d}) \displaystyle\int_o^L \rho(l)\,{\rm d}l = \langle\rho\rangle\kappa L \times B_\nu(T_{\rm d})$

Emission only

Hypothesis: homogeneous dust cloud of grains at thermal equilibrium, $T = T_{\rm d}$, with opacity κ.

Transfer equation: $\dfrac{\mathrm{d}I_\nu}{\mathrm{d}l} = \rho(l)\kappa B_\nu(T_{\rm d})$.

Surface brightness: $I_\nu(L) = \kappa B_\nu(T_{\rm d}) \displaystyle\int_o^L \rho(l)\,\mathrm{d}l = \langle\rho\rangle\kappa L \times B_\nu(T_{\rm d}) \Leftrightarrow \boxed{I_\nu(L) = \tau(L) \times B_\nu(T_{\rm d})}$.

Emission only

Hypothesis: homogeneous dust cloud of grains at thermal equilibrium, $T = T_{\rm d}$, with opacity κ.

Transfer equation: $\frac{{\rm d}I_\nu}{{\rm d}l} = \rho(l)\kappa B_\nu(T_{\rm d})$.

Surface brightness: $I_\nu(L) = \kappa B_\nu(T_{\rm d})\int_o^L \rho(l)\,{\rm d}l = \langle\rho\rangle\kappa L \times B_\nu(T_{\rm d}) \Leftrightarrow \boxed{I_\nu(L) = \tau(L)\times B_\nu(T_{\rm d})}$.

Absorption only

Emission only

Hypothesis: homogeneous dust cloud of grains at thermal equilibrium, $T = T_\mathrm{d}$, with opacity κ.

Transfer equation: $\dfrac{\mathrm{d}I_\nu}{\mathrm{d}l} = \rho(l)\kappa B_\nu(T_\mathrm{d})$.

Surface brightness: $I_\nu(L) = \kappa B_\nu(T_\mathrm{d}) \displaystyle\int_o^L \rho(l)\,\mathrm{d}l = \langle\rho\rangle\kappa L \times B_\nu(T_\mathrm{d}) \Leftrightarrow \boxed{I_\nu(L) = \tau(L) \times B_\nu(T_\mathrm{d})}$.

Absorption only

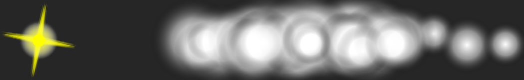

Emission only

Hypothesis: homogeneous dust cloud of grains at thermal equilibrium, $T = T_\mathrm{d}$, with opacity κ.

Transfer equation: $\frac{\mathrm{d}I_\nu}{\mathrm{d}l} = \rho(l)\kappa B_\nu(T_\mathrm{d})$.

Surface brightness: $I_\nu(L) = \kappa B_\nu(T_\mathrm{d}) \int_o^L \rho(l)\,\mathrm{d}l = \langle\rho\rangle\kappa L \times B_\nu(T_\mathrm{d}) \Leftrightarrow \boxed{I_\nu(L) = \tau(L) \times B_\nu(T_\mathrm{d})}$.

Absorption only

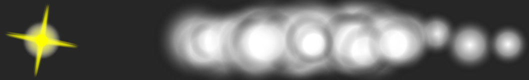

Hypothesis: dust cloud, with opacity κ, in front of a star of specific intensity $I_\nu^\star$.

Transfer | Analytical Solutions: Emission or Absorption

Emission only

Hypothesis: homogeneous dust cloud of grains at thermal equilibrium, $T = T_{\rm d}$, with opacity κ.

Transfer equation: $\frac{{\rm d}I_\nu}{{\rm d}l} = \rho(l)\kappa B_\nu(T_{\rm d})$.

Surface brightness: $I_\nu(L) = \kappa B_\nu(T_{\rm d}) \int_o^L \rho(l)\,{\rm d}l = \langle\rho\rangle\kappa L \times B_\nu(T_{\rm d}) \Leftrightarrow \boxed{I_\nu(L) = \tau(L) \times B_\nu(T_{\rm d})}$.

Absorption only

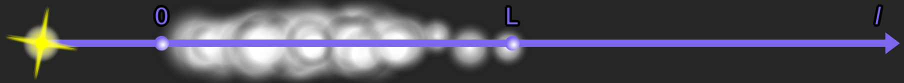

Hypothesis: dust cloud, with opacity κ, in front of a star of specific intensity $I_\nu^\star$.

Emission only

Hypothesis: homogeneous dust cloud of grains at thermal equilibrium, $T = T_\mathrm{d}$, with opacity κ.

Transfer equation: $\frac{\mathrm{d}I_\nu}{\mathrm{d}l} = \rho(l)\kappa B_\nu(T_\mathrm{d})$.

Surface brightness: $I_\nu(L) = \kappa B_\nu(T_\mathrm{d}) \int_o^L \rho(l)\,\mathrm{d}l = \langle\rho\rangle\kappa L \times B_\nu(T_\mathrm{d}) \Leftrightarrow \boxed{I_\nu(L) = \tau(L) \times B_\nu(T_\mathrm{d})}$.

Absorption only

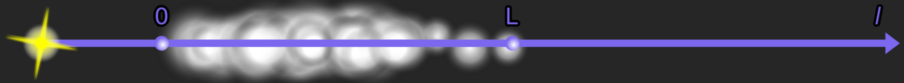

Hypothesis: dust cloud, with opacity κ, in front of a star of specific intensity $I_\nu^\star$.

Transfer equation: $\frac{\mathrm{d}I_\nu}{\mathrm{d}l} = -\alpha(l)I_\nu$

Emission only

Hypothesis: homogeneous dust cloud of grains at thermal equilibrium, $T = T_\mathrm{d}$, with opacity κ.

Transfer equation: $\frac{\mathrm{d}I_\nu}{\mathrm{d}l} = \rho(l)\kappa B_\nu(T_\mathrm{d})$.

Surface brightness: $I_\nu(L) = \kappa B_\nu(T_\mathrm{d}) \int_o^L \rho(l)\,\mathrm{d}l = \langle\rho\rangle\kappa L \times B_\nu(T_\mathrm{d}) \Leftrightarrow \boxed{I_\nu(L) = \tau(L) \times B_\nu(T_\mathrm{d})}$.

Absorption only

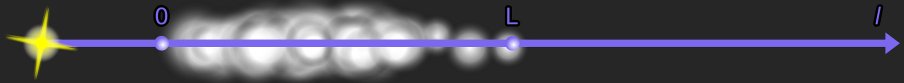

Hypothesis: dust cloud, with opacity κ, in front of a star of specific intensity $I_\nu^\star$.

Transfer equation: $\frac{\mathrm{d}I_\nu}{\mathrm{d}l} = -\alpha(l)I_\nu \Rightarrow I_\nu = I_\nu^\star \exp\left[-\kappa \int_0^L \alpha\,\mathrm{d}l\right]$

Emission only

Hypothesis: homogeneous dust cloud of grains at thermal equilibrium, $T = T_\mathrm{d}$, with opacity κ.

Transfer equation: $\frac{\mathrm{d}I_\nu}{\mathrm{d}l} = \rho(l)\kappa B_\nu(T_\mathrm{d})$.

Surface brightness: $I_\nu(L) = \kappa B_\nu(T_\mathrm{d}) \int_o^L \rho(l)\,\mathrm{d}l = \langle\rho\rangle\kappa L \times B_\nu(T_\mathrm{d}) \Leftrightarrow \boxed{I_\nu(L) = \tau(L) \times B_\nu(T_\mathrm{d})}$.

Absorption only

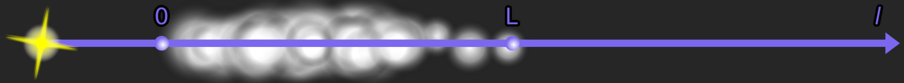

Hypothesis: dust cloud, with opacity κ, in front of a star of specific intensity $I_\nu^\star$.

Transfer equation: $\frac{\mathrm{d}I_\nu}{\mathrm{d}l} = -\alpha(l)I_\nu \Rightarrow I_\nu = I_\nu^\star \exp\left[-\kappa \int_0^L \alpha\,\mathrm{d}l\right] \Leftrightarrow \boxed{I_\nu(l) = I_\nu^\star \exp\left[-\tau(L)\right]}$.

Transfer equation: can be simplified using τ instead of l as a parameter: $\frac{dI_\nu}{d\tau} = -I_\nu + \underbrace{S_\nu}_{\text{source function}}$.

Transfer equation: can be simplified using τ instead of l as a parameter: $\frac{\mathrm{d}I_\nu}{\mathrm{d}\tau} = -I_\nu + \underbrace{S_\nu}_{\text{source function}}$.

Solution: $I_\nu(\tau) = I_\nu^\star \exp(-\tau) + \int_0^\tau \exp(\tau' - \tau) \times S_\nu(\tau')\,\mathrm{d}\tau'$

Transfer equation: can be simplified using τ instead of l as a parameter: $\frac{\mathrm{d}I_\nu}{\mathrm{d}\tau} = -I_\nu + \underbrace{S_\nu}_{\text{source function}}$.

Solution: $I_\nu(\tau) = I_\nu^\star \exp(-\tau) + \int_0^\tau \exp(\tau' - \tau) \times S_\nu(\tau')\,\mathrm{d}\tau'$

$\Rightarrow I_\nu = \underbrace{I_\nu^\star \exp(-\tau)}_{\text{stellar extinction}} +$

Transfer equation: can be simplified using τ instead of l as a parameter: $\frac{\mathrm{d}I_\nu}{\mathrm{d}\tau} = -I_\nu + \underbrace{S_\nu}_{\text{source function}}$.

Solution: $I_\nu(\tau) = I_\nu^\star \exp(-\tau) + \int_0^\tau \exp(\tau' - \tau) \times S_\nu(\tau')\,\mathrm{d}\tau'$

$$\Rightarrow I_\nu = \underbrace{I_\nu^\star \exp(-\tau)}_{\text{stellar extinction}} + \underbrace{B_\nu(T_\mathrm{d}) \times [1 - \exp(-\tau)]}_{\text{cloud self-absorption}}.$$

Transfer | Analytical Solutions: Emission & Absorption

Transfer equation: can be simplified using τ instead of l as a parameter: $\frac{dI_\nu}{d\tau} = -I_\nu + \underbrace{S_\nu}_{\text{source function}}$.

Solution: $I_\nu(\tau) = I_\nu^\star \exp(-\tau) + \int_0^\tau \exp(\tau' - \tau) \times S_\nu(\tau')\,d\tau'$

$$\Rightarrow I_\nu = \underbrace{I_\nu^\star \exp(-\tau)}_{\text{stellar extinction}} + \underbrace{B_\nu(T_\mathrm{d}) \times [1 - \exp(-\tau)]}_{\text{cloud self-absorption}}.$$

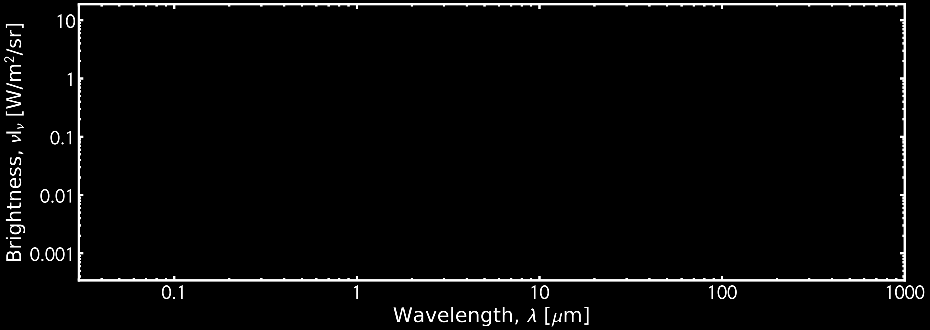

Transfer equation: can be simplified using τ instead of l as a parameter: $\frac{dI_\nu}{d\tau} = -I_\nu + \underbrace{S_\nu}_{\text{source function}}$.

Solution: $I_\nu(\tau) = I_\nu^\star \exp(-\tau) + \int_0^\tau \exp(\tau' - \tau) \times S_\nu(\tau')\, d\tau'$

$$\Rightarrow I_\nu = \underbrace{I_\nu^\star \exp(-\tau)}_{\text{stellar extinction}} + \underbrace{B_\nu(T_d) \times [1 - \exp(-\tau)]}_{\text{cloud self-absorption}}.$$

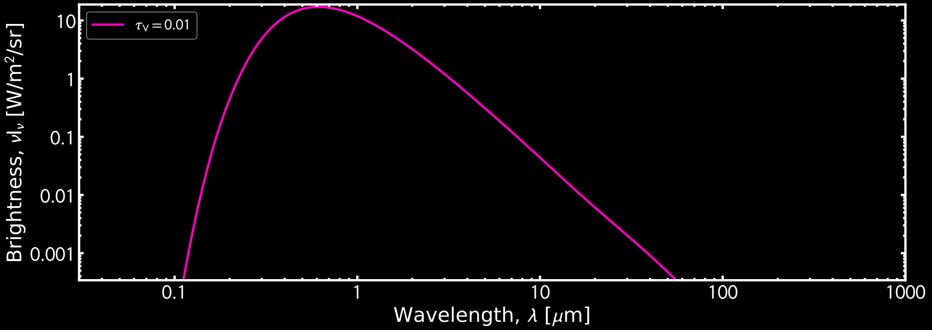

Transfer equation: can be simplified using τ instead of l as a parameter: $\frac{dI_\nu}{d\tau} = -I_\nu + \underbrace{S_\nu}_{\text{source function}}$.

Solution: $I_\nu(\tau) = I_\nu^\star \exp(-\tau) + \int_0^\tau \exp(\tau' - \tau) \times S_\nu(\tau')\, d\tau'$

$$\Rightarrow I_\nu = \underbrace{I_\nu^\star \exp(-\tau)}_{\text{stellar extinction}} + \underbrace{B_\nu(T_d) \times [1 - \exp(-\tau)]}_{\text{cloud self-absorption}}.$$

Optically thin: $\tau \ll 1 \Rightarrow I_\nu^{\text{cloud}} \simeq \tau B_\nu(T_d) \rightarrow$ "*grey body*".

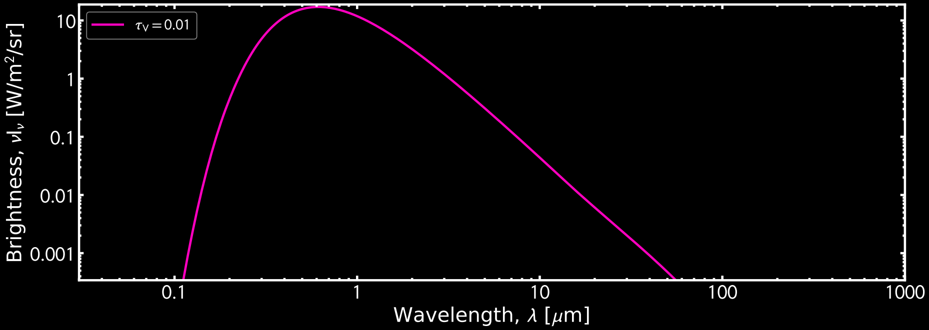

Transfer equation: can be simplified using τ instead of l as a parameter: $\frac{\mathrm{d}I_\nu}{\mathrm{d}\tau} = -I_\nu + \underbrace{S_\nu}_{\text{source function}}$.

Solution: $I_\nu(\tau) = I_\nu^\star \exp(-\tau) + \int_0^\tau \exp(\tau' - \tau) \times S_\nu(\tau')\,\mathrm{d}\tau'$

$$\Rightarrow I_\nu = \underbrace{I_\nu^\star \exp(-\tau)}_{\text{stellar extinction}} + \underbrace{B_\nu(T_\mathrm{d}) \times [1 - \exp(-\tau)]}_{\text{cloud self-absorption}}.$$

Optically thin: $\tau \ll 1 \Rightarrow I_\nu^{\mathrm{cloud}} \simeq \tau B_\nu(T_\mathrm{d}) \rightarrow$ "*grey body*".

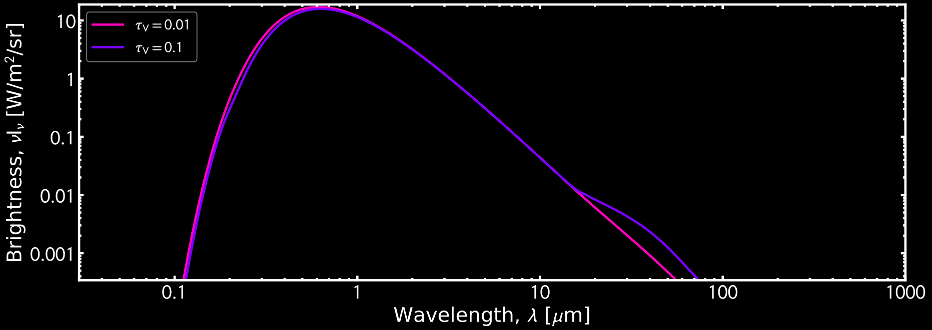

Transfer equation: can be simplified using τ instead of l as a parameter: $\frac{\mathrm{d}I_\nu}{\mathrm{d}\tau} = -I_\nu + \underbrace{S_\nu}_{\text{source function}}$.

Solution: $I_\nu(\tau) = I_\nu^\star \exp(-\tau) + \int_0^\tau \exp(\tau' - \tau) \times S_\nu(\tau')\,\mathrm{d}\tau'$

$$\Rightarrow I_\nu = \underbrace{I_\nu^\star \exp(-\tau)}_{\text{stellar extinction}} + \underbrace{B_\nu(T_\mathrm{d}) \times [1 - \exp(-\tau)]}_{\text{cloud self-absorption}}.$$

Optically thin: $\tau \ll 1 \Rightarrow I_\nu^{\text{cloud}} \simeq \tau B_\nu(T_\mathrm{d}) \rightarrow$ "*grey body*".

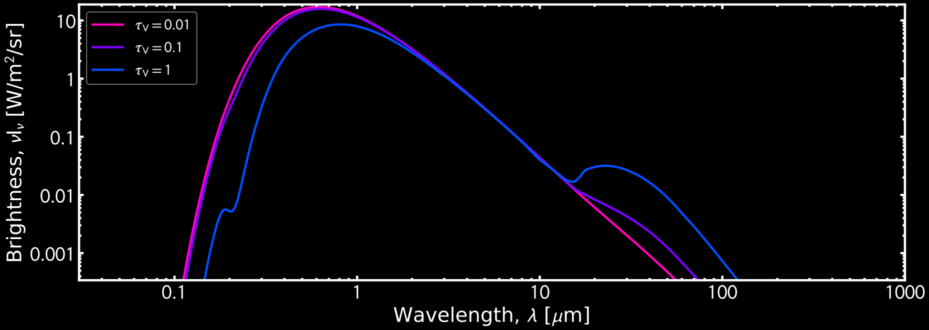

Transfer equation: can be simplified using τ instead of l as a parameter: $\frac{dI_\nu}{d\tau} = -I_\nu + \underbrace{S_\nu}_{\text{source function}}$.

Solution: $I_\nu(\tau) = I_\nu^\star \exp(-\tau) + \int_0^\tau \exp(\tau' - \tau) \times S_\nu(\tau')\, d\tau'$

$$\Rightarrow I_\nu = \underbrace{I_\nu^\star \exp(-\tau)}_{\text{stellar extinction}} + \underbrace{B_\nu(T_d) \times [1 - \exp(-\tau)]}_{\text{cloud self-absorption}}.$$

Optically thin: $\tau \ll 1 \Rightarrow I_\nu^{\text{cloud}} \simeq \tau B_\nu(T_d) \rightarrow$ "*grey body*".

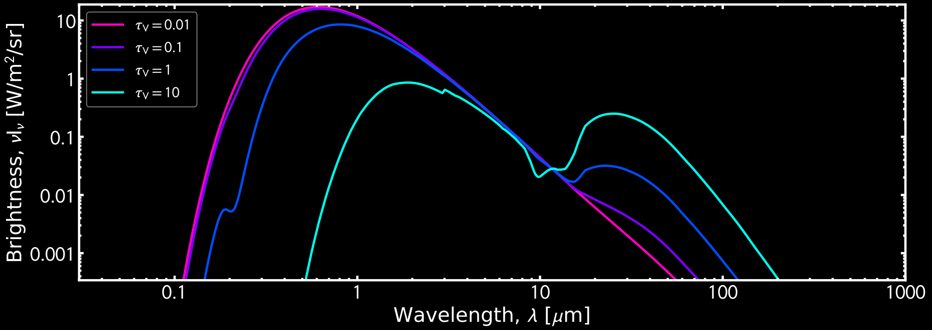

Transfer equation: can be simplified using τ instead of l as a parameter: $\frac{dI_\nu}{d\tau} = -I_\nu + \underbrace{S_\nu}_{\text{source function}}$.

Solution: $I_\nu(\tau) = I_\nu^\star \exp(-\tau) + \int_0^\tau \exp(\tau' - \tau) \times S_\nu(\tau')\,d\tau'$

$$\Rightarrow I_\nu = \underbrace{I_\nu^\star \exp(-\tau)}_{\text{stellar extinction}} + \underbrace{B_\nu(T_d) \times [1 - \exp(-\tau)]}_{\text{cloud self-absorption}}.$$

Optically thin: $\tau \ll 1 \Rightarrow I_\nu^{\text{cloud}} \simeq \tau B_\nu(T_d) \rightarrow$ "*grey body*".

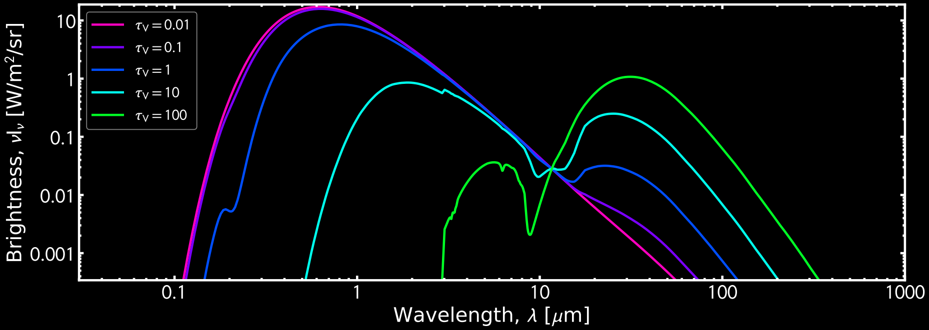

Transfer equation: can be simplified using τ instead of l as a parameter: $\frac{\mathrm{d}I_\nu}{\mathrm{d}\tau} = -I_\nu + \underbrace{S_\nu}_{\text{source function}}$.

Solution: $I_\nu(\tau) = I_\nu^\star \exp(-\tau) + \int_0^\tau \exp(\tau' - \tau) \times S_\nu(\tau')\,\mathrm{d}\tau'$

$$\Rightarrow I_\nu = \underbrace{I_\nu^\star \exp(-\tau)}_{\text{stellar extinction}} + \underbrace{B_\nu(T_\mathrm{d}) \times [1 - \exp(-\tau)]}_{\text{cloud self-absorption}}.$$

Optically thin: $\tau \ll 1 \Rightarrow I_\nu^{\text{cloud}} \simeq \tau B_\nu(T_\mathrm{d}) \rightarrow$ "*grey body*".

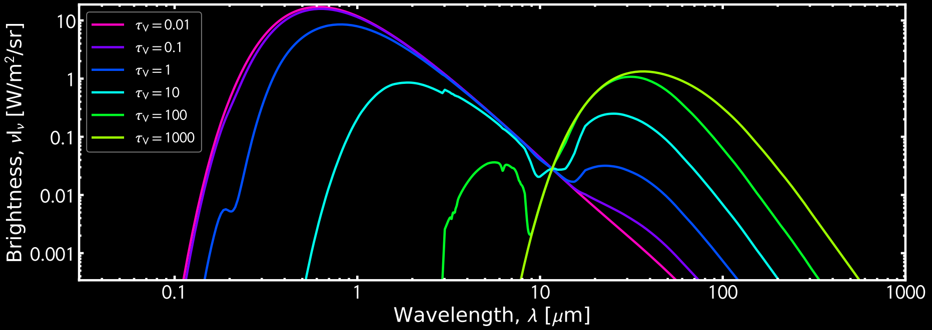

Transfer equation: can be simplified using τ instead of l as a parameter: $\frac{\mathrm{d}I_\nu}{\mathrm{d}\tau} = -I_\nu + \underbrace{S_\nu}_{\text{source function}}$.

Solution: $I_\nu(\tau) = I_\nu^\star \exp(-\tau) + \int_0^\tau \exp(\tau' - \tau) \times S_\nu(\tau')\,\mathrm{d}\tau'$

$$\Rightarrow I_\nu = \underbrace{I_\nu^\star \exp(-\tau)}_{\text{stellar extinction}} + \underbrace{B_\nu(T_\mathrm{d}) \times [1 - \exp(-\tau)]}_{\text{cloud self-absorption}}.$$

Optically thin: $\tau \ll 1 \Rightarrow I_\nu^{\text{cloud}} \simeq \tau B_\nu(T_\mathrm{d}) \rightarrow$ "*grey body*".

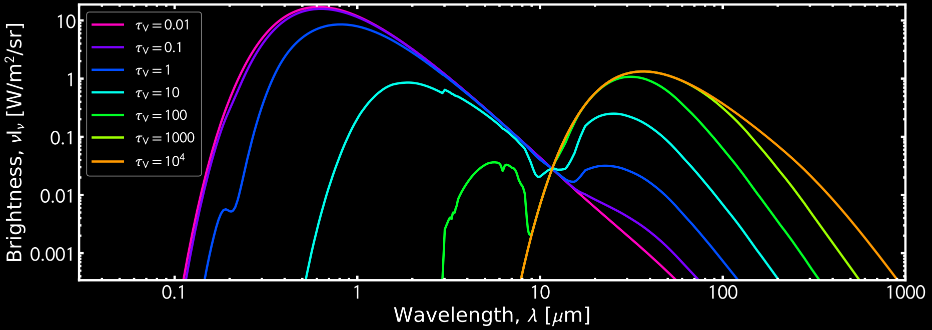

Transfer equation: can be simplified using τ instead of l as a parameter: $\frac{\mathrm{d}I_\nu}{\mathrm{d}\tau} = -I_\nu + \underbrace{S_\nu}_{\text{source function}}$.

Solution: $I_\nu(\tau) = I_\nu^\star \exp(-\tau) + \int_0^\tau \exp(\tau' - \tau) \times S_\nu(\tau')\,\mathrm{d}\tau'$

$$\Rightarrow I_\nu = \underbrace{I_\nu^\star \exp(-\tau)}_{\text{stellar extinction}} + \underbrace{B_\nu(T_\mathrm{d}) \times [1 - \exp(-\tau)]}_{\text{cloud self-absorption}}.$$

Optically thin: $\tau \ll 1 \Rightarrow I_\nu^{\text{cloud}} \simeq \tau B_\nu(T_\mathrm{d}) \rightarrow$ "*grey body*".

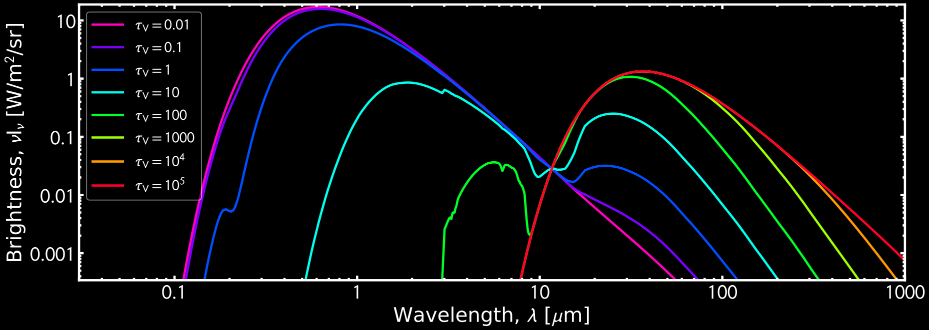

Transfer equation: can be simplified using τ instead of l as a parameter: $\frac{\mathrm{d}I_\nu}{\mathrm{d}\tau} = -I_\nu + \underbrace{S_\nu}_{\text{source function}}$.

Solution: $I_\nu(\tau) = I_\nu^\star \exp(-\tau) + \int_0^\tau \exp(\tau' - \tau) \times S_\nu(\tau')\,\mathrm{d}\tau'$

$$\Rightarrow I_\nu = \underbrace{I_\nu^\star \exp(-\tau)}_{\text{stellar extinction}} + \underbrace{B_\nu(T_\mathrm{d}) \times [1 - \exp(-\tau)]}_{\text{cloud self-absorption}}.$$

Optically thin: $\tau \ll 1 \Rightarrow I_\nu^{\text{cloud}} \simeq \tau B_\nu(T_\mathrm{d}) \rightarrow$ "*grey body*".

Optically thick: $\tau \gg 1 \Rightarrow I_\nu^{\text{cloud}} \simeq B_\nu(T_\mathrm{d}) \rightarrow$ "*black body*".

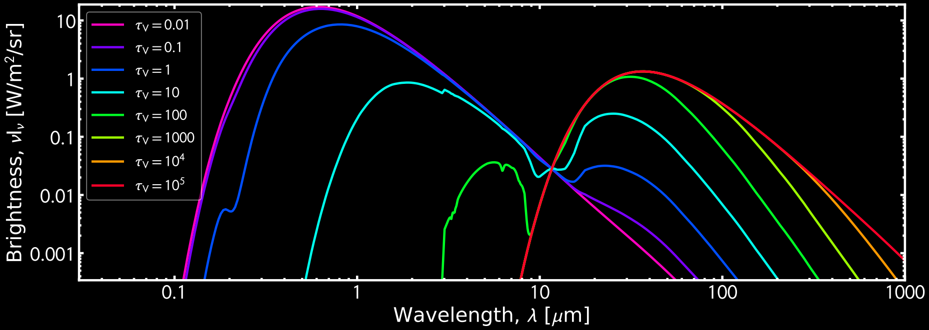

Radiastronomy convention

Radiastronomy convention

Rayleigh-Jeans approximation: $h\nu \ll kT \Rightarrow B_\nu(T) \simeq \frac{2kT\nu^2}{c^2}$.

Radiastronomy convention

Rayleigh-Jeans approximation: $h\nu \ll kT \Rightarrow B_\nu(T) \simeq \frac{2kT\nu^2}{c^2}$.

Brightness temperature: $T_\mathrm{b} \equiv \frac{I_\nu c^2}{2k\nu^2}$.

Radiastronomy convention

Rayleigh-Jeans approximation: $h\nu \ll kT \Rightarrow B_\nu(T) \simeq \frac{2kT\nu^2}{c^2}$.

Brightness temperature: $T_\mathrm{b} \equiv \frac{I_\nu c^2}{2k\nu^2}$.

Measuring H I gas temperature ("*spin temperature*")

Radiastronomy convention

Rayleigh-Jeans approximation: $h\nu \ll kT \Rightarrow B_\nu(T) \simeq \frac{2kT\nu^2}{c^2}$.

Brightness temperature: $T_\mathrm{b} \equiv \frac{I_\nu c^2}{2k\nu^2}$.

Measuring H I gas temperature ("*spin temperature*")

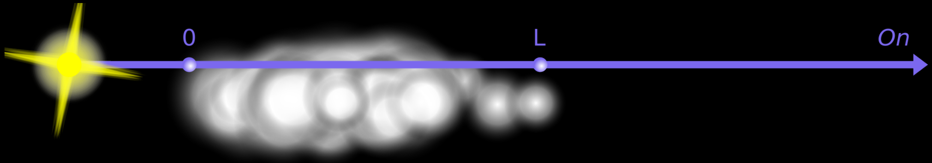

Radiastronomy convention

Rayleigh-Jeans approximation: $h\nu \ll kT \Rightarrow B_\nu(T) \simeq \frac{2kT\nu^2}{c^2}$.

Brightness temperature: $T_\mathrm{b} \equiv \frac{I_\nu c^2}{2k\nu^2}$.

Measuring H I gas temperature ("*spin temperature*")

Background source through a cloud: $T_\mathrm{b}^\mathrm{on} = T_\mathrm{QSO} \exp(-\tau) + T_\mathrm{H\,I}\,[1-\exp(-\tau)]$.

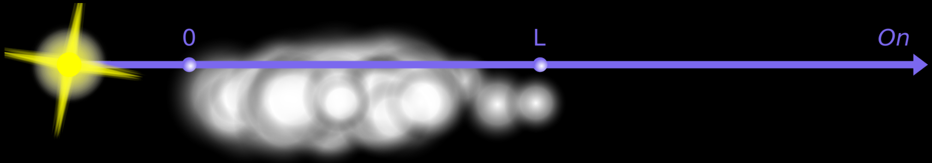

Radiastronomy convention

Rayleigh-Jeans approximation: $h\nu \ll kT \Rightarrow B_\nu(T) \simeq \frac{2kT\nu^2}{c^2}$.

Brightness temperature: $T_\mathrm{b} \equiv \frac{I_\nu c^2}{2k\nu^2}$.

Measuring H I gas temperature ("*spin temperature*")

Background source through a cloud: $T_\mathrm{b}^\mathrm{on} = T_\mathrm{QSO} \exp(-\tau) + T_\mathrm{H\,I}\,[1-\exp(-\tau)]$.

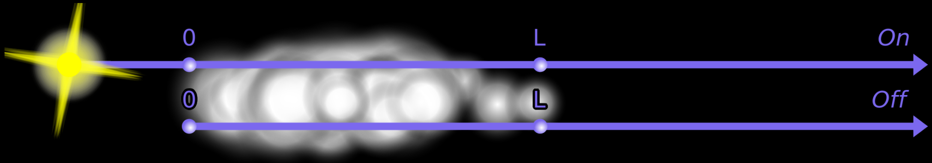

Radiastronomy convention

Rayleigh-Jeans approximation: $h\nu \ll kT \Rightarrow B_\nu(T) \simeq \frac{2kT\nu^2}{c^2}$.

Brightness temperature: $T_b \equiv \frac{I_\nu c^2}{2k\nu^2}$.

Measuring H I gas temperature ("*spin temperature*")

Background source through a cloud: $T_b^{on} = T_{QSO} \exp(-\tau) + T_{HI}[1 - \exp(-\tau)]$.

Cloud alone: $T_b^{off} = T_{HI}[1 - \exp(-\tau)]$.

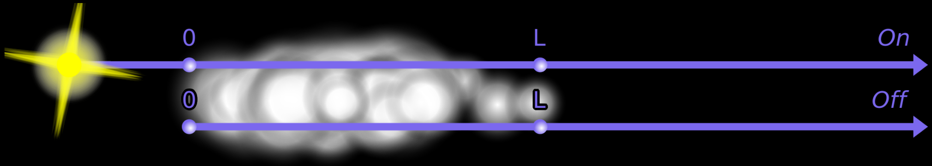

Radiastronomy convention

Rayleigh-Jeans approximation: $h\nu \ll kT \Rightarrow B_\nu(T) \simeq \frac{2kT\nu^2}{c^2}$.

Brightness temperature: $T_\mathrm{b} \equiv \frac{I_\nu c^2}{2k\nu^2}$.

Measuring H I gas temperature ("*spin temperature*")

Background source through a cloud: $T_\mathrm{b}^\mathrm{on} = T_\mathrm{QSO} \exp(-\tau) + T_\mathrm{H\,I}[1-\exp(-\tau)]$.

Cloud alone: $T_\mathrm{b}^\mathrm{off} = T_\mathrm{H\,I}[1-\exp(-\tau)]$.

Solution: (1) $\tau = \ln \frac{T_\mathrm{QSO}}{T_\mathrm{b}^\mathrm{on} - T_\mathrm{b}^\mathrm{off}}$

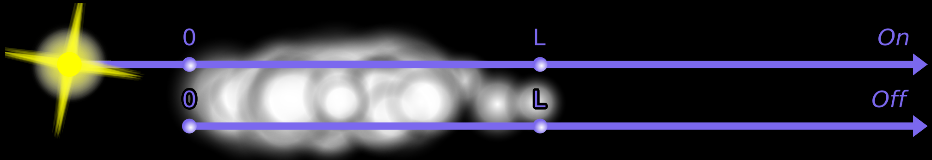

Radiastronomy convention

Rayleigh-Jeans approximation: $h\nu \ll kT \Rightarrow B_\nu(T) \simeq \frac{2kT\nu^2}{c^2}$.

Brightness temperature: $T_\mathrm{b} \equiv \frac{I_\nu c^2}{2k\nu^2}$.

Measuring H I gas temperature ("*spin temperature*")

Background source through a cloud: $T_\mathrm{b}^\mathrm{on} = T_\mathrm{QSO}\exp(-\tau) + T_\mathrm{H\,I}[1-\exp(-\tau)]$.

Cloud alone: $T_\mathrm{b}^\mathrm{off} = T_\mathrm{H\,I}[1-\exp(-\tau)]$.

Solution: (1) $\tau = \ln\frac{T_\mathrm{QSO}}{T_\mathrm{b}^\mathrm{on} - T_\mathrm{b}^\mathrm{off}}$ (2) $T_\mathrm{H\,I} = \frac{T_\mathrm{b}^\mathrm{off}}{1-\exp(-\tau)}$.

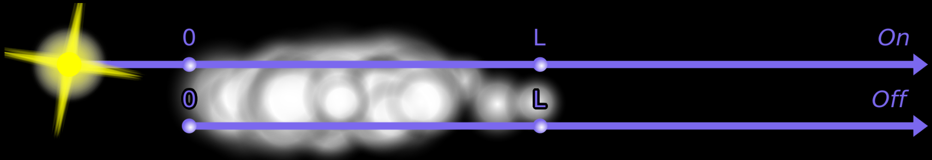

Drawing random photons in an arbitrary geometry

Drawing random photons in an arbitrary geometry

Sources of photons can be stars at any position $\rightarrow$ large number of photons at every wavelength.

Drawing random photons in an arbitrary geometry

Sources of photons can be stars at any position → large number of photons at every wavelength.

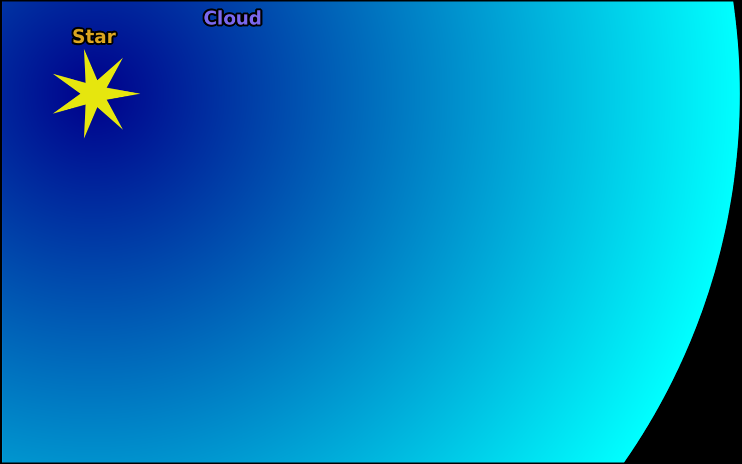

Drawing random photons in an arbitrary geometry

Sources of photons can be stars at any position → large number of photons at every wavelength.

Multiple scattering are then accounted for randomly, keeping in memory the weight of the ray.

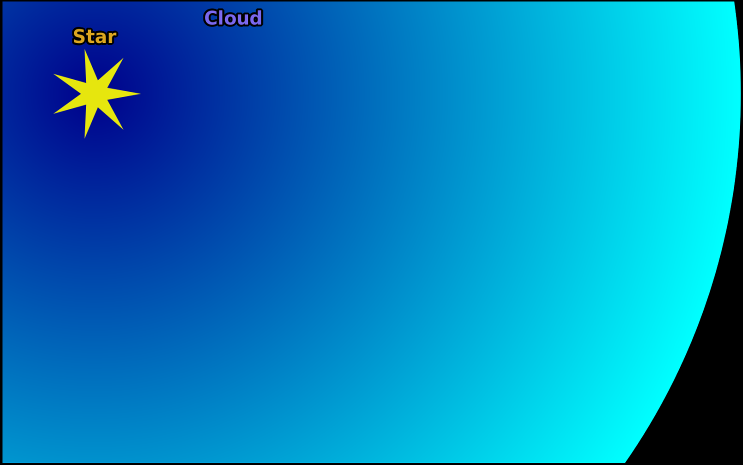

Drawing random photons in an arbitrary geometry

Sources of photons can be stars at any position → large number of photons at every wavelength.

Multiple scattering are then accounted for randomly, keeping in memory the weight of the ray.

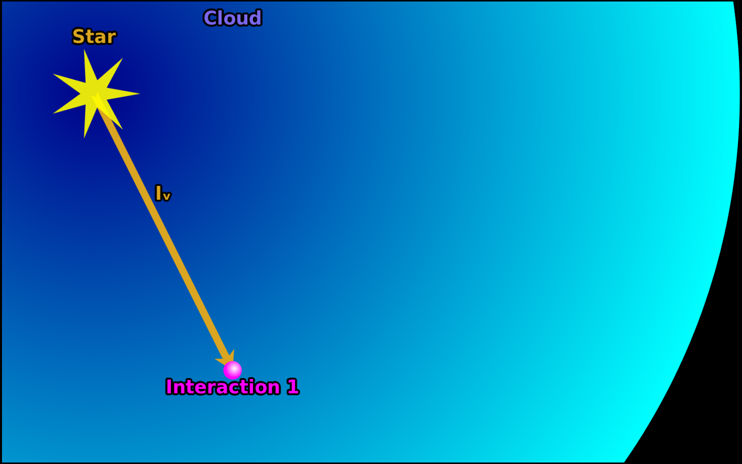

Drawing random photons in an arbitrary geometry

Sources of photons can be stars at any position → large number of photons at every wavelength.

Multiple scattering are then accounted for randomly, keeping in memory the weight of the ray.

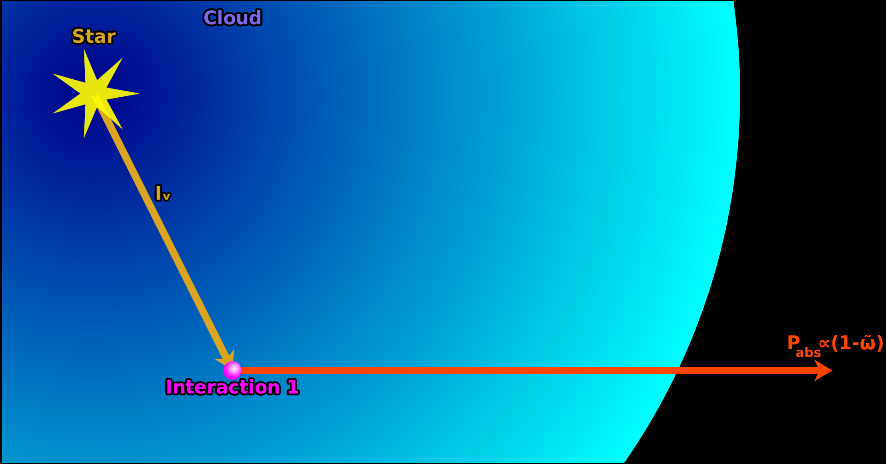

Drawing random photons in an arbitrary geometry

Sources of photons can be stars at any position → large number of photons at every wavelength.

Multiple scattering are then accounted for randomly, keeping in memory the weight of the ray.

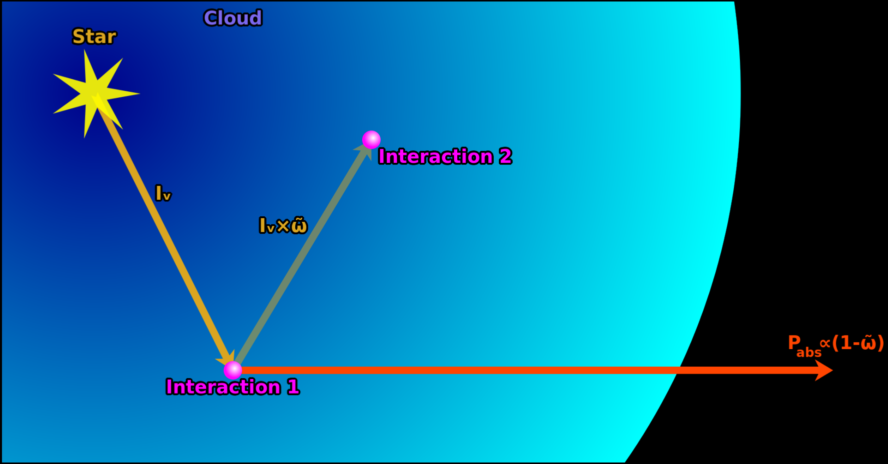

Drawing random photons in an arbitrary geometry

Sources of photons can be stars at any position → large number of photons at every wavelength.

Multiple scattering are then accounted for randomly, keeping in memory the weight of the ray.

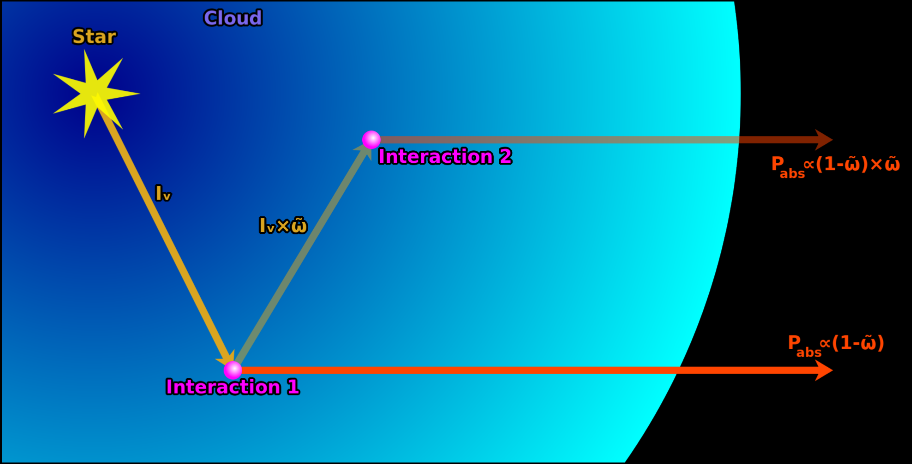

Drawing random photons in an arbitrary geometry

Sources of photons can be stars at any position → large number of photons at every wavelength.

Multiple scattering are then accounted for randomly, keeping in memory the weight of the ray.

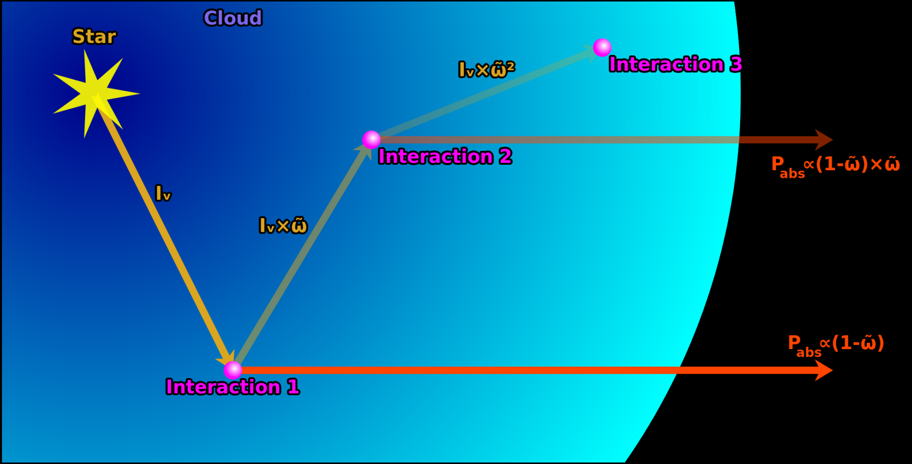

Drawing random photons in an arbitrary geometry

Sources of photons can be stars at any position → large number of photons at every wavelength.

Multiple scattering are then accounted for randomly, keeping in memory the weight of the ray.

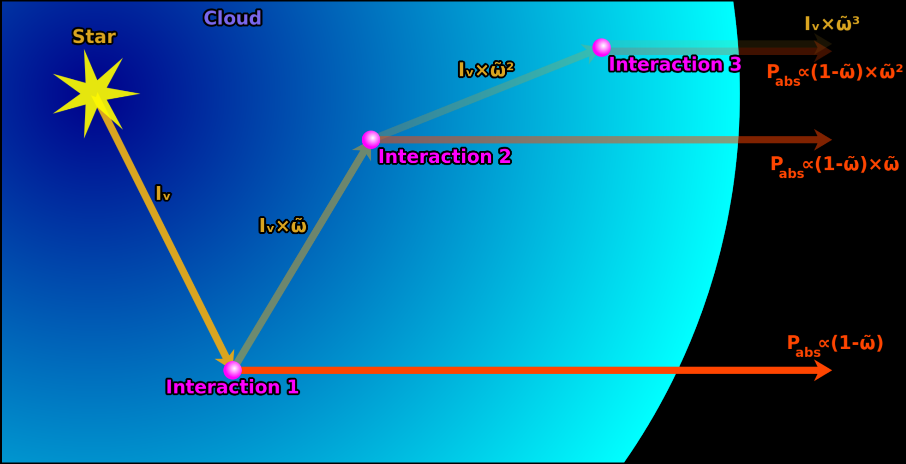

Drawing random photons in an arbitrary geometry

Sources of photons can be stars at any position → large number of photons at every wavelength.

Multiple scattering are then accounted for randomly, keeping in memory the weight of the ray.

Iterative process is required to compute atomic & molecular level populations & dust heating.

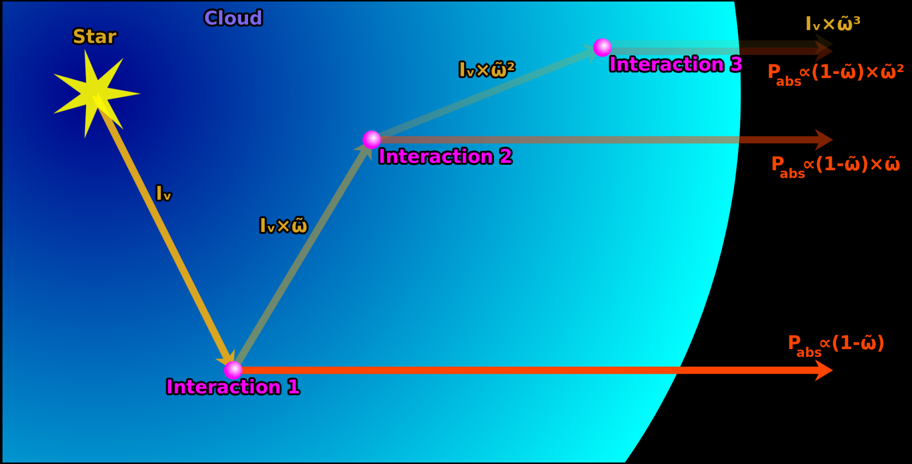

Transfer | Large-Scale Radiative Transfer of Galaxies

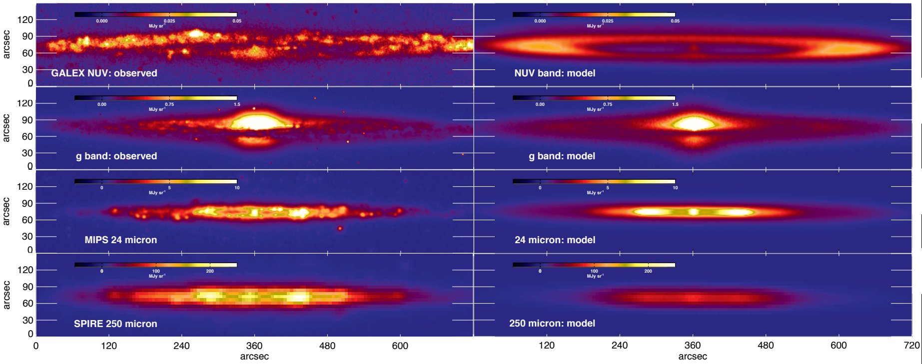

(De Looze et al., 2012)

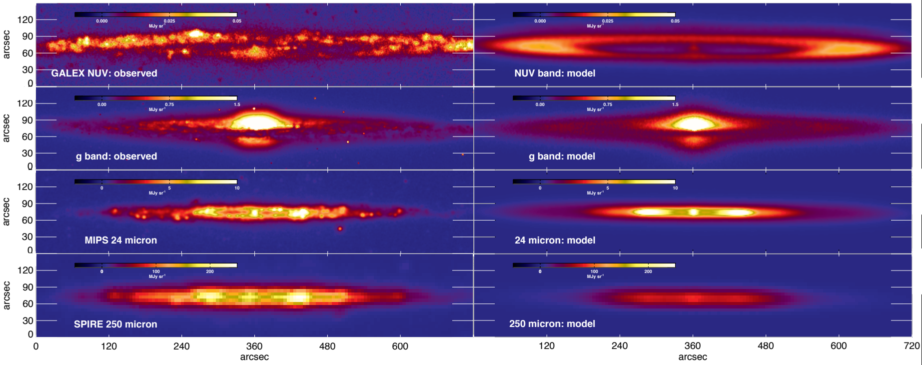

(De Looze et al., 2012)

Usefulness of these models:

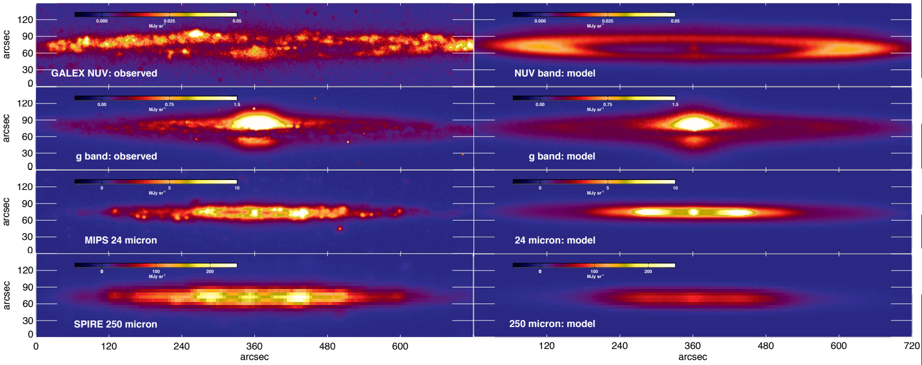

(De Looze et al., 2012)

Usefulness of these models:

1. Large-scale geometry: disk scale-height, opacity, *etc.*

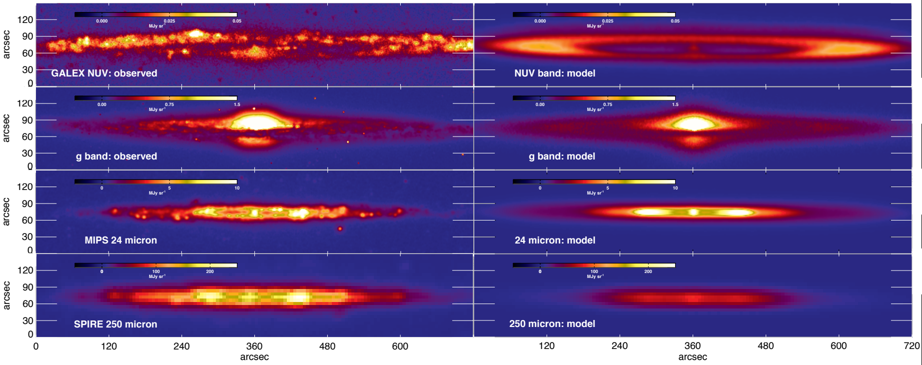

(De Looze et al., 2012)

Usefulness of these models:

1. Large-scale geometry: disk scale-height, opacity, *etc.*
2. Contribution to dust heating of ≠ stellar populations.

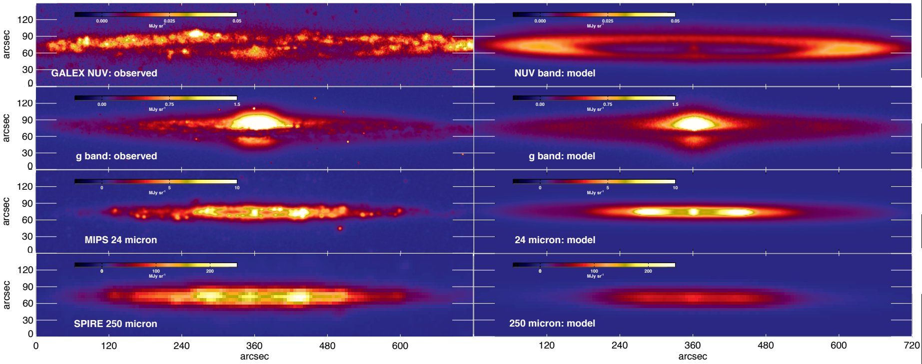

(De Looze et al., 2012)

Usefulness of these models:

1. Large-scale geometry: disk scale-height, opacity, *etc.*
2. Contribution to dust heating of $\neq$ stellar populations.

Simulations:

Monte Carlo radiative transfer models can also be used to post-process numerical simulations of star-forming regions or galaxies $\Rightarrow$ synthetic observables.

Outline of the Lecture

WIM: thermally stable phase ionized by diffuse UV photons escaping from H II regions.

WIM: thermally stable phase ionized by diffuse UV photons escaping from H II regions.

H II regions: short-lived, localized region ionized by nearby star cluster.

WIM: thermally stable phase ionized by diffuse UV photons escaping from H II regions.

H II regions: short-lived, localized region ionized by nearby star cluster.

Credit: IC 1396 (Kallias IOANNIDIS).

WIM: thermally stable phase ionized by diffuse UV photons escaping from H II regions.

H II regions: short-lived, localized region ionized by nearby star cluster.

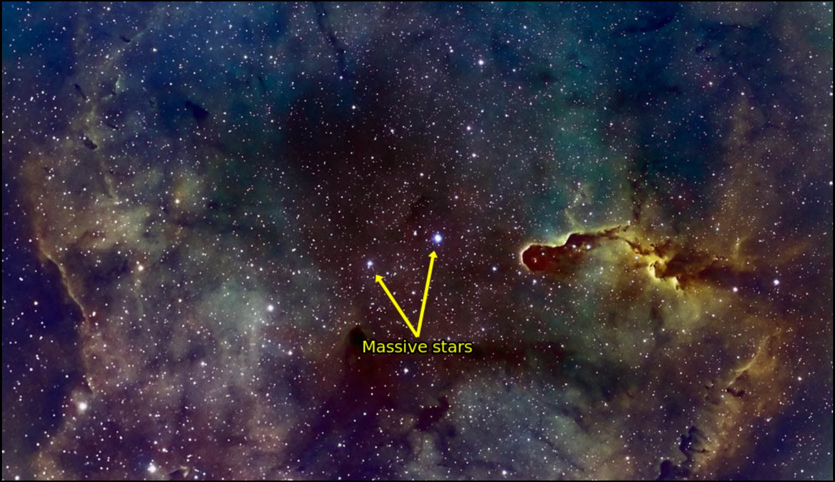

Credit: IC 1396 (Kallias IOANNIDIS).

WIM: thermally stable phase ionized by diffuse UV photons escaping from H II regions.

H II regions: short-lived, localized region ionized by nearby star cluster.

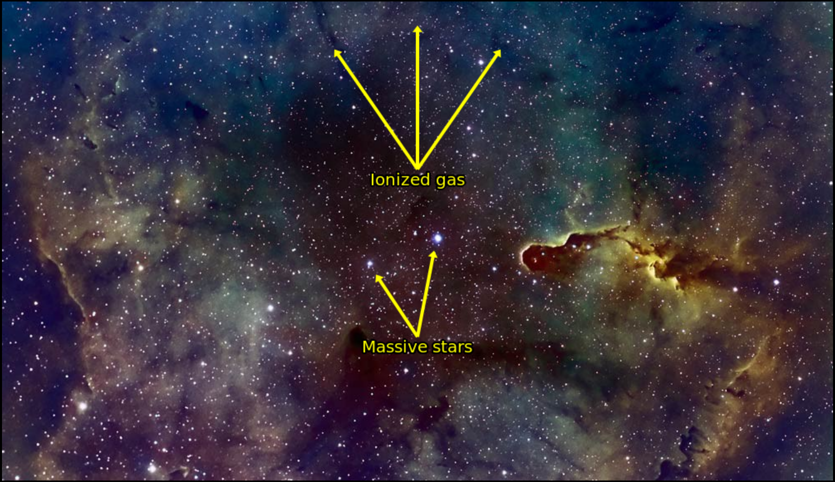

Credit: IC 1396 (Kallias IOANNIDIS).

WIM: thermally stable phase ionized by diffuse UV photons escaping from H II regions.

H II regions: short-lived, localized region ionized by nearby star cluster.

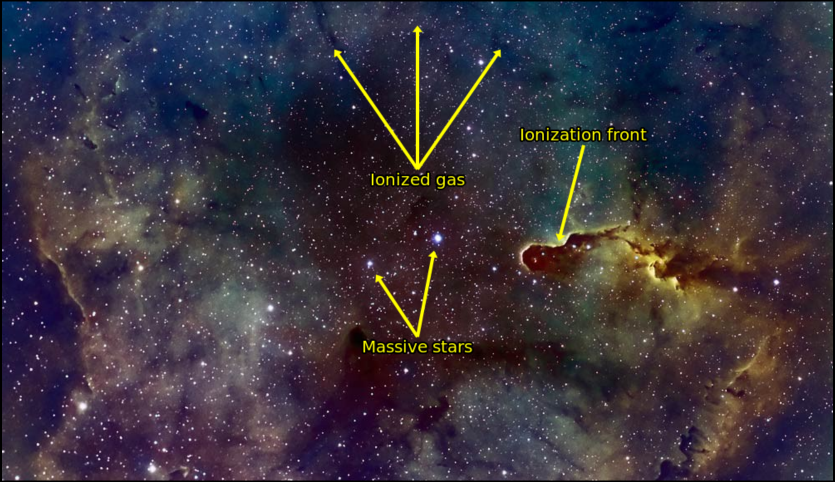

Credit: IC 1396 (Kallias IOANNIDIS).

WIM: thermally stable phase ionized by diffuse UV photons escaping from H II regions.

H II regions: short-lived, localized region ionized by nearby star cluster.

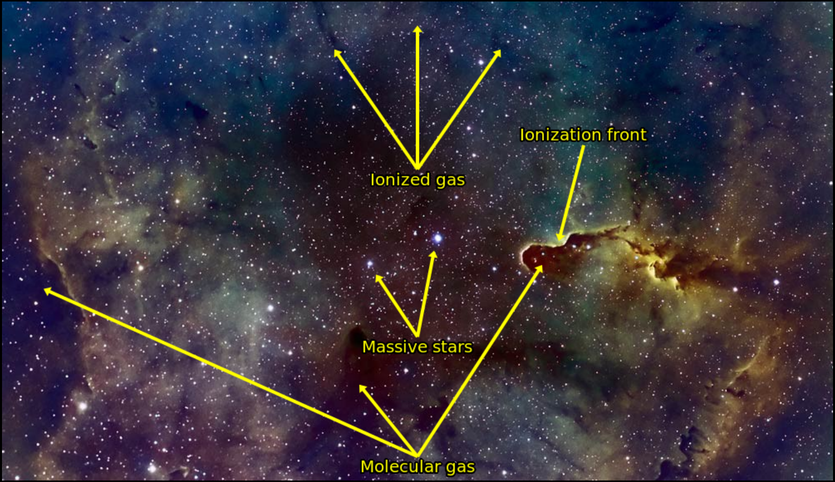

Credit: IC 1396 (Kallias IOANNIDIS).

(Habart et al., 2024)

(Habart et al., 2024)

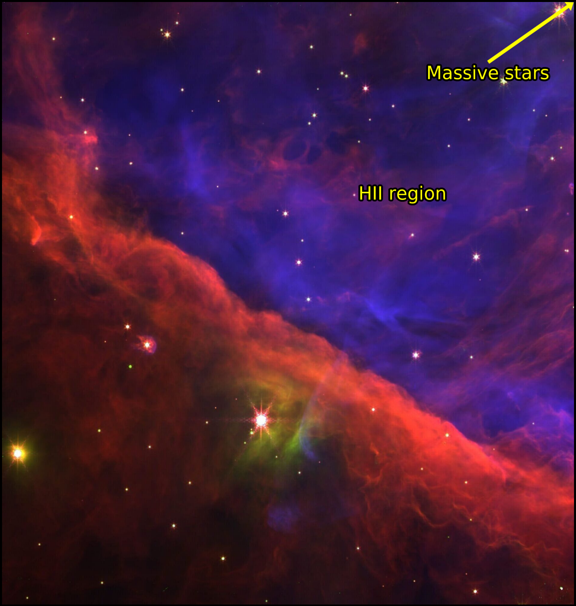

(Habart et al., 2024)

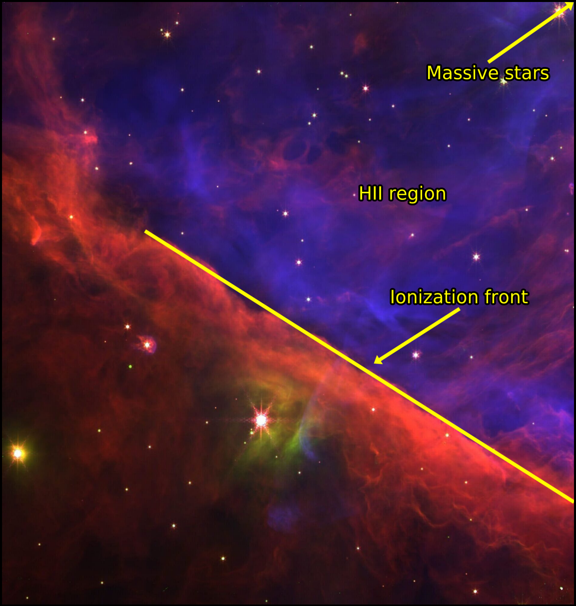

(Habart et al., 2024)

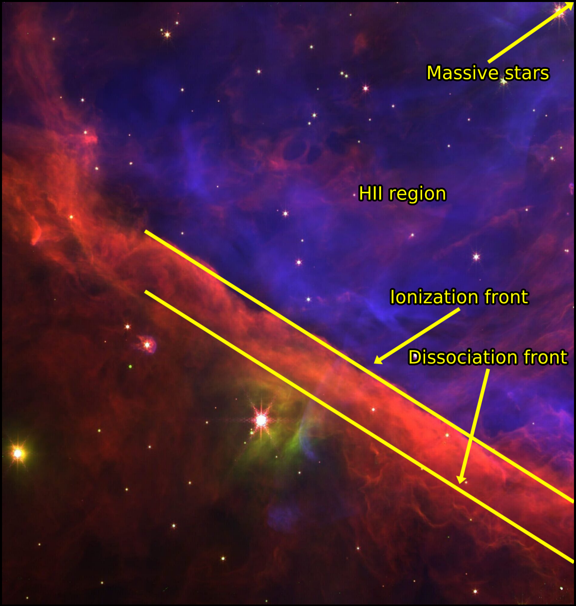

(Habart et al., 2024)

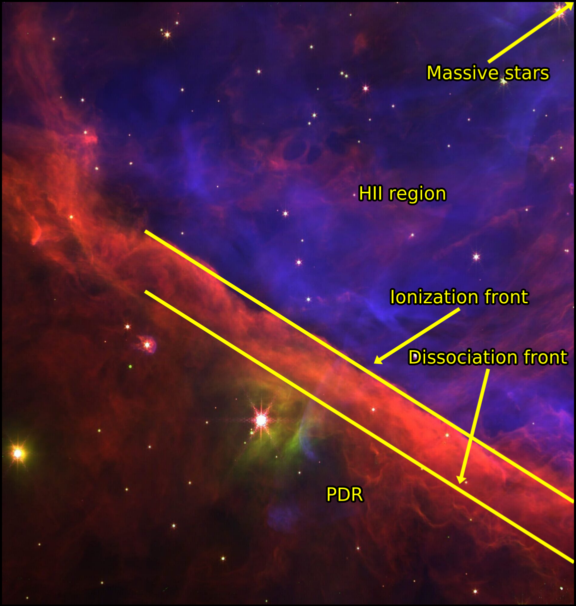

(Habart et al., 2024)

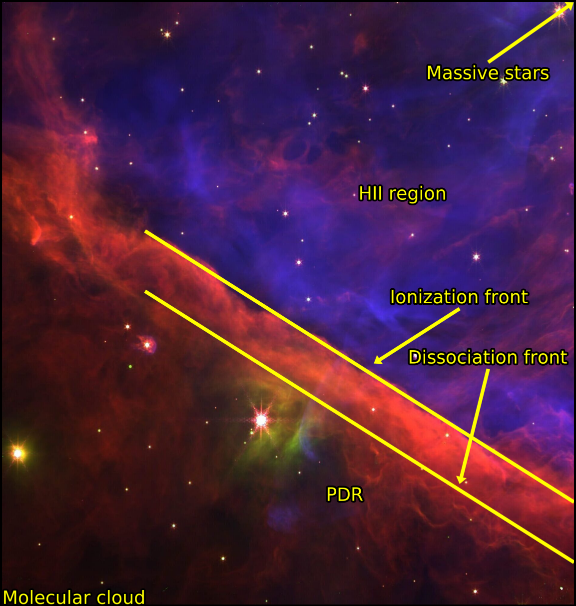

(Habart et al., 2024)

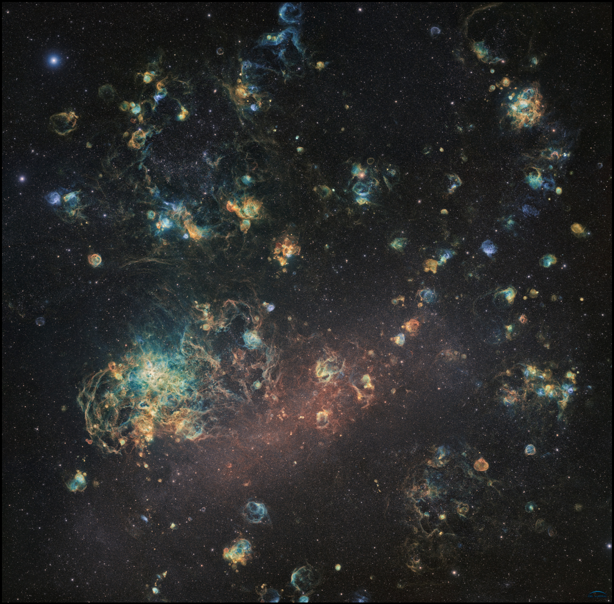

Credit: J. C. Canonne, N. Outters, P. Bernhard, D. Chaplain, L. Bourgon.

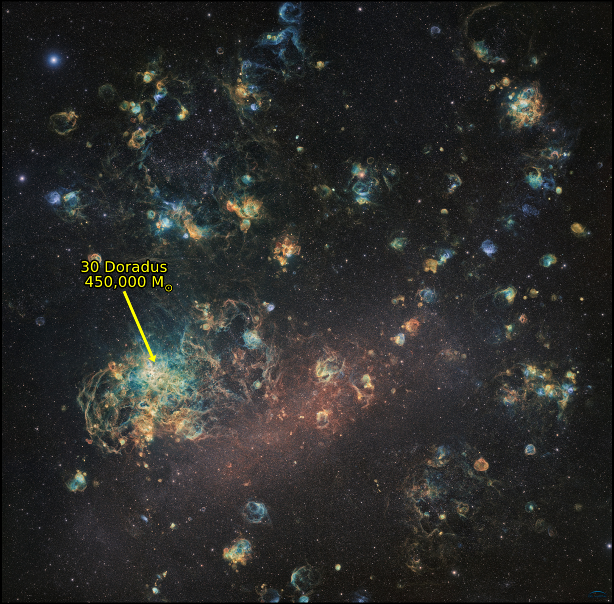

Credit: J. C. Canonne, N. Outters, P. Bernhard, D. Chaplain, L. Bourgon.

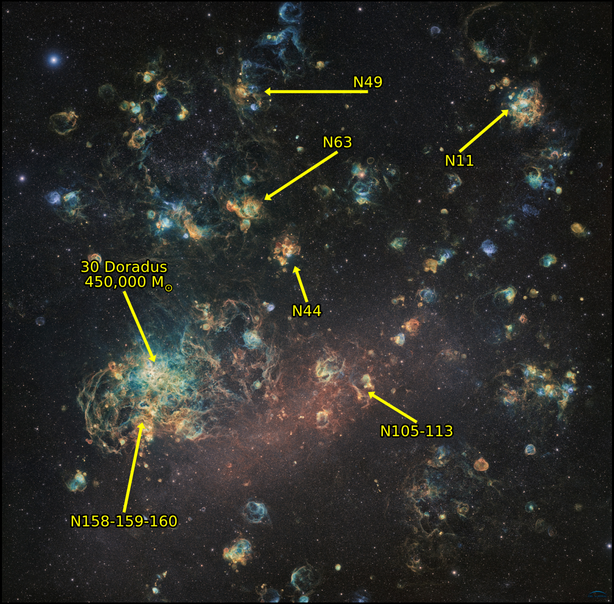

Credit: J. C. Canonne, N. Outters, P. Bernhard, D. Chaplain, L. Bourgon.

Name	Scope	Reference	Download link

(adapted from B. Godard)

Name	Scope	Reference	Download link
CLOUDY	H II regions, AGNs, XDRs, PDRs (3D)	Ferland et al. (2013, 2017)	https://www.nublado.org

(adapted from B. Godard)

Name	Scope	Reference	Download link
CLOUDY	H II regions, AGNs, XDRs, PDRs (3D)	Ferland et al. (2013, 2017)	https://www.nublado.org
MAPPINGS V	H II regions, shocks	Allen et al. (2008); Sutherland & Dopita (2017)	https://mappings.anu.edu.au/

(adapted from B. Godard)

Name	Scope	Reference	Download link
CLOUDY	H II regions, AGNs, XDRs, PDRs (3D)	Ferland et al. (2013, 2017)	https://www.nublado.org
MAPPINGS V	H II regions, shocks	Allen et al. (2008); Sutherland & Dopita (2017)	https://mappings.anu.edu.au/
Meudon PDR	PDRs	Le Petit et al. (2006); Le Bourlot et al. (2012)	https://ism.obspm.fr

(adapted from B. Godard)

Name	Scope	Reference	Download link
CLOUDY	H II regions, AGNs, XDRs, PDRs (3D)	Ferland et al. (2013, 2017)	https://www.nublado.org
MAPPINGS V	H II regions, shocks	Allen et al. (2008); Sutherland & Dopita (2017)	https://mappings.anu.edu.au/
Meudon PDR	PDRs	Le Petit et al. (2006); Le Bourlot et al. (2012)	https://ism.obspm.fr
Kosma-τ	PDRs	Röllig et al. (2006, 2013)	https://hera.ph1.uni-koeln.de/~pdr/

(adapted from B. Godard)

Name	Scope	Reference	Download link
CLOUDY	H II regions, AGNs, XDRs, PDRs (3D)	Ferland et al. (2013, 2017)	https://www.nublado.org
MAPPINGS V	H II regions, shocks	Allen et al. (2008); Sutherland & Dopita (2017)	https://mappings.anu.edu.au/
Meudon PDR	PDRs	Le Petit et al. (2006); Le Bourlot et al. (2012)	https://ism.obspm.fr
Kosma-τ	PDRs	Röllig et al. (2006, 2013)	https://hera.ph1.uni-koeln.de/~pdr/
UCL PDR	PDRs (3D)	Bell et al. (2005); Bisbas et al. (2012)	https://uclchem.github.io/

(adapted from B. Godard)

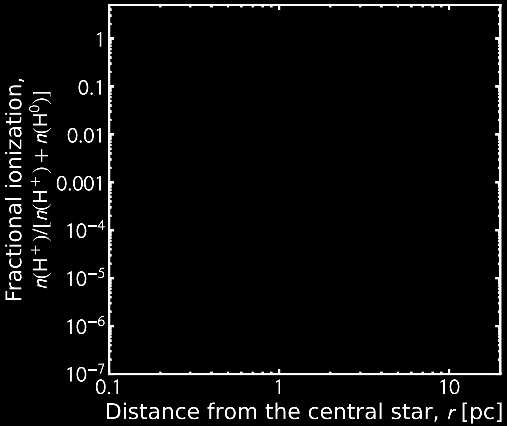
Fractional ionization,
n(H+)/[n(H+) + n(H0)]
1
0.1
0.01
0.001
10−4
10−5
10−6
10−7
0.1
1
10
Distance from the central star, r [pc]

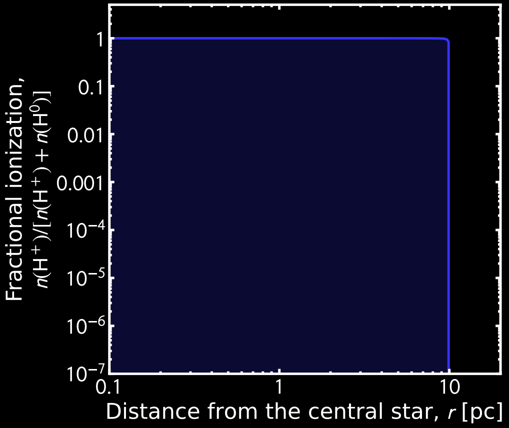
1
0.1
0.01
0.001
10^{-4}
10^{-5}
10^{-6}
10^{-7}
0.1
1
10
Fractional ionization, $n(H^+)/[n(H^+)+n(H^0)]$
Distance from the central star, r [pc]

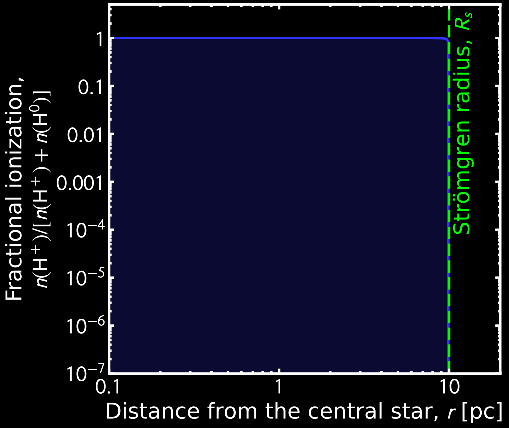

Fractional ionization,
$n(H^+)/[n(H^+)+n(H^0)]$
1
0.1
0.01
0.001
10^{-4}
10^{-5}
10^{-6}
10^{-7}
0.1
1
10
Distance from the central star, r [pc]
Strömgren radius, R_s

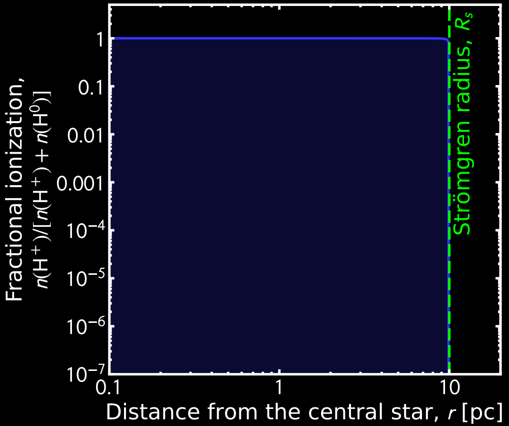
Fractional ionization,
$n(H^+)/[n(H^+)+n(H^0)]$
1
0.1
0.01
0.001
10^{-4}
10^{-5}
10^{-6}
10^{-7}
0.1
1
10
Distance from the central star, r [pc]
Strömgren radius, R_s

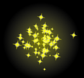

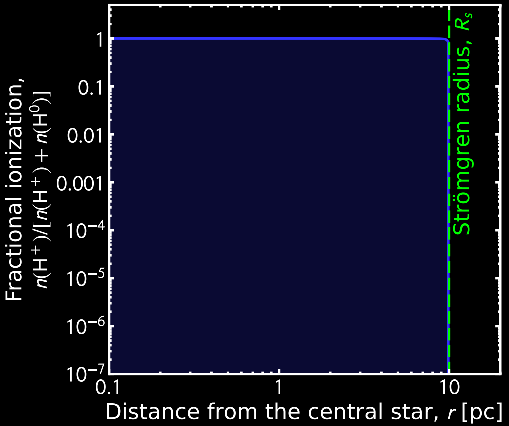
Fractional ionization,
$n(H^+)/[n(H^+)+n(H^0)]$
1
0.1
0.01
0.001
10^{-4}
10^{-5}
10^{-6}
10^{-7}
0.1
1
10
Distance from the central star, r [pc]
Strömgren radius, R_s

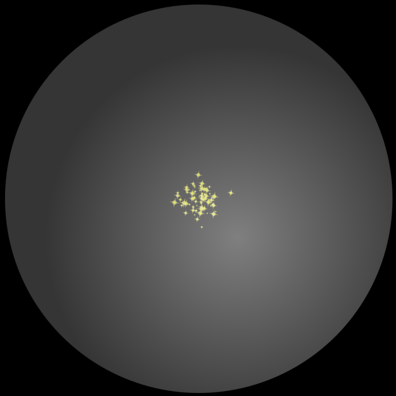

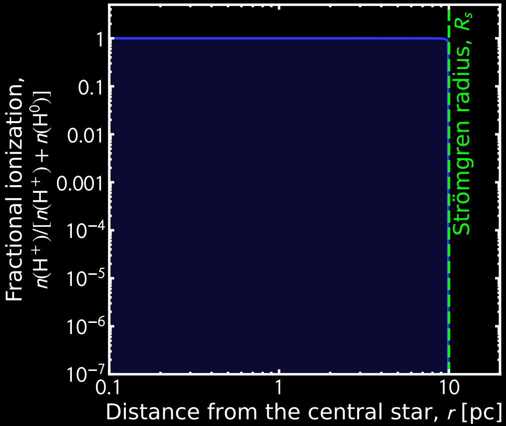
Fractional ionization,
$n(H^+)/[n(H^+)+n(H^0)]$
1
0.1
0.01
0.001
10^{-4}
10^{-5}
10^{-6}
10^{-7}
0.1
1
10
Distance from the central star, r [pc]
Strömgren radius, R_s

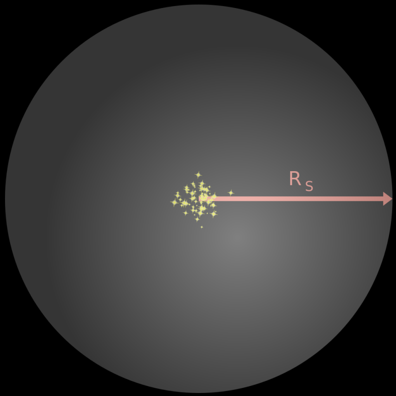
R_S

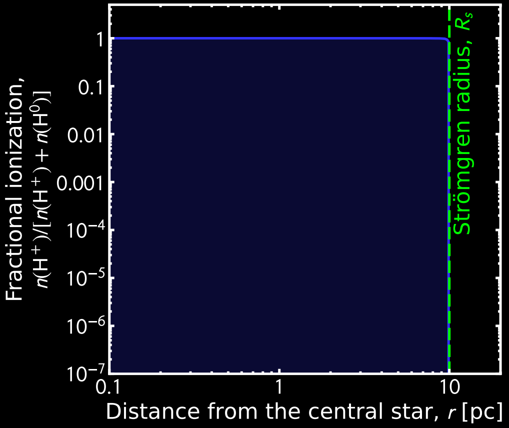

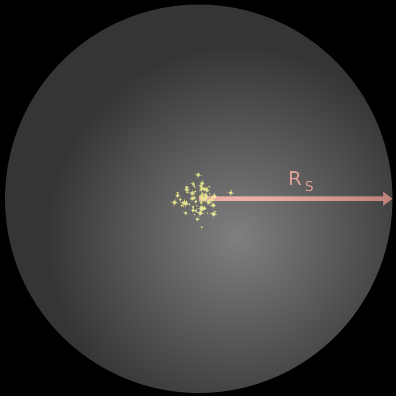

The size of an H II region (Strömgren, 1939)

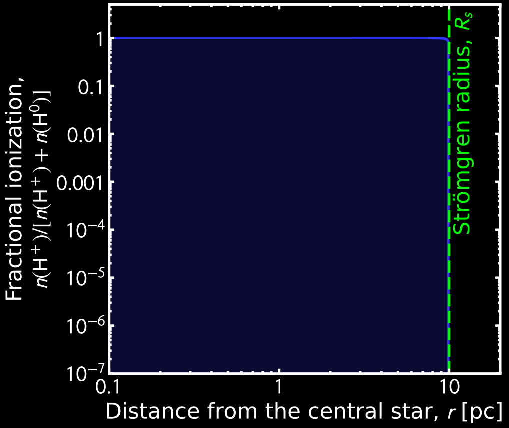

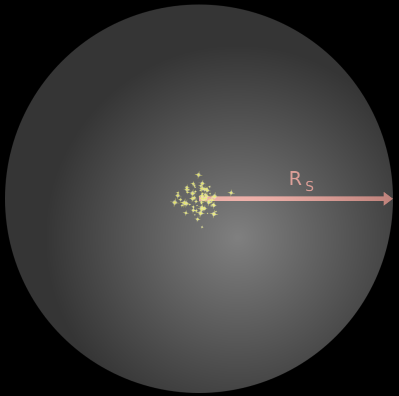

The size of an H II region (Strömgren, 1939)

$$\underbrace{Q_0}_{\text{total photoionization rate}} = \int_{\nu_{Ly}}^{\infty} \frac{L_\nu}{h\nu}\, d\nu$$

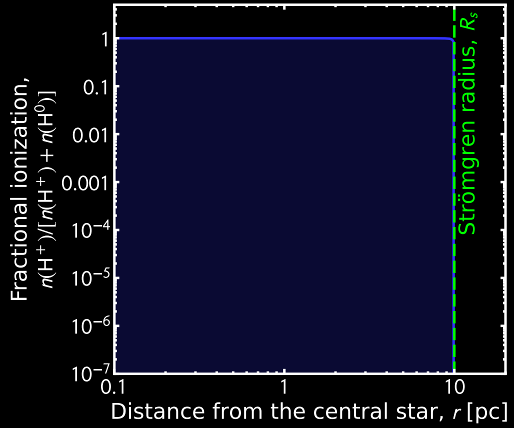

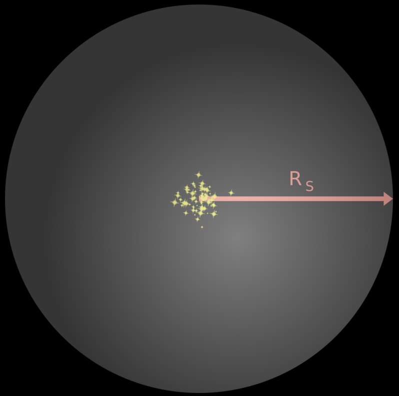

The size of an H II region (Strömgren, 1939)

$$\underbrace{Q_0}_{\text{total photoionization rate}} = \int_{\nu_{Ly}}^{\infty} \frac{L_\nu}{h\nu}\,\mathrm{d}\nu = \underbrace{\frac{4\pi}{3} R_s^3 n_\mathrm{p}}_{\text{number of protons}} \times \underbrace{n_e \alpha_\mathrm{B}}_{\text{recombination rate}}$$

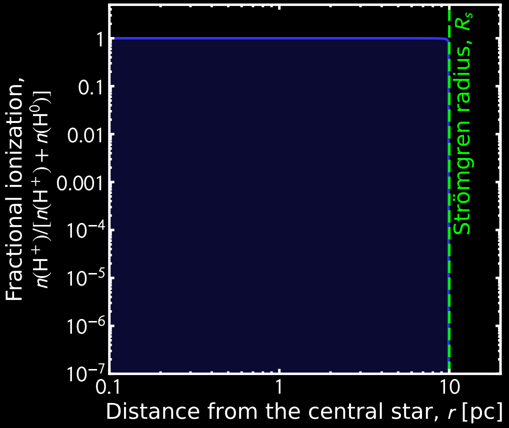

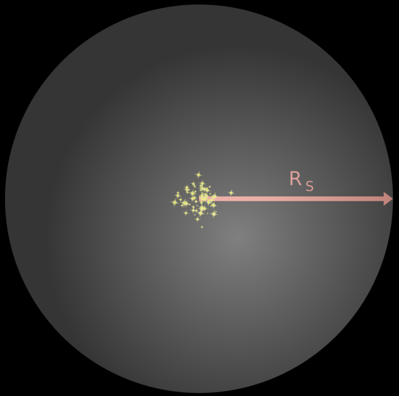

The size of an H II region (Strömgren, 1939)

$$\underbrace{Q_0}_{\text{total photoionization rate}} = \int_{\nu_{Ly}}^{\infty} \frac{L_\nu}{h\nu}\,\mathrm{d}\nu = \underbrace{\frac{4\pi}{3} R_s^3 n_p}_{\text{number of protons}} \times \underbrace{n_e \alpha_B}_{\text{recombination rate}} \Rightarrow \underbrace{R_s}_{\text{Strömgren radius}} = \left(\frac{3 Q_0}{4\pi n_{gas}^2 \alpha_B} \right)^{1/3}.$$

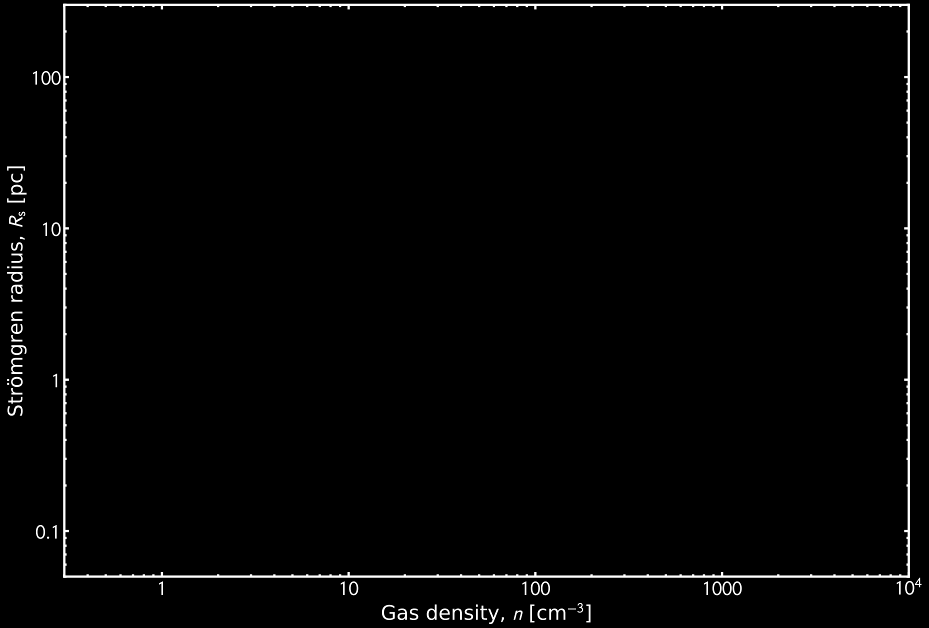
100
10
1
0.1
Strömgren radius, R_s [pc]
1
10
100
1000
10^4
Gas density, n [cm^{-3}]

SF regions | Effects of Density & Stellar Type on H II Region Sizes

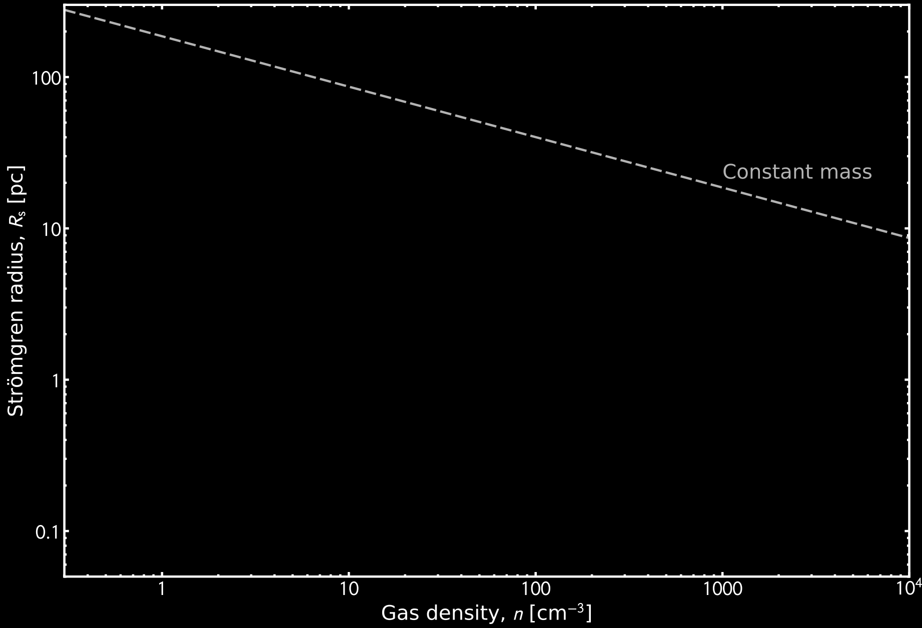

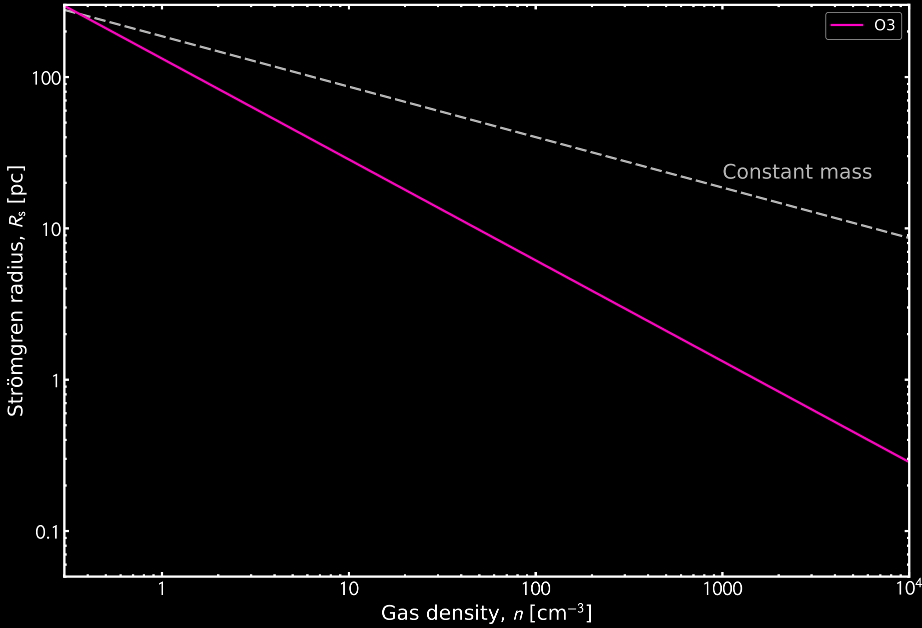
O3
Constant mass
100
10
1
0.1
Strömgren radius, R_s [pc]
1
10
100
1000
10^4
Gas density, n [cm^{-3}]

SF regions | Effects of Density & Stellar Type on H II Region Sizes

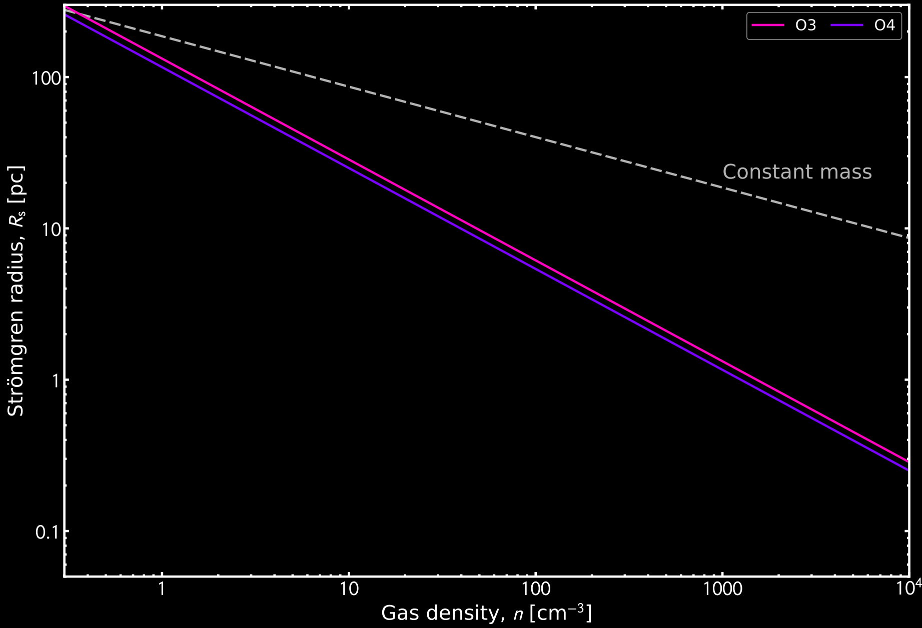

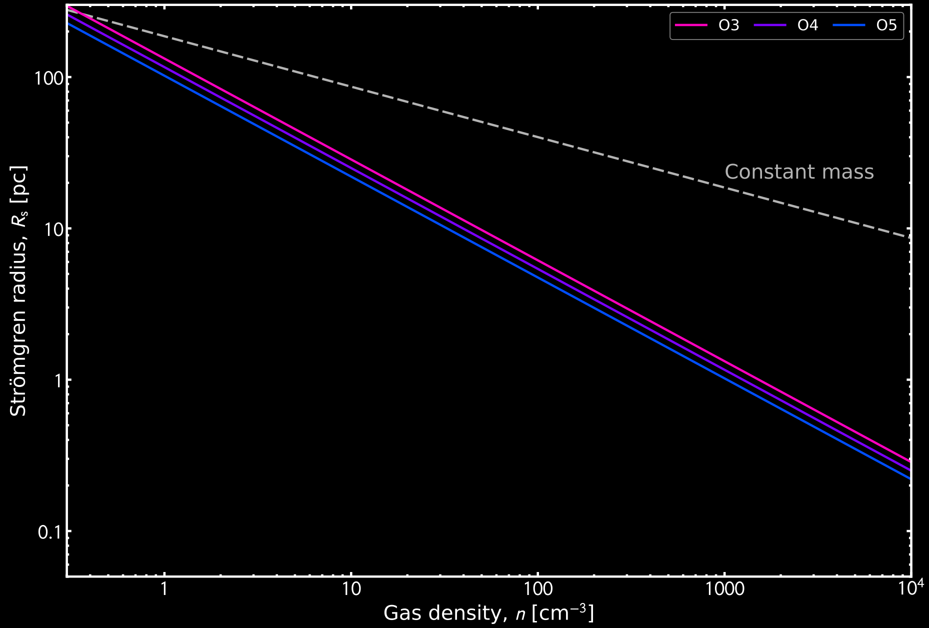
O3
O4
O5
Constant mass
100
10
1
0.1
Strömgren radius, R_s [pc]
1
10
100
1000
10^4
Gas density, n [cm^{-3}]

SF regions | Effects of Density & Stellar Type on H II Region Sizes

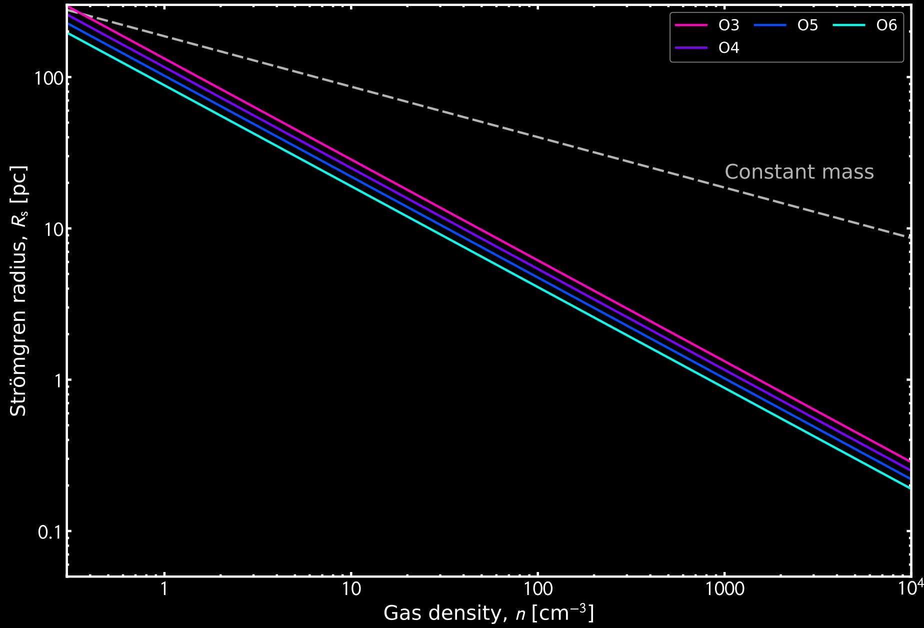

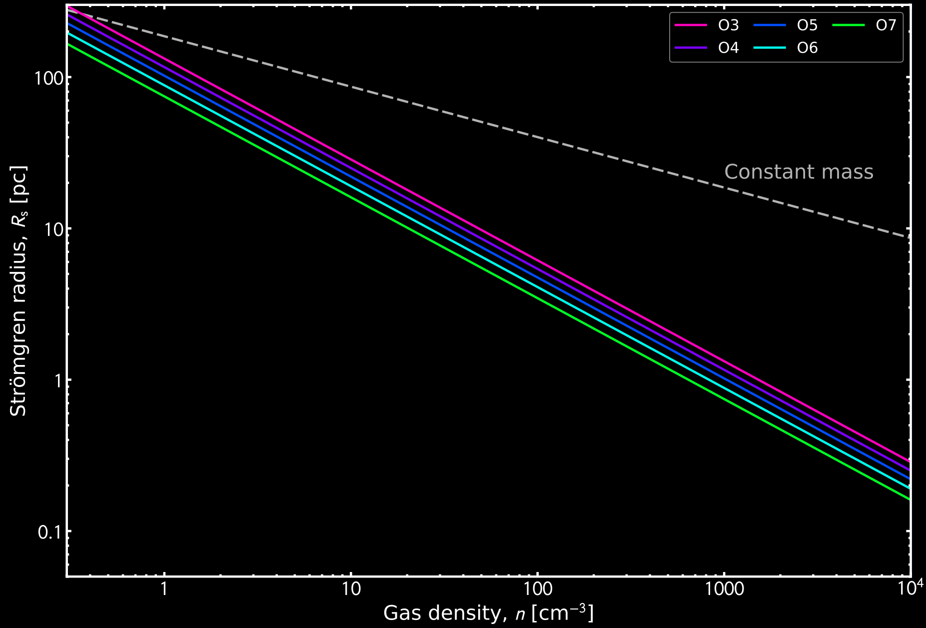
O3
O4
O5
O6
O7
Constant mass
Strömgren radius, R_s [pc]
100
10
1
0.1
1
10
100
1000
10^4
Gas density, n [cm^{-3}]

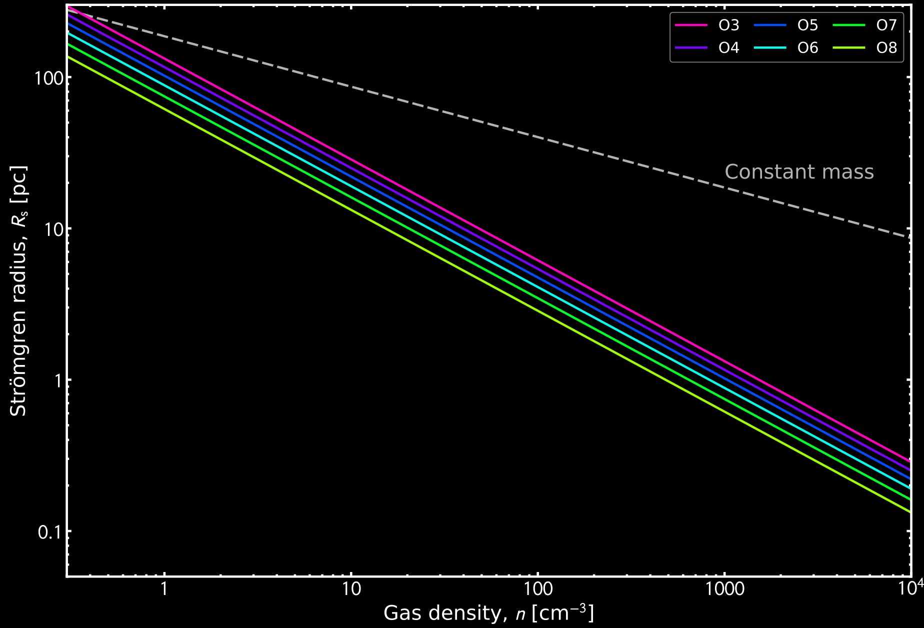
O3
O4
O5
O6
O7
O8
Constant mass
Strömgren radius, R_s [pc]
100
10
1
0.1
1
10
100
1000
10^4
Gas density, n [cm^{-3}]

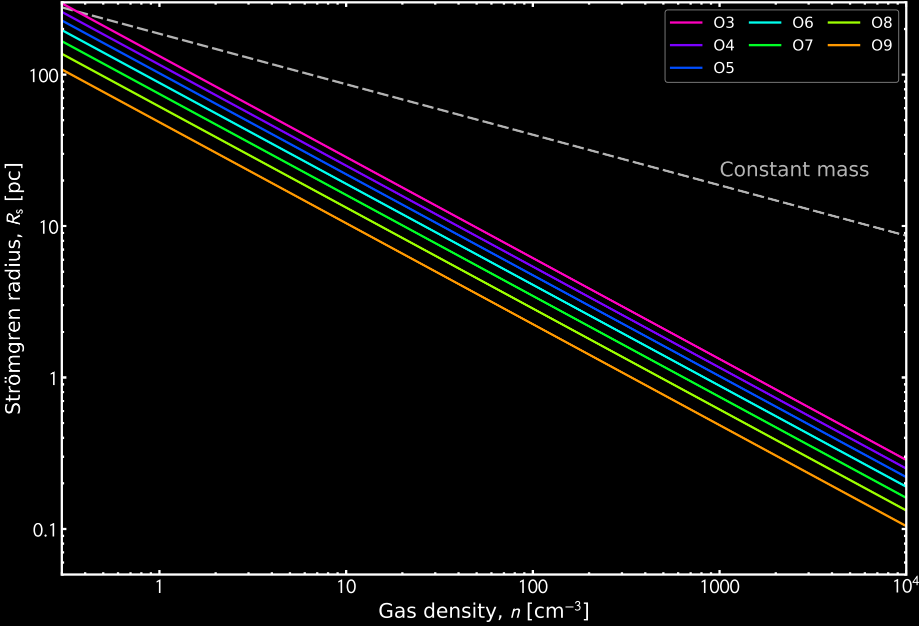

O3
O4
O5
O6
O7
O8
O9
Constant mass
Strömgren radius, R_s [pc]
100
10
1
0.1
Gas density, n [cm^{-3}]
1
10
100
1000
10^4

SF regions | Effects of Density & Stellar Type on H II Region Sizes

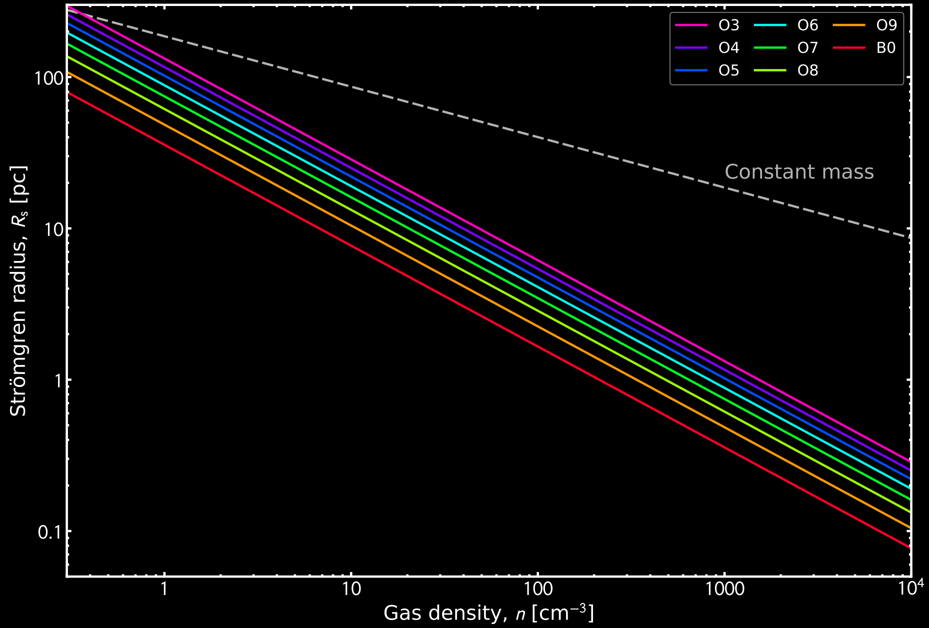

SF regions | The Modeled Spectrum of an H II Region

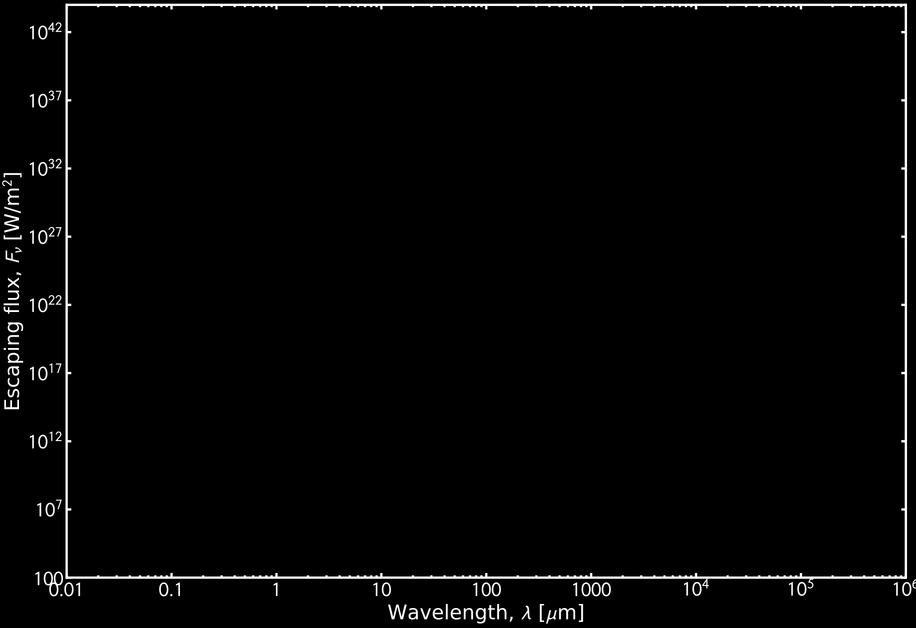

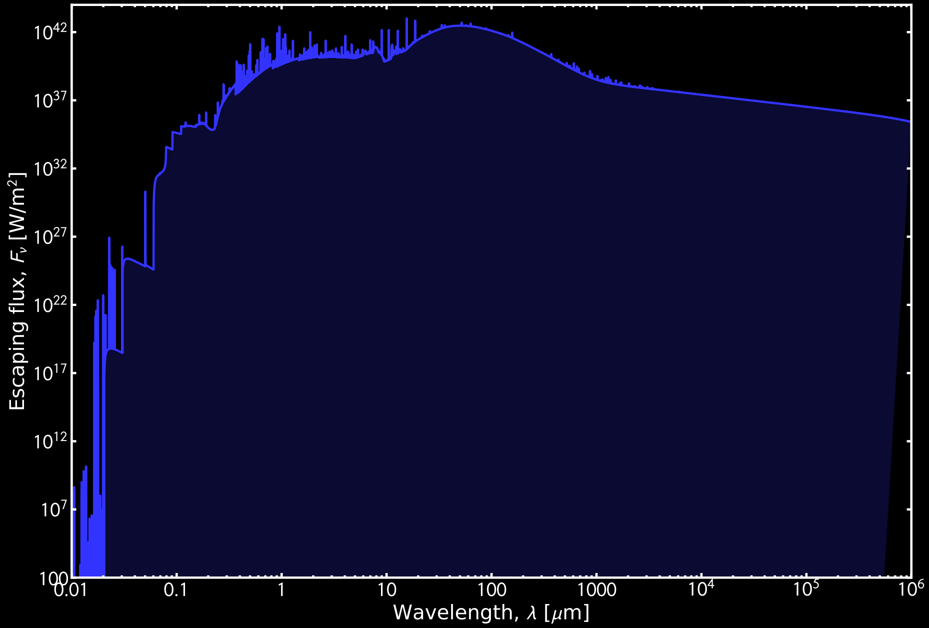
Escaping flux, F_ν [W/m^2]
10^{42}
10^{37}
10^{32}
10^{27}
10^{22}
10^{17}
10^{12}
10^{7}
100
0.01
0.1
1
10
100
1000
10^4
10^5
10^6
Wavelength, λ [μm]

Using Dust Emission

Using Dust Emission

- Young stars are extremelly luminous & enshrouded with dust.

Using Dust Emission

- Young stars are extremelly luminous & enshrouded with dust.

⇒ $L_{OB} \simeq L_{IR}$.

Using Dust Emission

- Young stars are extremelly luminous & enshrouded with dust.

⇒ $L_{\rm OB} \simeq L_{\rm IR}$.

⇒ SFR $[M_\odot/{\rm yr}] \simeq 10^{-10} \times L_{\rm IR}$ $[L_\odot]$, with reasonable assumptions about the *Initial Mass Function* (IMF), burst age & metallicity (Kennicutt, 1998).

Using Dust Emission

- Young stars are extremelly luminous & enshrouded with dust.

$\Rightarrow$ $L_{\rm OB} \simeq L_{\rm IR}$.

$\Rightarrow$ SFR $[M_\odot/\text{yr}] \simeq 10^{-10} \times L_{\rm IR}$ $[L_\odot]$, with reasonable assumptions about the *Initial Mass Function* (IMF), burst age & metallicity (Kennicutt, 1998).

Accounting for escaping UV photons

(Hao et al., 2011; Boquien et al., 2016)

Using Dust Emission

- Young stars are extremelly luminous & enshrouded with dust.

⇒ $L_{\rm OB} \simeq L_{\rm IR}$.

⇒ SFR $[M_\odot/{\rm yr}] \simeq 10^{-10} \times L_{\rm IR}\ [L_\odot]$, with reasonable assumptions about the *Initial Mass Function* (IMF), burst age & metallicity (Kennicutt, 1998).

Accounting for escaping UV photons

Photons absorbed by the dust: traced by $L_{\rm IR}$.

(Hao et al., 2011; Boquien et al., 2016)

Using Dust Emission

- Young stars are extremelly luminous & enshrouded with dust.

⇒ $L_{\rm OB} \simeq L_{\rm IR}$.

⇒ SFR $[M_\odot/\rm yr] \simeq 10^{-10} \times L_{\rm IR}$ $[L_\odot]$, with reasonable assumptions about the *Initial Mass Function* (IMF), burst age & metallicity (Kennicutt, 1998).

Accounting for escaping UV photons

Photons absorbed by the dust: traced by $L_{\rm IR}$.

Escaping photons: traced by far-UV or Hα measurements.

(Hao et al., 2011; Boquien et al., 2016)

The relevance of PDRs

The relevance of PDRs

- PDRs: continuation of H II regions where all ionizing photons have been absorbed $\Rightarrow$ H^0.

The relevance of PDRs

- PDRs: continuation of H II regions where all ionizing photons have been absorbed $\Rightarrow$ H^0.
- PDR $\Leftrightarrow$ UV-illuminated edges of molecular clouds. Broader nomenclature: most neutral & molecular clouds bathed with UV photons are PDRs.

The relevance of PDRs

- PDRs: continuation of H II regions where all ionizing photons have been absorbed $\Rightarrow$ H^0.
- PDR $\Leftrightarrow$ UV-illuminated edges of molecular clouds. Broader nomenclature: most neutral & molecular clouds bathed with UV photons are PDRs.
- They harbor a rich variety of chemical reactions $\longrightarrow$ H_2.

(*cf.* Bron et al. 2014)

The relevance of PDRs

- PDRs: continuation of H II regions where all ionizing photons have been absorbed ⇒ H^0.
- PDR ⇔ UV-illuminated edges of molecular clouds. Broader nomenclature: most neutral & molecular clouds bathed with UV photons are PDRs.
- They harbor a rich variety of chemical reactions → H_2.

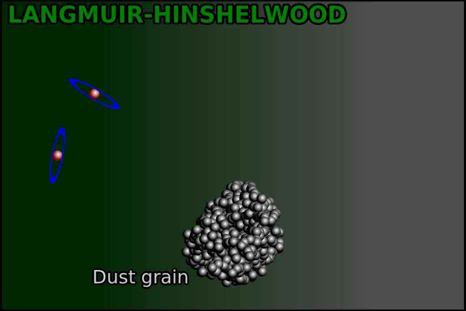

(*cf.* Bron et al. 2014)

The relevance of PDRs

- PDRs: continuation of H II regions where all ionizing photons have been absorbed ⇒ H^0.
- PDR ⇔ UV-illuminated edges of molecular clouds. Broader nomenclature: most neutral & molecular clouds bathed with UV photons are PDRs.
- They harbor a rich variety of chemical reactions → H_2.

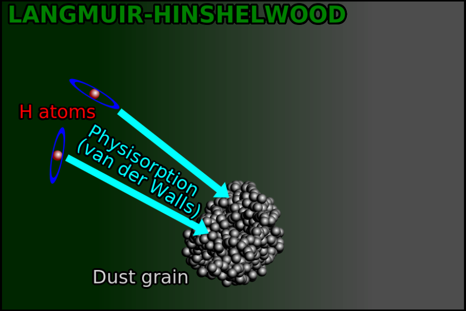

(*cf.* Bron et al. 2014)

The relevance of PDRs

- PDRs: continuation of H II regions where all ionizing photons have been absorbed ⇒ H^0.
- PDR ⇔ UV-illuminated edges of molecular clouds. Broader nomenclature: most neutral & molecular clouds bathed with UV photons are PDRs.
- They harbor a rich variety of chemical reactions → H_2.

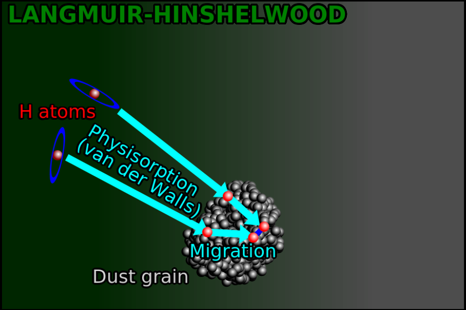

(*cf.* Bron et al. 2014)

The relevance of PDRs

- PDRs: continuation of H II regions where all ionizing photons have been absorbed ⇒ H^0.
- PDR ⇔ UV-illuminated edges of molecular clouds. Broader nomenclature: most neutral & molecular clouds bathed with UV photons are PDRs.
- They harbor a rich variety of chemical reactions → H_2.

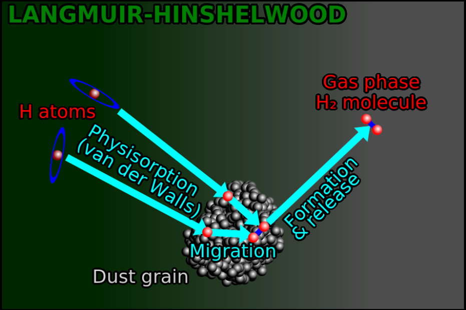

(*cf.* Bron et al. 2014)

The relevance of PDRs

- PDRs: continuation of H II regions where all ionizing photons have been absorbed ⇒ H^0.
- PDR ⇔ UV-illuminated edges of molecular clouds. Broader nomenclature: most neutral & molecular clouds bathed with UV photons are PDRs.
- They harbor a rich variety of chemical reactions → H_2.

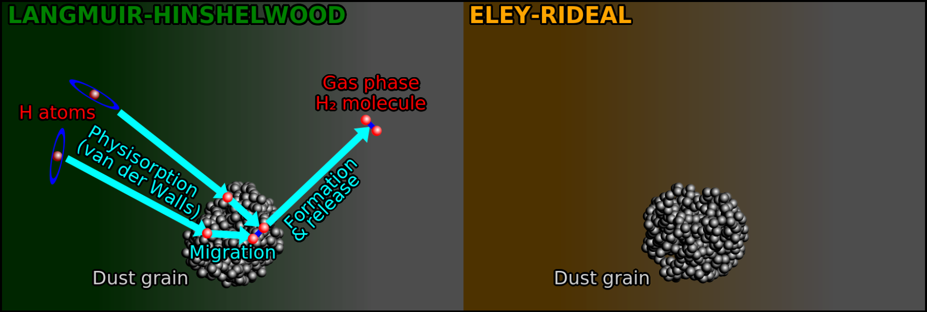

(*cf.* Bron et al. 2014)

The relevance of PDRs

- PDRs: continuation of H II regions where all ionizing photons have been absorbed ⇒ H^0.
- PDR ⇔ UV-illuminated edges of molecular clouds. Broader nomenclature: most neutral & molecular clouds bathed with UV photons are PDRs.
- They harbor a rich variety of chemical reactions → H_2.

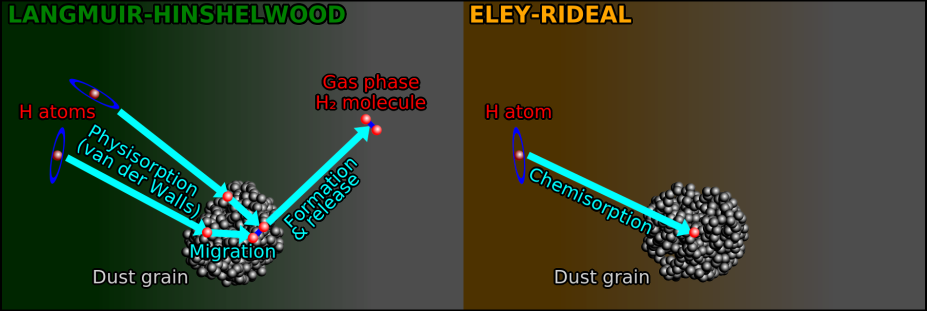

(*cf.* Bron et al. 2014)

The relevance of PDRs

- PDRs: continuation of H II regions where all ionizing photons have been absorbed ⇒ H^0.
- PDR ⇔ UV-illuminated edges of molecular clouds. Broader nomenclature: most neutral & molecular clouds bathed with UV photons are PDRs.
- They harbor a rich variety of chemical reactions → H_2.

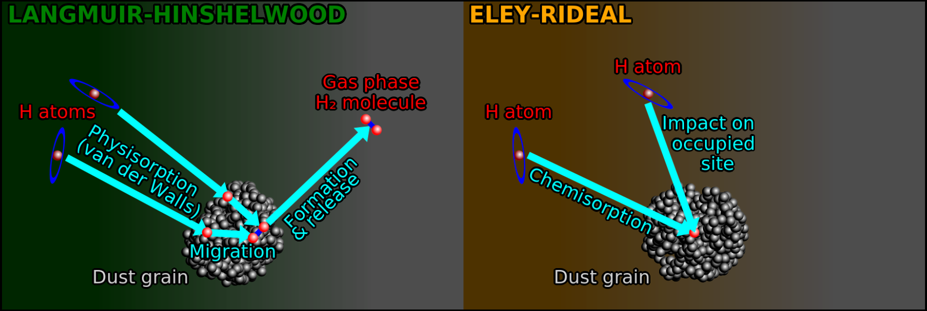

(*cf.* Bron et al. 2014)

The relevance of PDRs

- PDRs: continuation of H II regions where all ionizing photons have been absorbed $\Rightarrow$ H^0.
- PDR $\Leftrightarrow$ UV-illuminated edges of molecular clouds. Broader nomenclature: most neutral & molecular clouds bathed with UV photons are PDRs.
- They harbor a rich variety of chemical reactions $\rightarrow$ H_2.

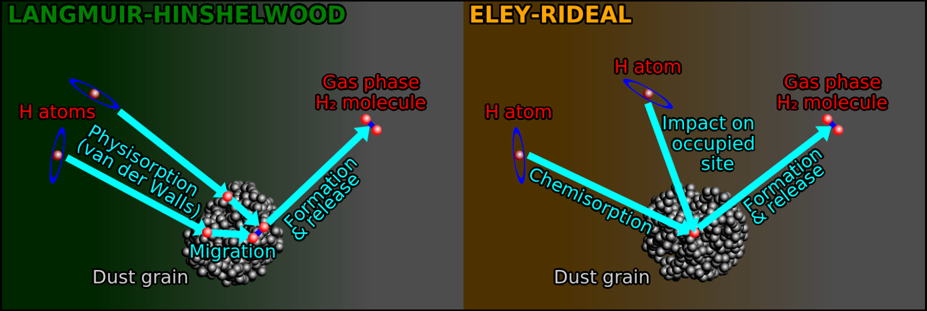

(*cf.* Bron et al. 2014)

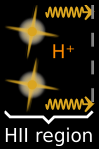
H+
HII region

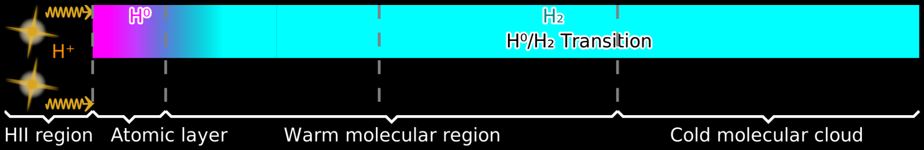
H⁰
H₂
H⁰/H₂ Transition
H⁺
HII region
Atomic layer
Warm molecular region
Cold molecular cloud

SF regions | The H^0/H_2 Transition

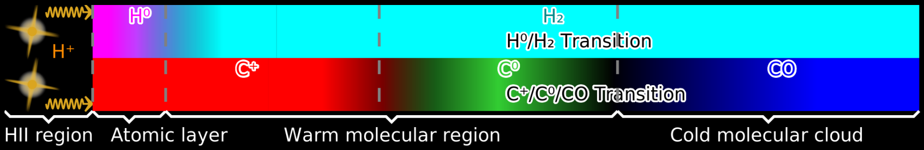

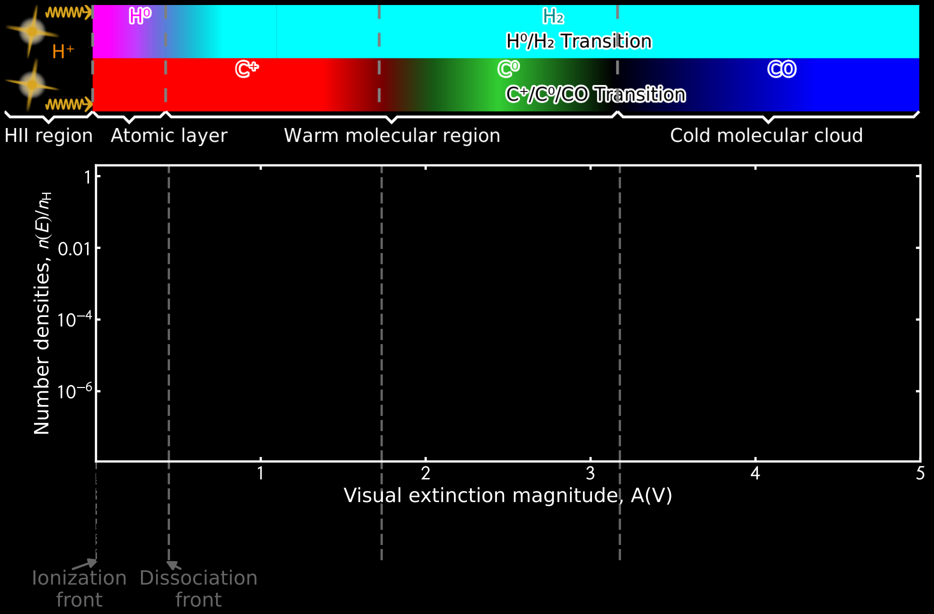
H⁰
H₂
H⁰/H₂ Transition
H⁺
C⁺
C⁰
CO
C⁺/C⁰/CO Transition
HII region
Atomic layer
Warm molecular region
Cold molecular cloud
Number densities, n(E)/n_H
1
0.01
10⁻⁴
10⁻⁶
1
2
3
4
5
Visual extinction magnitude, A(V)
Ionization front
Dissociation front

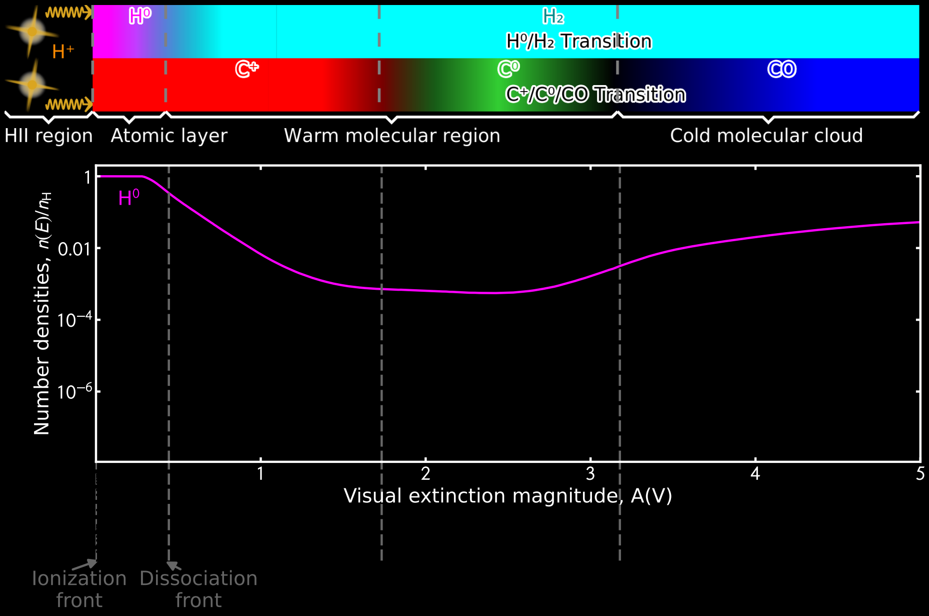
H⁰
H₂
H⁰/H₂ Transition
H⁺
C⁺
C⁰
CO
C⁺/C⁰/CO Transition
HII region
Atomic layer
Warm molecular region
Cold molecular cloud
1
0.01
10⁻⁴
10⁻⁶
Number densities, n(E)/n_H
H⁰
1
2
3
4
5
Visual extinction magnitude, A(V)
Ionization front
Dissociation front

SF regions | The H^0/H_2 Transition

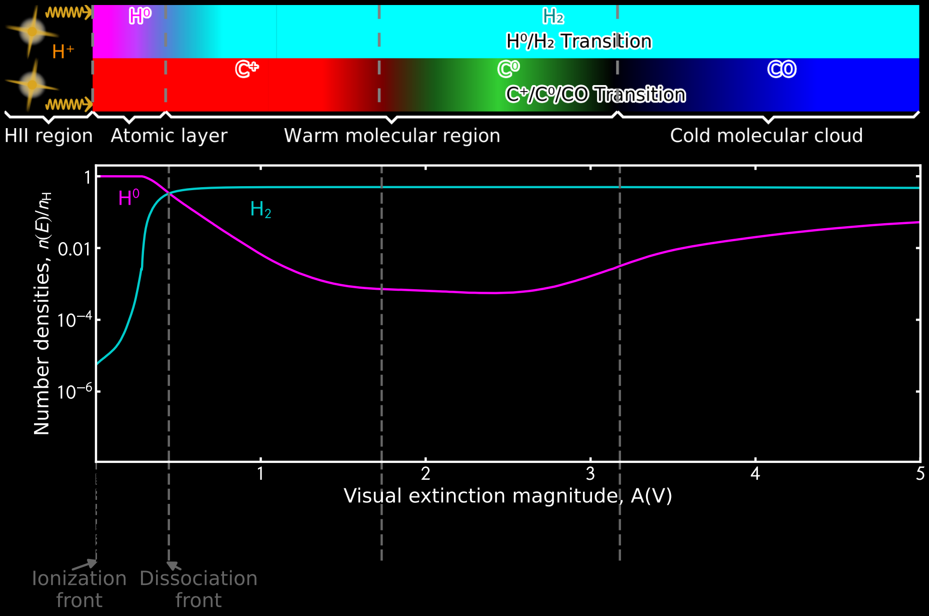

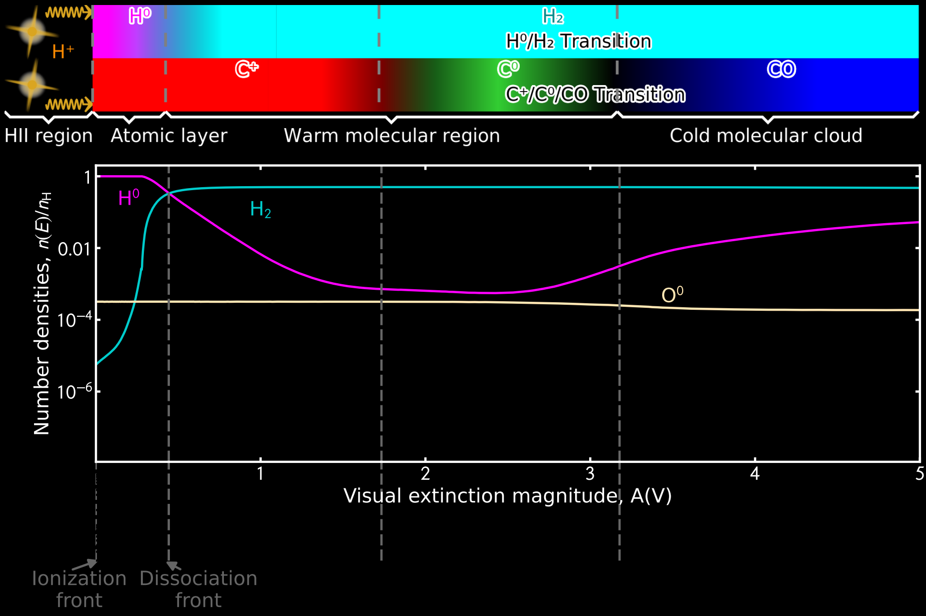

H⁰
H₂
H⁺
H⁰/H₂ Transition
C⁺
C⁰
CO
C⁺/C⁰/CO Transition
HII region
Atomic layer
Warm molecular region
Cold molecular cloud
Number densities, n(E)/n_H
H⁰
H₂
O⁰
1
0.01
10⁻⁴
10⁻⁶
1
2
3
4
5
Visual extinction magnitude, A(V)
Ionization front
Dissociation front

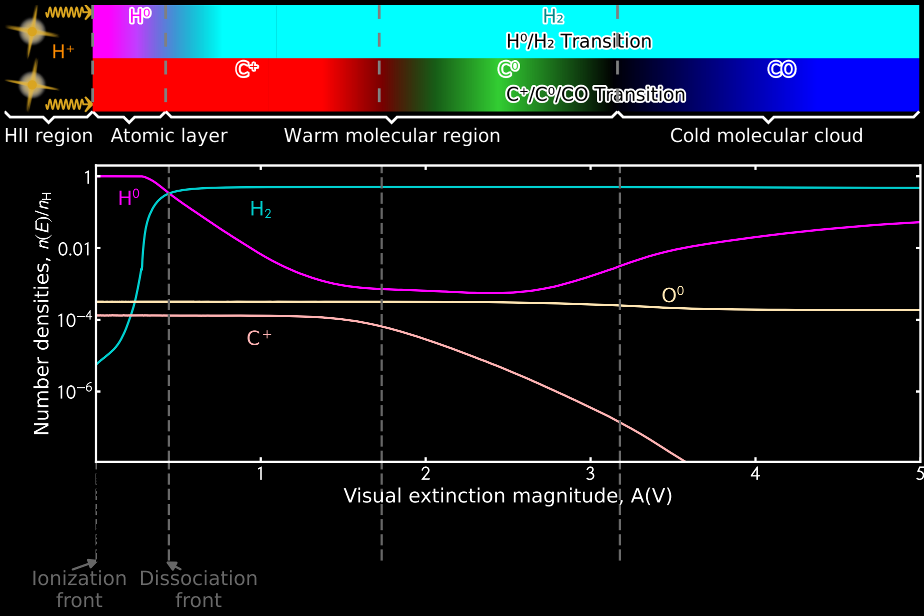
H+
H0
H2
H0/H2 Transition
C+
C0
CO
C+/C0/CO Transition
HII region
Atomic layer
Warm molecular region
Cold molecular cloud
1
0.01
10−4
10−6
H0
H2
O0
C+
1
2
3
4
5
Number densities, n(E)/nH
Visual extinction magnitude, A(V)
Ionization front
Dissociation front

SF regions | The H^0/H_2 Transition

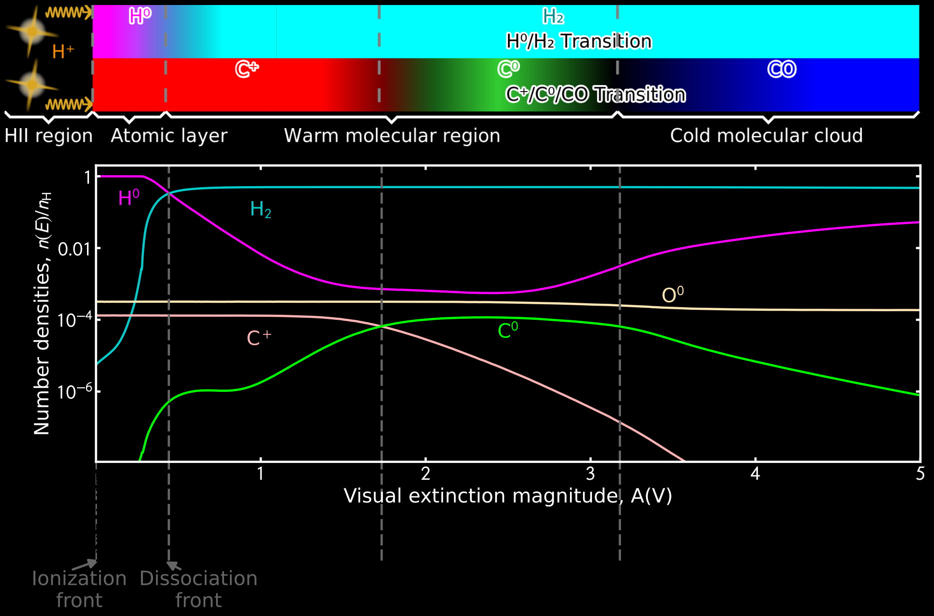

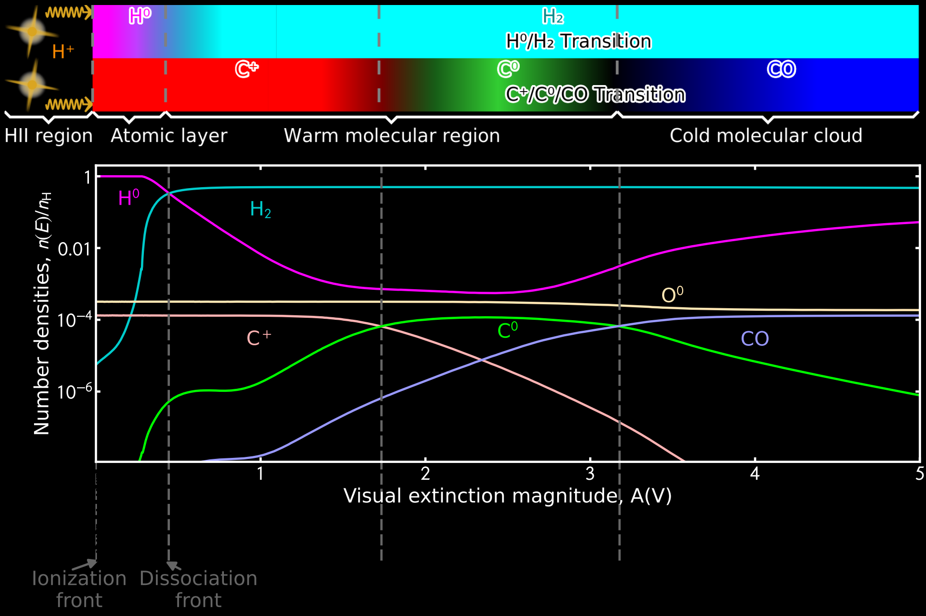

H⁰
H₂
H⁰/H₂ Transition
H⁺
C⁺
C⁰
CO
C⁺/C⁰/CO Transition
HII region
Atomic layer
Warm molecular region
Cold molecular cloud
1
0.01
10⁻⁴
10⁻⁶
Number densities, n(E)/n_H
H⁰
H₂
O⁰
C⁺
C⁰
CO
1
2
3
4
5
Visual extinction magnitude, A(V)
Ionization front
Dissociation front

SF regions | The H^0/H_2 Transition

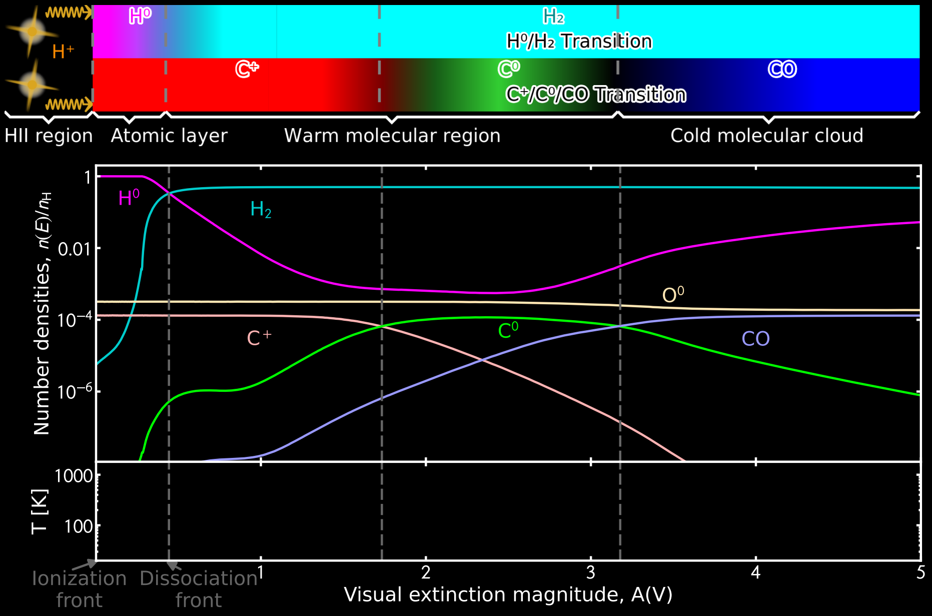

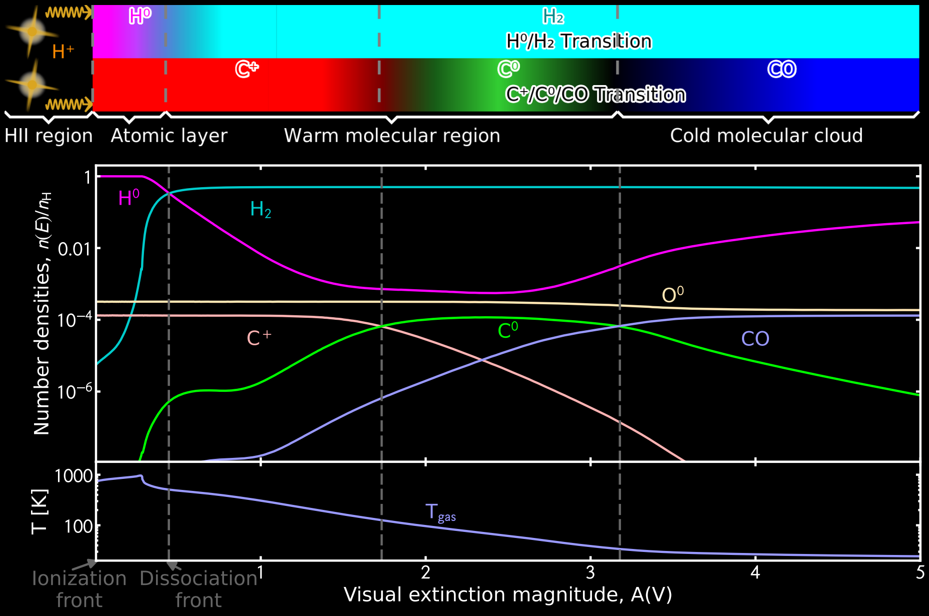
H⁰
H₂
H⁺
H⁰/H₂ Transition
C⁺
C⁰
CO
C⁺/C⁰/CO Transition
HII region
Atomic layer
Warm molecular region
Cold molecular cloud
Number densities, n(E)/n_H
1
0.01
10⁻⁴
10⁻⁶
H⁰
H₂
O⁰
C⁺
C⁰
CO
T [K]
1000
100
T_gas
Ionization front
Dissociation front
1
2
3
4
5
Visual extinction magnitude, A(V)

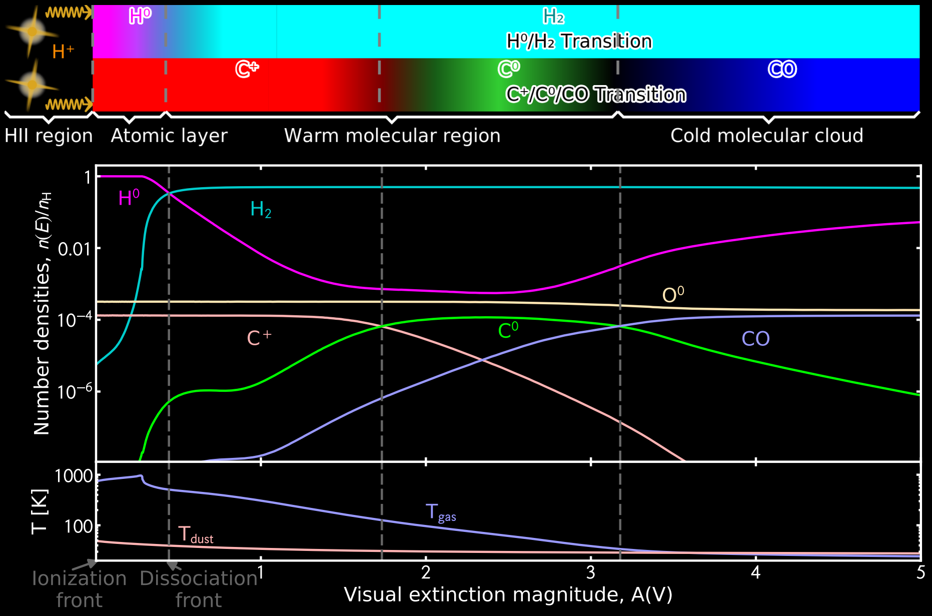
H+
H0
H2
H0/H2 Transition
C+
C0
CO
C+/C0/CO Transition
HII region
Atomic layer
Warm molecular region
Cold molecular cloud
Number densities, n(E)/nH
1
0.01
10−4
10−6
H0
H2
O0
C+
C0
CO
T [K]
1000
100
Tgas
Tdust
Ionization front
Dissociation front
1
2
3
4
5
Visual extinction magnitude, A(V)

Measuring molecular gas masses

Measuring molecular gas masses

- H_2 symmetry $\Rightarrow$ no rotational lines

Measuring molecular gas masses

- H_2 symmetry $\Rightarrow$ no rotational lines $\Rightarrow$ Rely on CO to trace molecular gas.

Measuring molecular gas masses

- H_2 symmetry ⇒ no rotational lines ⇒ Rely on CO to trace molecular gas.
- CO photodissociation at low $Z \rightarrow \simeq$ 70-100 % of H_2 not traced by CO (Madden et al., 2020).

Measuring molecular gas masses

- H_2 symmetry $\Rightarrow$ no rotational lines $\Rightarrow$ Rely on CO to trace molecular gas.
- CO photodissociation at low $Z \rightarrow \simeq$ 70-100 % of H_2 not traced by CO (Madden et al., 2020).

Measuring molecular gas masses

- H_2 symmetry $\Rightarrow$ no rotational lines $\Rightarrow$ Rely on CO to trace molecular gas.
- CO photodissociation at low Z $\rightarrow$ $\simeq$ 70-100 % of H_2 not traced by CO (Madden et al., 2020).

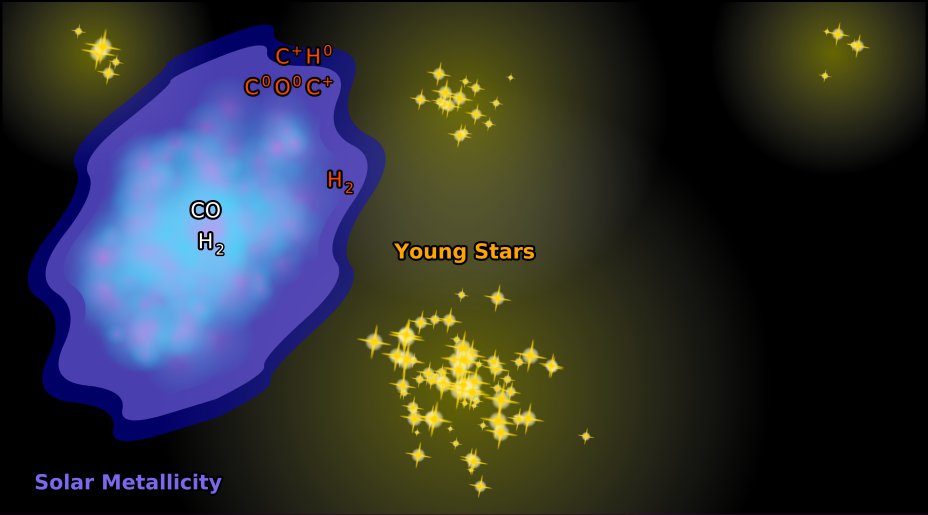

Measuring molecular gas masses

- H_2 symmetry ⇒ no rotational lines ⇒ Rely on CO to trace molecular gas.
- CO photodissociation at low Z → ≃ 70-100 % of H_2 not traced by CO (Madden et al., 2020).

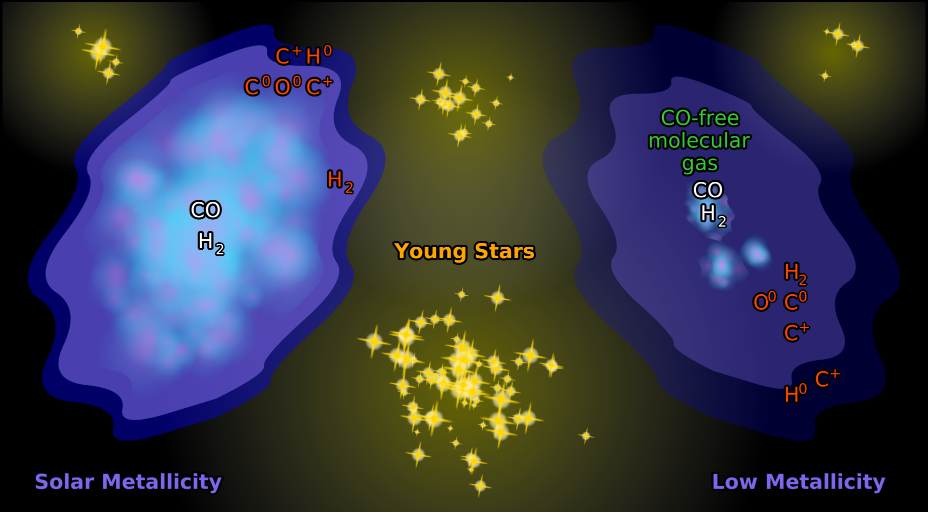

Outline of the Lecture

Balance between gas heating & cooling – the phases of the ISM

Conclusion | Take-Away Points

Balance between gas heating & cooling – the phases of the ISM

- The *Cold Neutral Medium* (CNM; $n \simeq 30\ \text{cm}^{-3}$; $T \simeq 100$ K) & the *Warm Neutral Medium* (WNM; $n \simeq 0.3\ \text{cm}^{-3}$; $T \simeq 10^4$ K) are at pressure equilibrium → the only 2 stable H I phases.

Conclusion | Take-Away Points

Balance between gas heating & cooling – the phases of the ISM

- The *Cold Neutral Medium* (CNM; $n \simeq 30\ \text{cm}^{-3}$; $T \simeq 100$ K) & the *Warm Neutral Medium* (WNM; $n \simeq 0.3\ \text{cm}^{-3}$; $T \simeq 10^4$ K) are at pressure equilibrium → the only 2 stable H I phases.
- So are the *Warm Ionized Medium* (WIM; $n \simeq 0.1\ \text{cm}^{-3}$; $T = 10^4$ K) & the *Hot Ionized Medium* (HIM; $n \simeq 0.003\ \text{cm}^{-3}$; $T \simeq 10^6$ K; $\simeq 50\,\%$ of the volume of the Galaxy).

Conclusion | Take-Away Points

Balance between gas heating & cooling – the phases of the ISM

- The *Cold Neutral Medium* (CNM; $n \simeq 30$ cm^{-3}; $T \simeq 100$ K) & the *Warm Neutral Medium* (WNM; $n \simeq 0.3$ cm^{-3}; $T \simeq 10^4$ K) are at pressure equilibrium $\rightarrow$ the only 2 stable H I phases.
- So are the *Warm Ionized Medium* (WIM; $n \simeq 0.1$ cm^{-3}; $T = 10^4$ K) & the *Hot Ionized Medium* (HIM; $n \simeq 0.003$ cm^{-3}; $T \simeq 10^6$ K; $\simeq 50\,\%$ of the volume of the Galaxy).
- Molecular clouds exhibit a large range of densities ($n \simeq 10^2 - 10^6$ cm^{-3}).

Balance between gas heating & cooling – the phases of the ISM

- The *Cold Neutral Medium* (CNM; $n \simeq 30$ cm^{-3}; $T \simeq 100$ K) & the *Warm Neutral Medium* (WNM; $n \simeq 0.3$ cm^{-3}; $T \simeq 10^4$ K) are at pressure equilibrium $\rightarrow$ the only 2 stable H I phases.
- So are the *Warm Ionized Medium* (WIM; $n \simeq 0.1$ cm^{-3}; $T = 10^4$ K) & the *Hot Ionized Medium* (HIM; $n \simeq 0.003$ cm^{-3}; $T \simeq 10^6$ K; $\simeq 50\,\%$ of the volume of the Galaxy).
- Molecular clouds exhibit a large range of densities ($n \simeq 10^2 - 10^6$ cm^{-3}).

Radiative transfer

Balance between gas heating & cooling – the phases of the ISM

- The *Cold Neutral Medium* (CNM; $n \simeq 30\ \text{cm}^{-3}$; $T \simeq 100$ K) & the *Warm Neutral Medium* (WNM; $n \simeq 0.3\ \text{cm}^{-3}$; $T \simeq 10^4$ K) are at pressure equilibrium $\rightarrow$ the only 2 stable H I phases.
- So are the *Warm Ionized Medium* (WIM; $n \simeq 0.1\ \text{cm}^{-3}$; $T = 10^4$ K) & the *Hot Ionized Medium* (HIM; $n \simeq 0.003\ \text{cm}^{-3}$; $T \simeq 10^6$ K; $\simeq 50\,\%$ of the volume of the Galaxy).
- Molecular clouds exhibit a large range of densities ($n \simeq 10^2 - 10^6\ \text{cm}^{-3}$).

Radiative transfer

- The radiative transfer equations solves the propagation of light in the ISM, accounting for absorption, scattering out & in the sightline & emission by the ISM.

Balance between gas heating & cooling – the phases of the ISM

- The *Cold Neutral Medium* (CNM; $n \simeq 30$ cm^{-3}; $T \simeq 100$ K) & the *Warm Neutral Medium* (WNM; $n \simeq 0.3$ cm^{-3}; $T \simeq 10^4$ K) are at pressure equilibrium $\rightarrow$ the only 2 stable H I phases.
- So are the *Warm Ionized Medium* (WIM; $n \simeq 0.1$ cm^{-3}; $T = 10^4$ K) & the *Hot Ionized Medium* (HIM; $n \simeq 0.003$ cm^{-3}; $T \simeq 10^6$ K; $\simeq 50$ % of the volume of the Galaxy).
- Molecular clouds exhibit a large range of densities ($n \simeq 10^2 - 10^6$ cm^{-3}).

Radiative transfer

- The radiative transfer equations solves the propagation of light in the ISM, accounting for absorption, scattering out & in the sightline & emission by the ISM.
- The optical depth, $\tau(\lambda)$, is related to the mean free path of photons.

Conclusion | Take-Away Points

Balance between gas heating & cooling – the phases of the ISM

- The *Cold Neutral Medium* (CNM; $n \simeq 30$ cm^{-3}; $T \simeq 100$ K) & the *Warm Neutral Medium* (WNM; $n \simeq 0.3$ cm^{-3}; $T \simeq 10^4$ K) are at pressure equilibrium $\rightarrow$ the only 2 stable H I phases.
- So are the *Warm Ionized Medium* (WIM; $n \simeq 0.1$ cm^{-3}; $T = 10^4$ K) & the *Hot Ionized Medium* (HIM; $n \simeq 0.003$ cm^{-3}; $T \simeq 10^6$ K; $\simeq 50\,\%$ of the volume of the Galaxy).
- Molecular clouds exhibit a large range of densities ($n \simeq 10^2 - 10^6$ cm^{-3}).

Radiative transfer

- The radiative transfer equations solves the propagation of light in the ISM, accounting for absorption, scattering out & in the sightline & emission by the ISM.
- The optical depth, $\tau(\lambda)$, is related to the mean free path of photons.
- The Monte Carlo method is the most flexible solution when dealing with complex geometries.

Conclusion | Take-Away Points

Balance between gas heating & cooling – the phases of the ISM

- The *Cold Neutral Medium* (CNM; $n \simeq 30$ cm^{-3}; $T \simeq 100$ K) & the *Warm Neutral Medium* (WNM; $n \simeq 0.3$ cm^{-3}; $T \simeq 10^4$ K) are at pressure equilibrium $\rightarrow$ the only 2 stable H I phases.
- So are the *Warm Ionized Medium* (WIM; $n \simeq 0.1$ cm^{-3}; $T = 10^4$ K) & the *Hot Ionized Medium* (HIM; $n \simeq 0.003$ cm^{-3}; $T \simeq 10^6$ K; $\simeq 50\,\%$ of the volume of the Galaxy).
- Molecular clouds exhibit a large range of densities ($n \simeq 10^2 - 10^6$ cm^{-3}).

Radiative transfer

- The radiative transfer equations solves the propagation of light in the ISM, accounting for absorption, scattering out & in the sightline & emission by the ISM.
- The optical depth, $\tau(\lambda)$, is related to the mean free path of photons.
- The Monte Carlo method is the most flexible solution when dealing with complex geometries.

Star-forming regions

Balance between gas heating & cooling – the phases of the ISM

- The *Cold Neutral Medium* (CNM; $n \simeq 30$ cm^{-3}; $T \simeq 100$ K) & the *Warm Neutral Medium* (WNM; $n \simeq 0.3$ cm^{-3}; $T \simeq 10^4$ K) are at pressure equilibrium $\rightarrow$ the only 2 stable H I phases.
- So are the *Warm Ionized Medium* (WIM; $n \simeq 0.1$ cm^{-3}; $T = 10^4$ K) & the *Hot Ionized Medium* (HIM; $n \simeq 0.003$ cm^{-3}; $T \simeq 10^6$ K; $\simeq 50\,\%$ of the volume of the Galaxy).
- Molecular clouds exhibit a large range of densities ($n \simeq 10^2 - 10^6$ cm^{-3}).

Radiative transfer

- The radiative transfer equations solves the propagation of light in the ISM, accounting for absorption, scattering out & in the sightline & emission by the ISM.
- The optical depth, $\tau(\lambda)$, is related to the mean free path of photons.
- The Monte Carlo method is the most flexible solution when dealing with complex geometries.

Star-forming regions

- The size of H II regions, the Strömgren radius, is determined by the photoionization equilibrium.

Conclusion | Take-Away Points

Balance between gas heating & cooling – the phases of the ISM

- The *Cold Neutral Medium* (CNM; $n \simeq 30$ cm^{-3}; $T \simeq 100$ K) & the *Warm Neutral Medium* (WNM; $n \simeq 0.3$ cm^{-3}; $T \simeq 10^4$ K) are at pressure equilibrium $\rightarrow$ the only 2 stable H I phases.
- So are the *Warm Ionized Medium* (WIM; $n \simeq 0.1$ cm^{-3}; $T = 10^4$ K) & the *Hot Ionized Medium* (HIM; $n \simeq 0.003$ cm^{-3}; $T \simeq 10^6$ K; $\simeq 50\,\%$ of the volume of the Galaxy).
- Molecular clouds exhibit a large range of densities ($n \simeq 10^2 - 10^6$ cm^{-3}).

Radiative transfer

- The radiative transfer equations solves the propagation of light in the ISM, accounting for absorption, scattering out & in the sightline & emission by the ISM.
- The optical depth, $\tau(\lambda)$, is related to the mean free path of photons.
- The Monte Carlo method is the most flexible solution when dealing with complex geometries.

Star-forming regions

- The size of H II regions, the Strömgren radius, is determined by the photoionization equilibrium.
- PhotoDissociation Regions (PDRs) harbor complex chemistry at the UV-illuminated edge of molecular clouds.

Conclusion | Take-Away Points

Balance between gas heating & cooling – the phases of the ISM

- The *Cold Neutral Medium* (CNM; $n \simeq 30\ \text{cm}^{-3}$; $T \simeq 100$ K) & the *Warm Neutral Medium* (WNM; $n \simeq 0.3\ \text{cm}^{-3}$; $T \simeq 10^4$ K) are at pressure equilibrium → the only 2 stable H I phases.
- So are the *Warm Ionized Medium* (WIM; $n \simeq 0.1\ \text{cm}^{-3}$; $T = 10^4$ K) & the *Hot Ionized Medium* (HIM; $n \simeq 0.003\ \text{cm}^{-3}$; $T \simeq 10^6$ K; $\simeq 50\,\%$ of the volume of the Galaxy).
- Molecular clouds exhibit a large range of densities ($n \simeq 10^2 - 10^6\ \text{cm}^{-3}$).

Radiative transfer

- The radiative transfer equations solves the propagation of light in the ISM, accounting for absorption, scattering out & in the sightline & emission by the ISM.
- The optical depth, $\tau(\lambda)$, is related to the mean free path of photons.
- The Monte Carlo method is the most flexible solution when dealing with complex geometries.

Star-forming regions

- The size of H II regions, the Strömgren radius, is determined by the photoionization equilibrium.
- PhotoDissociation Regions (PDRs) harbor complex chemistry at the UV-illuminated edge of molecular clouds.
- At low metallicity, the photodissociation of CO biases molecular mass estimates.

Allen, M. G., Groves, B. A., Dopita, M. A., Sutherland, R. S., & Kewley, L. J. 2008, ApJS, 178, 20

Bakes, E. L. O. & Tielens, A. G. G. M. 1994, ApJ, 427, 822

Bell, T. A., Viti, S., Williams, D. A., Crawford, I. A., & Price, R. J. 2005, MNRAS, 357, 961

Bisbas, T. G., Bell, T. A., Viti, S., Yates, J., & Barlow, M. J. 2012, MNRAS, 427, 2100

Boquien, M., Kennicutt, R., Calzetti, D., et al. 2016, A&A, 591, A6

Bron, E., Le Bourlot, J., & Le Petit, F. 2014, A&A, 569, A100

Cormier, D., Abel, N. P., Hony, S., et al. 2019, A&A, 626, A23

Dalgarno, A. & McCray, R. A. 1972, ARA&A, 10, 375

Dame, T. M., Hartmann, D., & Thaddeus, P. 2001, ApJ, 547, 792

De Looze, I., Baes, M., Bendo, G. J., et al. 2012, MNRAS, 427, 2797

Dopita, M. A. & Sutherland, R. S. 2003, Astrophysics of the diffuse universe (Springer)

Draine, B. T. 2011, Physics of the Interstellar and Intergalactic Medium (Princeton University Press)

Ferland, G. J., Chatzikos, M., Guzmán, F., et al. 2017, RMxAA, 53, 385

Ferland, G. J., Porter, R. L., van Hoof, P. A. M., et al. 2013, RMxAA, 49, 137

Galliano, F. 2022, HDR, Université Paris-Saclay

Habart, E., Peeters, E., Berné, O., et al. 2024, A&A, 685, A73

Hao, C.-N., Kennicutt, R. C., Johnson, B. D., et al. 2011, ApJ, 741, 124

Kalberla, P. M. W. & Kerp, J. 2009, ARA&A, 47, 27

Kennicutt, Jr., R. C. 1998, ApJ, 498, 541

Kimura, H. 2016, MNRAS, 459, 2751

Krügel, E. 2003, The physics of interstellar dust (IoP)

Le Bourlot, J., Le Petit, F., Pinto, C., Roueff, E., & Roy, F. 2012, A&A, 541, A76

Le Petit, F., Nehmé, C., Le Bourlot, J., & Roueff, E. 2006, ApJS, 164, 506

Madden, S. C., Cormier, D., Hony, S., et al. 2020, A&A, 643, A141

Mathis, J. S., Mezger, P. G., & Panagia, N. 1983, A&A, 128, 212

Osterbrock, D. E. & Ferland, G. J. 2006, Astrophysics of gaseous nebulae and active galactic nuclei (University Science Books)

Röllig, M., Ossenkopf, V., Jeyakumar, S., Stutzki, J., & Sternberg, A. 2006, A&A, 451, 917

Röllig, M., Szczerba, R., Ossenkopf, V., & Glück, C. 2013, A&A, 549, A85

Rybicky, G. B. & Lightman, A. P. 1979, Radiative processes in astrophysics (Wiley)

Schure, K. M., Kosenko, D., Kaastra, J. S., Keppens, R., & Vink, J. 2009, A&A, 508, 751

Steinacker, J., Baes, M., & Gordon, K. D. 2013, ARA&A, 51, 63

Strömgren, B. 1939, ApJ, 89, 526

Sutherland, R. S. & Dopita, M. A. 2017, ApJS, 229, 34

Conclusion | References (3/3)

Tielens, A. 2021, Molecular Astrophysics (Cambridge University Press)

Tielens, A. G. G. M. 2005, The Physics and Chemistry of the Interstellar Medium (Cambridge University Press)

Weingartner, J. C. & Draine, B. T. 2001, ApJS, 134, 263

Wolfire, M. G., Hollenbach, D., McKee, C. F., Tielens, A. G. G. M., & Bakes, E. L. O. 1995, ApJ, 443, 152

Wolfire, M. G., Vallini, L., & Chevance, M. 2022, ARA&A, 60, 247